

Enzymatic Conversion of CO₂: From Natural to Artificial Utilization

Sarah Bierbaumer, Maren Nattermann,^{||} Luca Schulz,^{||} Reinhard Zschoche, Tobias J. Erb, Christoph K. Winkler,^{*} Matthias Tinzl,^{*} and Silvia M. Glueck^{*}



Cite This: *Chem. Rev.* 2023, 123, 5702–5754



Read Online

ACCESS |



Metrics & More

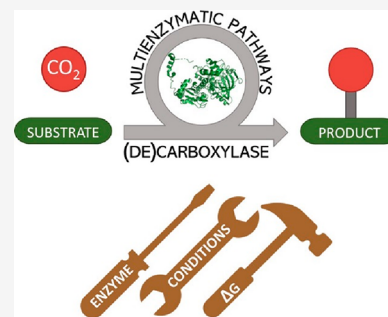


Article Recommendations



Supporting Information

ABSTRACT: Enzymatic carbon dioxide fixation is one of the most important metabolic reactions as it allows the capture of inorganic carbon from the atmosphere and its conversion into organic biomass. However, due to the often unfavorable thermodynamics and the difficulties associated with the utilization of CO₂, a gaseous substrate that is found in comparatively low concentrations in the atmosphere, such reactions remain challenging for biotechnological applications. Nature has tackled these problems by evolution of dedicated CO₂-fixing enzymes, i.e., carboxylases, and embedding them in complex metabolic pathways. Biotechnology employs such carboxylating and decarboxylating enzymes for the carboxylation of aromatic and aliphatic substrates either by embedding them into more complex reaction cascades or by shifting the reaction equilibrium via reaction engineering. This review aims to provide an overview of natural CO₂-fixing enzymes and their mechanistic similarities. We also discuss biocatalytic applications of carboxylases and decarboxylases for the synthesis of valuable products and provide a separate summary of strategies to improve the efficiency of such processes. We briefly summarize natural CO₂ fixation pathways, provide a roadmap for the design and implementation of artificial carbon fixation pathways, and highlight examples of biocatalytic cascades involving carboxylases. Additionally, we suggest that biochemical utilization of reduced CO₂ derivatives, such as formate or methanol, represents a suitable alternative to direct use of CO₂ and provide several examples. Our discussion closes with a techno-economic perspective on enzymatic CO₂ fixation and its potential to reduce CO₂ emissions.



CONTENTS

1. Introduction	5703	3.3.1. CO ₂ Source	5723
2. Enzymatic CO ₂ Fixation Mechanisms and Thermodynamic Considerations	5703	3.3.2. Product Removal	5725
2.1. General Mechanistic Steps of Enzymatic Carboxylation Reactions	5704	3.3.3. Engineering of the Biocatalyst	5725
2.2. Thermodynamic Point of View	5704	3.3.4. Optimization of the Reaction Conditions and the Formulation of the Biocatalyst	5725
3. Enzymatic Carboxylation and CO ₂ Utilization Systems	5706	4. CO ₂ Fixation Pathways and Cascades	5726
3.1. Carboxylases Involved in Natural CO ₂ Fixation and Utilization	5707	4.1. Natural CO ₂ Fixation Pathways	5729
3.1.1. CO ₂ -Fixing Enzymes without External Reductant	5707	4.1.1. CBB Cycle	5729
3.1.2. CO ₂ -Converting Enzymes with External Reductant	5710	4.1.2. rTCA Cycle	5730
3.2. Reversing Decarboxylases for CO ₂ Fixation	5714	4.1.3. WL and Reductive Glycine Pathway	5730
3.2.1. Bivalent Metal-Dependent (De)-carboxylases	5714	4.1.4. Dicarboxylate, 3HP/4HB Cycle, and 3HP Bicycle	5730
3.2.2. Cofactor-Independent (De)carboxylases	5717	4.2. Development and Current State of Synthetic CO ₂ Fixation Pathways	5731
3.2.3. prFMN-Dependent (De)carboxylases	5717	4.2.1. Motivation	5731
3.2.4. TPP-Dependent Keto Acid Decarboxylases	5722	4.2.2. Design	5731
3.2.5. Decarboxylases from Tannin Degradation	5722	4.2.3. Realization and Implementation	5732
3.3. Reaction Engineering of Enzymatic Carboxylation Reactions	5722	4.3. Biocatalytic Cascades Using CO ₂ as C1 Building Block for Fine Chemicals	5733

Special Issue: Bridging the Gaps: Learning from Catalysis across Boundaries

Received: August 18, 2022

Published: January 24, 2023



5. Approaches to Use CO ₂ Derivatives	5734
5.1. Benefits to a Bioeconomy Based on Soluble One-Carbon Compounds	5734
5.2. The Diversity of Natural C1 Assimilation	5735
5.3. Tetrahydrofolate (THF) Cascade	5735
5.4. WL Pathway and Metal Cofactors	5735
5.5. Serine Cycle and Pyridoxal Phosphate Dependent Enzymes	5736
5.6. RuMP Pathway and RuBisCO-like Reactions	5737
5.7. XuMP Pathway and Thiamine Pyrophosphate Dependent Reactions	5738
5.8. Pyruvate Formate-lyase: Exploiting Reverse Reactions	5738
6. Techno-economic Perspective	5739
7. Outlook and Opportunities	5741
Associated Content	5742
Supporting Information	5742
Author Information	5742
Corresponding Authors	5742
Authors	5742
Author Contributions	5742
Funding	5742
Notes	5743
Biographies	5743
Acknowledgments	5743
Abbreviations	5743
References	5744

1. INTRODUCTION

Over billions of years, nature has evolved extremely powerful tools to use CO₂ as a building block for the formation of biomass. In fact, CO₂ is likely the most ancient carbon source on the planet. In the course of evolution, all three kingdoms of life have evolved and/or acquired carboxylases that allow them to utilize CO₂ via different mechanistic pathways. Humankind has recently started to exploit these biocatalysts and concepts for biotechnological and synthetic purposes.^{1–5} In such applications, CO₂ represents an attractive alternative to building blocks derived from fossil feedstock. As a result, carboxylases as well as decarboxylases from both primary and secondary metabolism of various microbial sources have been used for synthetic CO₂ utilization.^{6–14}

Herein, we provide an overview of carboxylating enzymes that occur in nature and biocatalysts that have potential for biotechnological applications. We discuss and guide the implementation of single enzymes in highly complex artificial pathways and cascades. Furthermore, we highlight the biotechnological potential of other one-carbon (C1) metabolites derived from CO₂ and give a techno-economic perspective of the field.

In the first section of the review, we provide a general introduction to enzymatic carboxylation reactions by discussing their chemical and energetic aspects. We thereby identify common mechanistic strategies employed by carboxylases to overcome the reaction's thermodynamic challenges (section 2). The following section (section 3) is focused on illustrating the structural and mechanistic details of natural carboxylases, and (de)carboxylases, which can be employed as carboxylases by reversing the direction of the reaction. Additionally, we provide a summary of strategies that are applied to increase the productivity of in vitro single-enzyme carboxylation systems for the synthesis of chemicals. We then turn our attention from

single enzymes to CO₂-fixing (autotrophic) pathways (section 4). Following a brief overview of naturally occurring autotrophic carbon fixation pathways, we provide a roadmap for the design and realization of new-to-nature CO₂ fixation pathways. The section closes with an overview of carboxylation cascades that utilize CO₂ as a synthetic C1 building block and directly aim for a product of synthetic or chemical value. section 5 further extends the concept of enzymatic carbon fixation toward C1 compounds (formate, formaldehyde, methanol) that can be generated through the reduction of CO₂. The current state of carbon fixation technology and the necessary next technological advances are summarized in section 6 from an industrial perspective. Finally, section 7 highlights the immediate challenges and the exciting opportunities for enzymatic carbon fixation.

As this review aims at providing an integrated view on enzymatic carbon fixation, we realize that our discussions are necessarily incomplete. For further details and insights into selected topics, we want to refer the reader to a number of excellent recent reviews on carboxylating enzymes,^{6,9,12} synthetic applications of carboxylases,^{10,11} engineering of artificial fixation pathways,¹⁵ as well as thermodynamic considerations.¹⁶

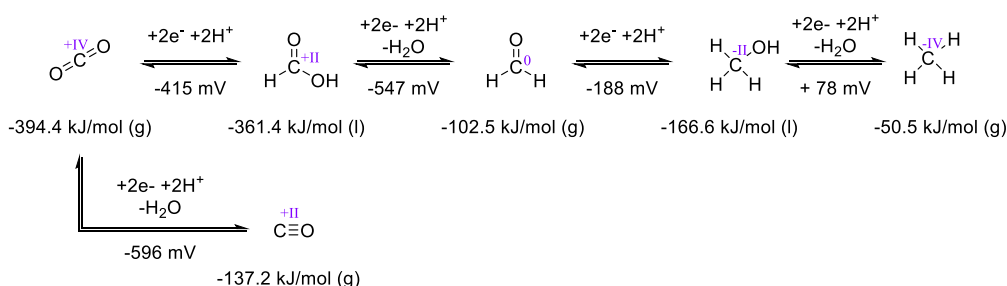
2. ENZYMATIC CO₂ FIXATION MECHANISMS AND THERMODYNAMIC CONSIDERATIONS

From a chemical perspective, carboxylation reactions are intriguing, as they allow introducing C1 units as building blocks into a target molecule, starting from the abundant and easily accessible carbon source, CO₂.^{10,17} However, the chemical utilization of CO₂ as a building block comes with a number of challenges. Most importantly, carbon in CO₂ is in its highest oxidation state, and therefore any functionalization must be reductive. As was recently put, CO₂ is at the “bottom of the potential energy well”,¹⁸ and energy must be invested to utilize it. This is nicely illustrated by the low Gibbs energy of formation of CO₂ compared to other C1 molecules with a more reduced carbon center, as well as by its comparably low reduction potential (Scheme 1).^{19,20}

Although CO₂ is abundant in the atmosphere, current concentrations (about 412 ppm in 2021²¹) do not allow direct use of atmospheric air for carboxylation chemistry. Additionally, when a gas is used as reagent in synthesis, its phase transfer into solution and its solubility (up to 1.7 g L^{−1} at atmospheric pressure and 20 °C), i.e., the availability of the building block in solution, need to be considered. As CO₂ undergoes hydration in aqueous solution, CO₂ availability is strongly pH-dependent, with bicarbonate (HCO₃[−]) being the most prevalent form at neutral to alkaline pH.

Biocatalytic carboxylation is applied to overcome the mentioned obstacles.^{3,5,22} The high efficiency of enzymes allows acceleration of challenging reactions and the substrate affinity of enzymes permits nature to operate them under the low CO₂ concentrations in air.^{10–12,14,15} An impressive example of the catalytic efficiency of enzymes that utilize CO₂ are carbonic anhydrases which belong to the fastest catalysts known to date and accelerate the equilibration of bicarbonate and CO₂ (aq) by 6 orders of magnitude.²³ Evolution has provided a broad portfolio of carboxylases that exhibit different binding and activation modes of CO₂ and different attack modes of the carbon nucleophile onto the respective electrophilic CO₂ species. The required electrons for the reduction of CO₂ are either provided

Scheme 1. Standard Molar Gibbs Energy of Formation ($\Delta_f G^\circ$) and Experimental Reduction Potentials of Carbon Dioxide, Carbon Monoxide, Formic Acid, Formaldehyde, Methanol, and Methane, at 298.15 K in kJ/mol (Oxidation States of Carbon Are Given As Roman Numerals)^{19,20}



by the substrate itself or in form of reduced cofactors, in particular, nicotinamides (NAD(P)H) or ferredoxin.

2.1. General Mechanistic Steps of Enzymatic Carboxylation Reactions

The general mechanistic steps of enzymatic carboxylations are highly similar for almost all carboxylases:^{9,12} (a) generation of an enol or enolate to create a nucleophile, (b) binding and stabilization of the enol (or enolate), (c) accommodation and/or activation of CO₂ (e.g., as carboxyphosphate), (d) C–C bond formation via nucleophilic attack of the enol (or enolate) onto the carbon of CO₂, and finally (e) potential follow up reactions such as cleavage of the product from the cofactor (Scheme 2).

Enzymes that do not follow these general steps are the pyridoxal-5'-phosphate (PLP)-dependent glycine cleavage system (GCS)²⁴ that is discussed in section 3.1.2, the ferulic acid decarboxylases that depend on a novel prenylated FMN cofactor to catalyze the reversible decarboxylation of ferulic acids via a 1,3-cycloaddition²⁵ (compare section 3.2.3), and enzymes that directly reduce CO₂, such as CO dehydrogenase²⁶ or formate dehydrogenase²⁷ (compare section 3.1.2). Below, we discuss the key steps for bio(techno)logically relevant carboxylases in detail, with a focus on (step a) enol formation and (step c) CO₂ activation. Note that for reversible decarboxylases, carboxylation is herein interpreted as the reversed decarboxylation mechanism. For details on specific mechanisms, refer to the subsections of the respective enzyme family (section 3).

Enols, enolates, and enamines serve as carbon nucleophiles, not only in synthetic organic chemistry but also in biochemistry. It is therefore no surprise that nature has evolved a range of different ways for their formation. The most straightforward reaction to form an enolate proceeds via α -deprotonation of carbonyls. For example, in the reaction catalyzed by RuBisCO, the hydroxy-keto moiety of D-ribulose-1,5-bisphosphate is deprotonated, forming an enediolate, which is stabilized by the active site Mg²⁺ (Scheme 3, I, see also section 3.1.1).²⁸ Similarly, enolates are formed via deprotonation in isocitrate dehydrogenases and acetyl-CoA carboxylases, which feature an acetyl-CoA anion (Scheme 3, II) that eventually attacks carboxybiotin (VIII, as discussed below; see also section 3.1.2). Also, the reversed reaction of bivalent metal-dependent decarboxylases (section 3.2.1) and the cofactor-independent decarboxylases (section 3.2.2) require initial activation of the substrate via deprotonation of the substrate's phenolic hydroxy group. In the first case, the phenolate is bound by a bivalent metal ion in the active site and the ortho-carbon, possessing the character of an enolate, attacks CO₂ (Scheme 3, III, Zn²⁺ can also be Mg²⁺ or Mn²⁺).^{29,30} For cofactor-independent

decarboxylases, the reaction proceeds via a quasi-trienolate (Scheme 3, IV).³¹ A mechanistic alternative for enolate formation is the 1,4-addition of a hydride from NADPH to α,β -unsaturated CoA esters, as in the case of enoyl-CoA carboxylases/reductases, such as crotonyl-CoA carboxylase/reductase (Scheme 3, V; compare to section 3.1.2).³²

In the case of phosphoenolpyruvate carboxylase (PEPC, see also section 3.1.1), the substrate itself (phosphoenolpyruvate) is already an enol-ester, and, upon cleavage of the phosphoester group with bicarbonate, the enolate is released (stabilized by an active site Mg²⁺; Scheme 3, VI). In parallel, this reaction also activates CO₂ as the mixed anhydride carboxyphosphate which serves as carboxylation source (Scheme 3, VII).³³

A similar activation of CO₂ as carboxyphosphate is also a key-step in other carboxylation mechanisms, such as the reaction catalyzed by acetyl-CoA carboxylases (see also section 3.1.1). In the first mechanistic step, these enzymes convert bicarbonate in an ATP-dependent reaction into carboxyphosphate (Scheme 3, VII). This is followed by the formation of carboxybiotin, another activated CO₂ equivalent (Scheme 3, VIII) which in turn facilitates the carboxylation of an acetyl-CoA enolate (Scheme 3, II).³⁴

Enzymes that depend on prenylated FMN (prFMN) as cofactor show a range of different carboxylation mechanisms (see section 3.2.3). The *para*-carboxylation of phenolic substrates proceeds via a substrate that is covalently bound to prFMN via a quasi-dienolate (Scheme 3, IX).³⁵

Finally, the mechanism of enzymes that depend on thiamin pyrophosphate (TPP) differs from the above-mentioned cases, as the nucleophile is not an enolate but an enamine. In the case of 2-ketoglutarate:ferredoxin oxidoreductase or pyruvate:ferredoxin oxidoreductase, the carbonyl of the respective acyl-CoA is turned into a nucleophile via an Umpolung. The reaction requires two electrons, provided by ferredoxins, leading to formation of a TPP-bound enamine intermediate that can attack CO₂ (Scheme 3, X; compare also section 3.1.2).^{36–38} The same intermediate is produced from aldehydes by pyruvate decarboxylase, however, in this case no reduction is required (compare to section 3.2.4).³⁹

2.2. Thermodynamic Point of View

For thermodynamically controlled reactions, such as carboxylations, the change in Gibbs free energy (ΔG) is a key parameter that needs to be considered (in contrast to kinetically controlled reactions, where the individual reaction rates are more relevant).⁴⁰ In nature and synthesis, carboxylation reactions are accomplished either by reducing the required reaction energy ($\Delta_r G$ or the activation energy) or by shifting the reaction equilibrium using Le Chatelier's principle.¹⁴ Nature

embeds carboxylations within metabolic pathways that are exergonic (cf. section 4.1). The same principle was applied for the development of artificial CO₂-fixing enzyme cascades (cf. section 4.2). Besides shifting the equilibrium, the energy demand^{41–43} of the overall reaction is reduced by several strategies that are discussed below (Scheme 4).^{12,14} Note that the $\Delta_r G^\circ$ values given in this section were calculated using the eQuilibrator tool^{42,43} at standard conditions (1 M concentration of the involved species, 25 °C and 1 bar; and at pH 7.5 and an ionic strength of 0.25 M) and compared to values reported in literature, whenever possible.^{14,16}

Strategies to render carboxylation reactions more favorable include:

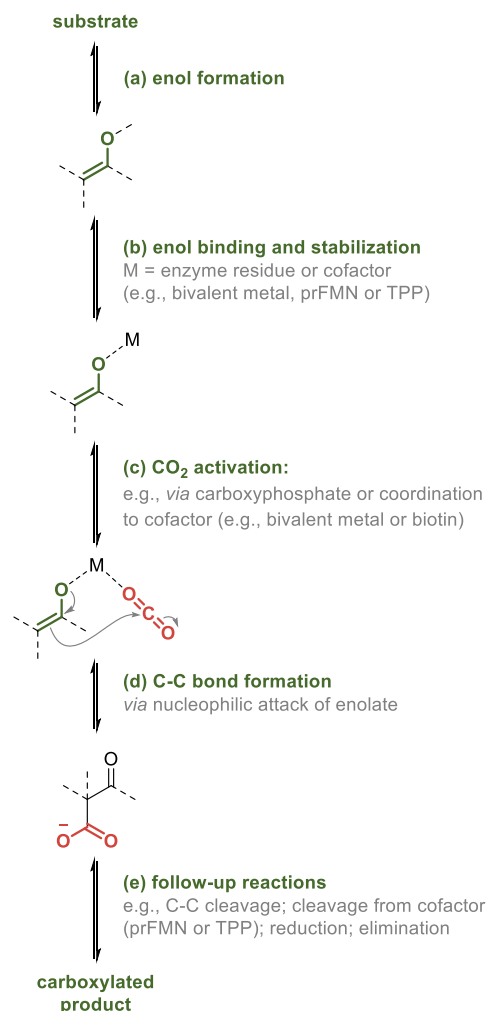
(i) Using high energy starting materials: This is the case for many CO₂-fixing enzymes that do not depend on external reductants. Examples are the reactions catalyzed by RuBisCO⁴⁴ or PEPC.⁴⁵ Both reactions are energetically favored, with a $\Delta_r G^\circ$ of -32.2 kJ/mol for PEPC^{16,42} and $\Delta_r G^\circ = -32.0$ kJ/mol for RuBisCO, which in addition benefits from the energy provided by the hydrolysis of the carboxylation product, i.e., from the fact that two “low energy” products are formed (see section 3.1.1).^{16,42}

(ii) Activation of CO₂: As previously discussed, many structurally distinct carboxylases share the mechanistic feature of CO₂ coordination to a bivalent metal in the active site (Mg²⁺, Zn²⁺, or Mn²⁺). Examples include PEPC, isocitrate dehydrogenase, or the metal-dependent phenolic acid decarboxylases.^{11,12} Furthermore, CO₂ (or HCO₃[−]) is often directly activated by ATP, forming the reactive carboxyphosphate. Hydrolysis of one phosphate group of ATP provides between 26 and 43 kJ/mol, depending on the Mg²⁺ concentration.^{16,42} Examples include the biotin-dependent acetyl-CoA and propionyl-CoA carboxylases. The free energy of the ATP-dependent enzymatic carboxylation of acetyl-CoA, for example, sums up to -9.1 kJ/mol.^{16,42} Catalysis proceeds via the formation of carboxyphosphate and the carboxylation of biotin (see also section 3.1.1).

(iii) Supply of external reducing equivalents: Electron donors that are commonly utilized are either NADPH, providing up to approximately 65 kJ/mol (for two electrons), or ferredoxins, worth up to approximately 40 kJ/mol per electron.^{16,19} 2-Ketoglutarate synthases, which utilize the TPP cofactor to carboxylate CoA thioesters forming α -keto acids, are examples of ferredoxin-dependent reductive carboxylases. Crotonyl-CoA carboxylase/reductases and isocitrate dehydrogenases depend either on NADPH or NADH and are energetically favorable with $\Delta_r G^\circ = -14.2$ kJ/mol and $\Delta_r G^\circ = -5.4$ kJ/mol, respectively. However, at millimolar substrate concentrations the isocitrate dehydrogenase reaction becomes unfavorable. The glycine cleavage system requires additional energy to run in the carboxylation direction ($\Delta_r G^\circ = 3.2$ kJ/mol).^{16,42} Propionyl-CoA synthase, an enzyme that catalyzes the conversion of 3-hydroxypropionate to propionyl-CoA, harbors a promiscuous NADPH-dependent carboxylation activity ($\Delta_r G^\circ = -43$ kJ/mol) that was recently enhanced by engineering.⁴⁶ Pyruvate:ferredoxin oxidoreductase can only catalyze the formation of pyruvate from CO₂ and acetyl-CoA if either reduced cofactor or highly reducing ferredoxins are present in sufficient amounts.⁴⁷ In addition to these carboxylases, enzymes that perform direct reduction of CO₂, namely formate dehydrogenase and CO-dehydrogenase, also require either NADPH or ferredoxin as electron donor.

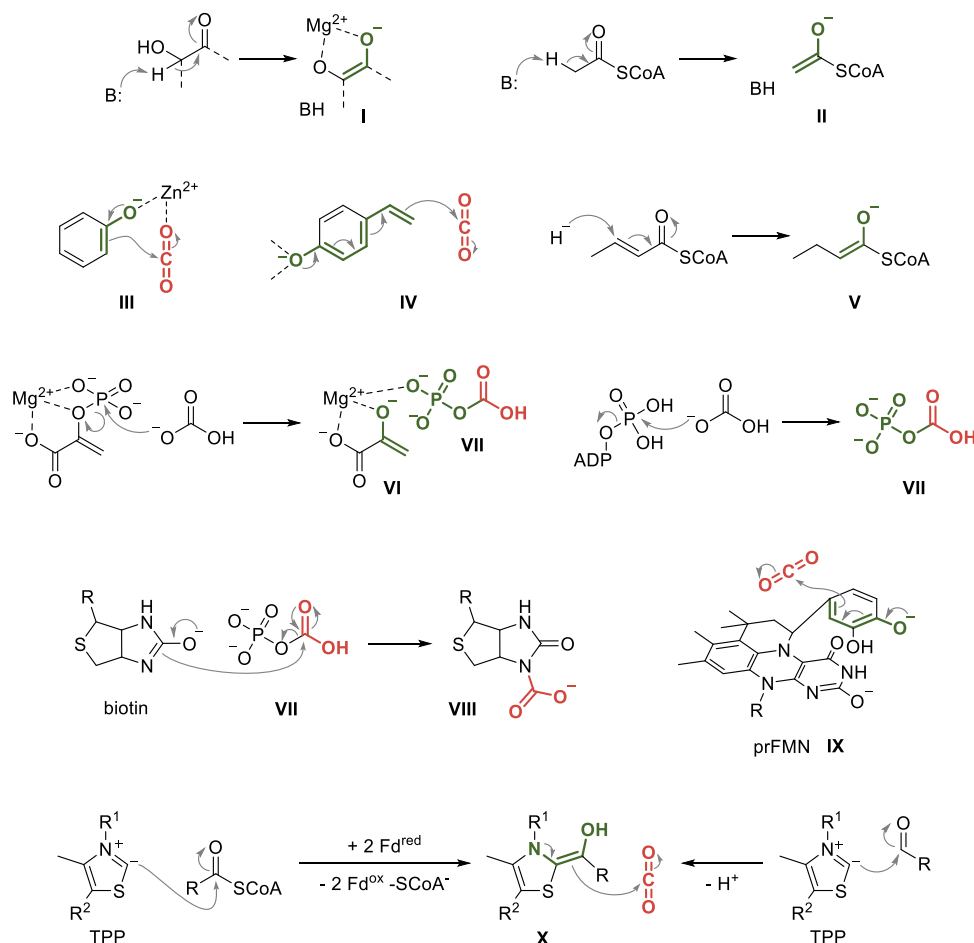
(iv) Formation of low energy products: the carboxylation of phenolic compounds, as performed by the enzymes of the UbiX-

Scheme 2. General Mechanistic Steps of Enzymatic Carboxylations



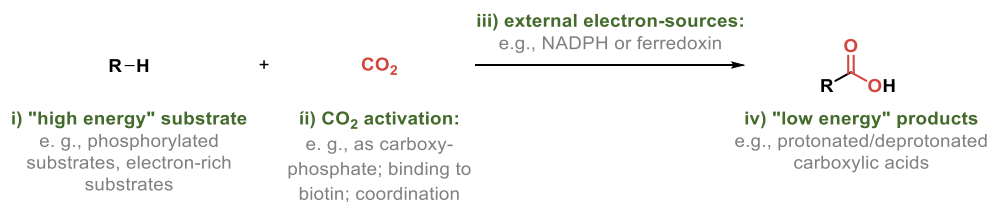
UbiD family, or by the metal-dependent decarboxylases, yields carboxylic acids.^{10–12} The reaction, however, is endergonic and the experimentally measured free standard energy demand of the reaction of approximately 22 kJ/mol⁴⁸ fits roughly to the calculated value of 15.9 kJ/mol ($\Delta_r G^\circ$; $\Delta_r G' = 33.0$ kJ/mol at concentrations of 1 mM).⁴² The thermodynamically expected reduction of the reactions free energy demand via increasing the concentration of the CO₂-donor bicarbonate was experimentally demonstrated.²⁹

In (synthetic) metabolic pathways, the overall energy demand is usually not given in kJ/mol but instead is measured as the number of ATP and NADPH equivalents consumed per molecule of CO₂ fixed.¹⁵ For example, the Calvin–Benson–Bassham cycle (CBB cycle) requires 8.5 ATP equivalents per equivalent of fixed CO₂. In comparison, the reductive oxidative citric acid cycle (rTCA cycle) only consumes 5 such equivalents per CO₂ (Table 5). Natural CO₂ fixation pathways were recently classified as “energy-intensive” if the total change in Gibbs free energy per mol of fixed carbon is more negative than -60 kJ/mol and “energy-saving” if it is less negative.¹⁶ Interestingly, while pathways from aerobic organisms are thermodynamically favorable, they generally have a high demand of ATP. In contrast, anaerobic organisms tend to resort to pathways which proceed with a lower gain in overall free energy but require less ATP (“energy-saving pathways”). This is most likely due to the

Scheme 3. Mechanistic Strategies for the Activation of the Nucleophile (Enol- or Enamine-Formation) and CO₂^a

^a(I) Endiolate stabilized by Mg²⁺, formed in the mechanism of RuBisCO. (II) Enolate formed by acetyl-CoA carboxylases. (III) Phenolate bound to Zn²⁺ in the active site of bivalent metal-dependent decarboxylases. (IV) Trienolate attack onto CO₂ by the cofactor-independent decarboxylases. (V) Hydride attack (NADPH) onto crotonyl-CoA by enoyl-CoA carboxylases/reductases, forming the intermediary enolate. (VI) Cleavage of the phosphate ester of phosphoenolpyruvate by pyruvate carboxylase. (VII) Carboxyphosphate, formed either from phosphoenolpyruvate or ATP and bicarbonate. (VIII) Formation of carboxybiotin by acetyl-CoA carboxylases. (IX) Intermediary dienolate, covalently bound to prFMN, in the mechanism of AroY-type enzymes. (X) Umpolung of the carbonyl center of either acyl-CoA (2-ketoglutarate synthase or pyruvate synthase) or aldehyde substrates (pyruvate decarboxylase) with TPP as cofactor.

Scheme 4. Nature's Strategies for Reducing the Free Energy of Carboxylation Reactions



ability of aerobic organisms to synthesize ATP via oxidative phosphorylation, thereby lifting ATP efficiency restrictions. To allow a better comparison of the different pathways, herein we normalized their energy demand to acetyl-CoA as final product (see section 4, Table 5 and Supporting Information). However, not only the overall reaction energy is important. For the development of synthetic carbon fixation pathways, the thermodynamic profile of reaction sequences plays an important role, as further discussed in section 4. Note that the recently investigated correlation of the reduction potential with basic reaction types allows a quick identification of the reactions that provide energetic barriers.²⁰

3. ENZYMATIC CARBOXYLATION AND CO₂ UTILIZATION SYSTEMS

The currently available enzymatic carboxylation systems may be categorized into two classes: carboxylases that perform CO₂ fixation or modification as their natural function, i.e. RuBisCO and other enzymes that are involved in natural CO₂ fixation pathways (section 3.1), and decarboxylases that naturally perform the decarboxylation reaction but that can be “tricked” into carboxylation (section 3.2). While enzymes involved in central metabolism are in general highly specific for their respective substrates, decarboxylases, which are mostly part of biodegradation pathways, accept a broad range of substrates.¹⁴

Table 1. Overview of Naturally Occurring Carboxylases^a

carboxylase	carbon species	cofactor	pathway	O ₂ sensitivity	reducing equivalents/ reduced species	ref
ribulose-1,5-bisphosphate carboxylase/oxygenase (RuBisCO)	CO ₂	Mg ²⁺	CBB	no, but side reactivity	substrate	49,50
phosphoenolpyruvate carboxylase (PEPC)	HCO ₃ [−]	Mg ²⁺	dicarboxylate	no	substrate	33,45,51
acetyl-CoA carboxylase (ACC)	HCO ₃ [−]	Mg ²⁺ , ATP, biotin	3HP bicycle, 3HP/4HB	no	substrate	34,52
propionyl-CoA carboxylase (ACPCC)	HCO ₃ [−]	Mg ²⁺ , ATP, biotin	3HP bicycle, 3HP/4HB	no	substrate	53,54,34,55,56
2-ketoglutarate:ferredoxin oxidoreductase (2KFOR)	CO ₂	ferredoxin, TPP	rTCA	yes	ferredoxin	57
pyruvate:ferredoxin oxidoreductase (PFOR)	CO ₂	ferredoxin, TPP	dicarboxylate cycle	yes	ferredoxin	36,38,58
isocitrate dehydrogenase (IDH)	CO ₂	NAD(P)H	rTCA	no	NADPH	59–61
glycine cleavage system (GCS)	CO ₂	NAD(P)H, PLP, lipoate	rGlycine	no	NADPH	24,62
crotonyl-CoA carboxylase/reductase (CCR)	CO ₂	NAD(P)H	ethylmalonyl-CoA pathway	no	NADPH	32,63
formate dehydrogenase (FDH)	CO ₂	ferredoxin, NADH	WL/rGlycine	yes	ferredoxin	64–66
CO dehydrogenase (CODH)	CO ₂	Ni4Fe4S	WL	yes	ferredoxin	67–69
phosphogluconate dehydrogenase (Gnd)	CO ₂	NADPH	GED	no	NADPH	70
pyruvate carboxylase	HCO ₃ [−]	Mg ²⁺ , ATP, biotin	anaplerosis	no	substrate	71,72
methylcrotonyl-CoA carboxylase	HCO ₃ [−]	Mg ²⁺ , ATP, biotin	leucine degradation	no	substrate	34,56
acetone carboxylase	HCO ₃ [−]	Mn ²⁺ /Zn ²⁺	acetone degradation	no	substrate	73,74
urea carboxylase	HCO ₃ [−]	Mg ²⁺ , ATP, biotin	urea degradation	no	substrate	75,76
vitamin K-dependent carboxylase	CO ₂	vitamin K	glutamate carboxylation	no	vitamin K	77,78
phenylphosphate carboxylase	CO ₂	K ⁺ , Mg ²⁺ or Mn ²⁺	phenol degradation	yes	substrate	79,80

^aCBB, Calvin–Benson–Bassham; 3HP, 3-hydroxypropionate; WL, Wood–Ljungdahl; DC, dicarboxylate; 3HP/4HB, 3-hydroxypropionate/4-hydroxybutyrate; rGlycine, reductive glycine; rTCA, reverse tricarboxylic acid cycle; RuBisCO, ribulose-1,5-bisphosphate carboxylase/oxygenase. Carboxylases below the double dashed line are not described in detail.

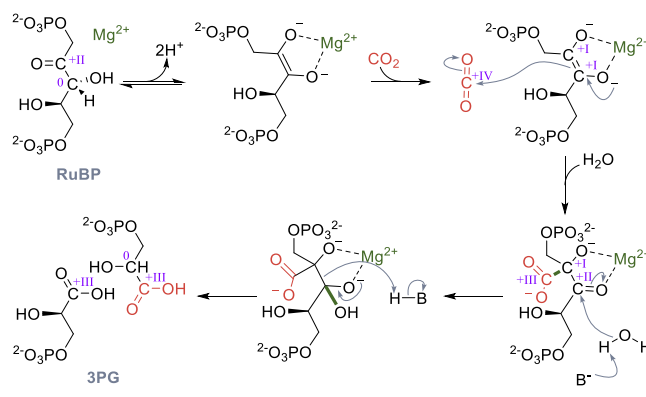
Building on these carboxylation systems, several reaction parameters can be tuned in order to reach higher conversion or productivity as summarized in section 3.3.

3.1. Carboxylases Involved in Natural CO₂ Fixation and Utilization

CO₂ is necessarily reduced in any chemical carbon fixation reaction. This reduction requires electrons which can be either provided by an external reductant or by oxidation of the substrate/reaction product itself.⁹ As this difference represents an important mechanistic distinction, we discuss natural CO₂-fixing enzymes according to these two categories: (i) enzymes which *do not* use external reductants (section 3.1.1) and (ii) enzymes which *do* require external reductants (section 3.1.2). Table 1 provides orientation within the natural carboxylases, highlighting the respective enzyme's cofactors, its natural role (i.e., the pathway it belongs to), its oxygen-sensitivity, and the source of reducing equivalents.

3.1.1. CO₂-Fixing Enzymes without External Reductant. **3.1.1.1. Ribulose-1,5-bisphosphate Carboxylase/Oxygenase (RuBisCO).** RuBisCO is the most important carbon fixing enzyme on the planet. Its relevance is illustrated by the fact that the total biomass of RuBisCO (roughly 0.7 Gt)⁸¹ exceeds the biomass of the entire human population (0.06 Gt)⁸² by 1 order of magnitude. RuBisCO is found in all domains of life, suggesting that it is an evolutionarily old protein. Four classes of RuBisCOs (forms I–IV) are known, three of which (forms I–III) catalyze the carboxylation reaction of ribulose-1,5-bisphosphate (RuBP), and the subsequent hydrolysis of the product, thereby forming two molecules of 3-phosphoglycerate (3PG, Scheme 5, Figure 1).^{83–86} Form I RuBisCOs, which are

Scheme 5. Catalytic Cycle of RuBisCO; Changes of the Oxidation State of Selected Carbons Are Given in Roman Numerals



found in plants and cyanobacteria⁸⁴ generally form hexadecameric complexes composed of eight large and eight small subunits. The small subunit is only found in form I RuBisCOs and is not essential for catalysis but contributes to specificity.⁸⁷ The catalytically active large subunits form four dimers, with the active sites located at the dimer–dimer interface. Form II RuBisCOs are found in purple nonsulfur bacteria, dinoflagellates, and other chemoautotrophic bacteria⁸⁶ and they are on average faster than form I RuBisCOs but tend to be less specific in distinguishing oxygen and CO₂. Form III RuBisCO, which is found in archaea and anaerobic bacteria, has long been thought to be unable to support autotrophy. However, it has been shown that the thermophilic bacterium *Thermodesulfobium acidophilum*

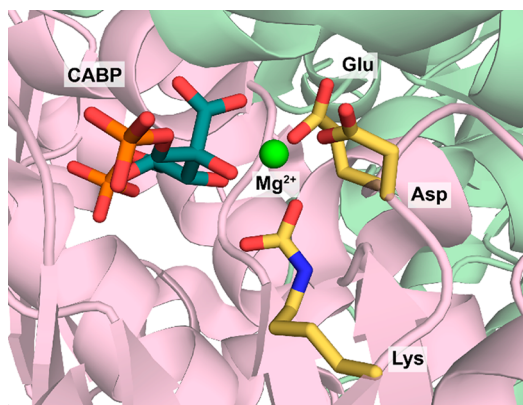


Figure 1. Active site of *Spinacia oleracea* RuBisCO (PDB 8RUC) lies at the dimer–dimer interface of two large subunits (pink and green) and features a Mg^{2+} ion (green). Here, the active site is occupied by the transition state analogue 2-carboxyarabinitol biphosphate (CABP, forest green).

can utilize its form III RuBisCO to sustain autotrophic growth, using the transaldolase variant of the CBB cycle.⁸⁸ Both form II and form III RuBisCOs are often found as dimers but more exotic oligomers such as hexamers⁸⁹ or decameric structures⁹⁰ have also been reported. Apart from the three carboxylating RuBisCO forms (forms I–III), another group of RuBisCOs (form IV, also called RuBisCO-like proteins, RLPs) exists.⁹¹ Only a handful of RLPs have been characterized, but all of them work with substrates structurally related to RuBP and share conserved steps in their catalytic cycle. However, their biological functions are diverse, ranging from simple proton abstractions,⁹² over isomerization reactions,⁹³ to decarboxylations⁹⁴ and oxygenations.⁹⁵

To form a catalytically competent complex, RuBisCOs require binding of a Mg^{2+} as well as carbamylation of a conserved lysine residue, which coordinates to the Mg^{2+} (Figure 1).^{83,84} The catalytic cycle of RuBisCO has been studied in detail. After coordination of RuBP to the Mg^{2+} , a proton is abstracted from the C3 carbon (Scheme 5). Then, the enediolate directly reacts with CO_2 to form an intermediate that subsequently undergoes hydrolysis, yielding two molecules of 3PG. The formal reduction of CO_2 is achieved by concomitant oxidation of the C3 carbon of RuBP. Therefore, the overall reaction catalyzed by RuBisCO is redox neutral. Note, that formation of an enediolate is also central to the mechanism of RLPs, while the subsequent steps in their reaction mechanisms (i.e., reprotonation, oxygenation, *trans*-carboxylation) differ, giving rise to the diverse reactions, catalyzed by RLPs.

RuBisCO works under ambient conditions and does not have a dedicated CO_2 binding site like crotonyl-CoA carboxylase/reductase (CCR, discussed below). During RuBisCO's catalytic cycle, side reactions with other gaseous molecules, such as oxygen⁴⁴ can occur, and indeed represent a major inefficiency in the metabolism of plants.⁹⁶ Approximately 20% of RuBisCO's catalytic cycles incorporate oxygen into biomass instead of CO_2 .⁹⁷ The products of this unwanted reaction are 3PG and 2-phosphoglycolate (2PG), a toxic compound which has to be recycled in an energy intensive process that releases previously fixed CO_2 known as photorespiration.⁹⁸

Notably, reaction of RuBisCO's singlet enediol intermediate with ground-state triplet O_2 is spin-forbidden and should thus (if at all) proceed very slowly due to the high-energy barrier

involved in the reaction.⁹⁹ Oxygenation in RuBisCO as well as in other carboxylases likely proceeds via a single electron transfer (SET) mechanism, in which a single electron is transferred from the RuBP enediolate to reduce O_2 and yield a superoxide radical, which can subsequently form a RuBP peroxide intermediate.¹⁰⁰ A suited dielectric environment in RuBisCO's active site enables this reaction sequence.¹⁰⁰ The propensity of carboxylases to react with O_2 instead of CO_2 likely depends on a multitude of factors, including the involved metal center, the metal center's coordination environment, outer shell protein environments, and the dielectric environment of the active site.¹⁰⁰

To suppress RuBisCO's oxygenation reaction, nature has developed several carbon concentrating mechanisms (CCMs) to increase local CO_2 concentrations around RuBisCO to favor carboxylation over oxygenation. Prominent examples for naturally occurring CCMs include the bacterial carboxysome,¹⁰¹ the pyrenoid present in algae¹⁰² as well as the C4 and Crassulacean acid metabolism (CAM) in plants.¹⁰³ Recent efforts in synthetic biology created a synthetic photorespiration pathway that converts 2PG back into the CBB cycle intermediate 3PG through tartronyl-CoA carboxylase, a new-to-nature CO_2 -fixing enzyme that compensates for the missed carboxylation reaction of RuBisCO.⁵⁵

A less commonly discussed side reactivity of RuBisCO is reprotonation of the reactive enediolate intermediate producing xylulose 1,5-bisphosphate, 3-ketoarabinitol 1,5-bisphosphate, or 3-ketoribitol 1,5-bisphosphate.^{104–106} These compounds can act as potent RuBisCO inhibitors and nature has developed dedicated chaperones to remove these inhibitors from the active site.¹⁰⁷

3.1.1.2. Phosphoenolpyruvate Carboxylase (PEPC).

Although phosphoenolpyruvate carboxylase (PEPC) is one of the carbon-fixing enzymes in the anaerobic dicarboxylate cycle, PEPC is not oxygen sensitive and is present in many aerobic organisms, most notably in the mesophyll of C4 plants.⁴⁵ The enzyme catalyzes the formation of oxaloacetate from PEP using bicarbonate as substrate. Like RuBisCO, PEPC features a Mg^{2+} in the active site. The Mg^{2+} is coordinated by a glutamate, an aspartate, and four water molecules (Figure 2).

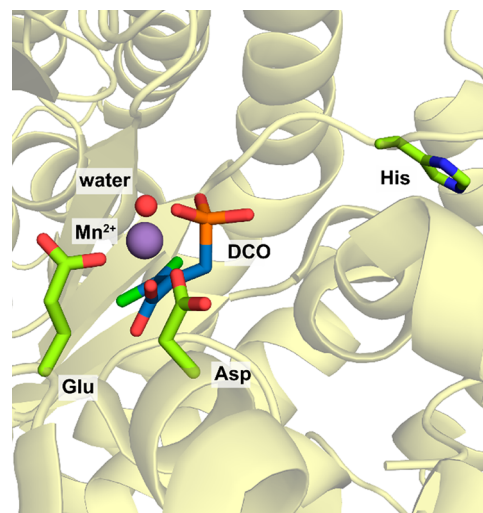
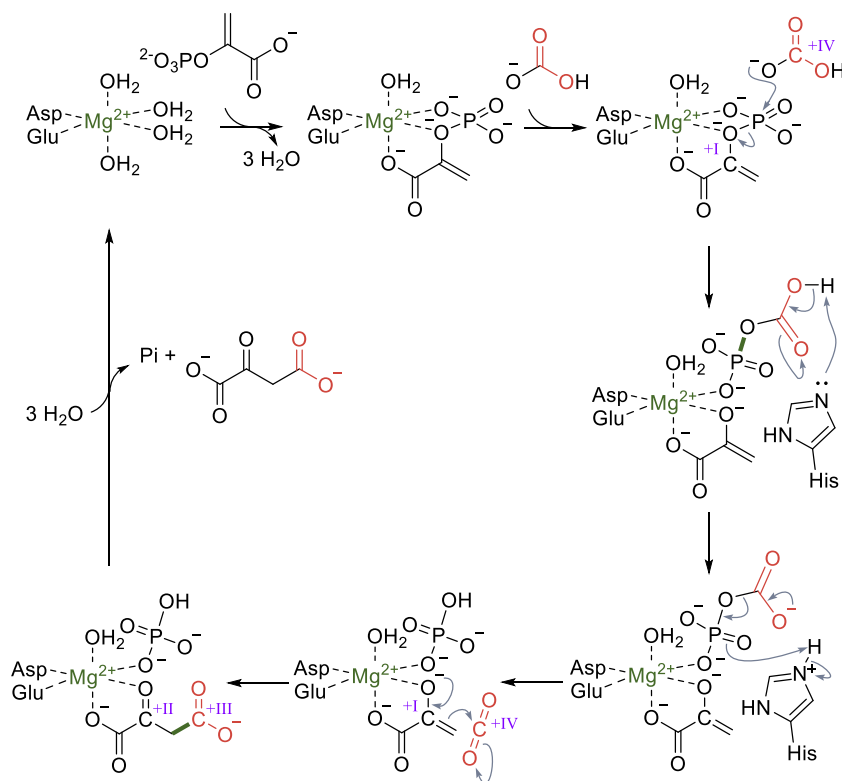
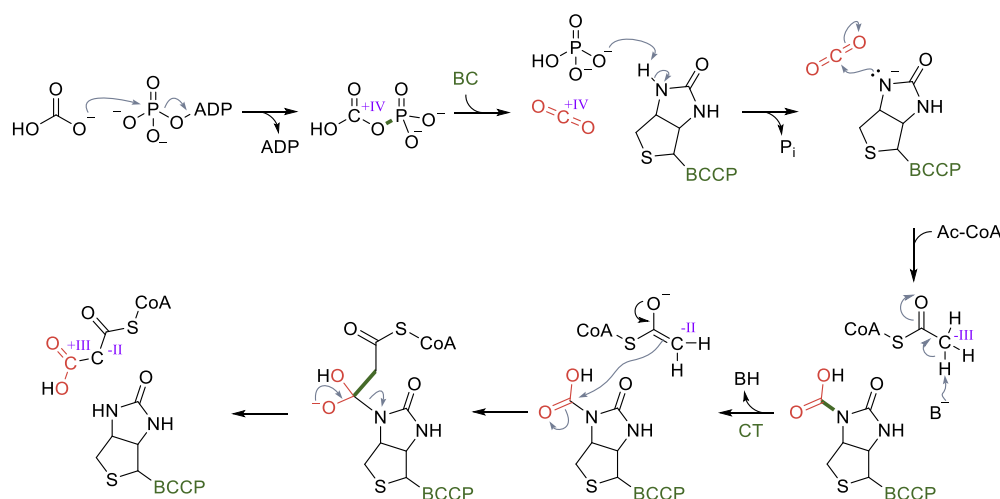


Figure 2. Active site of *E. coli* PEPC (PDB 1JQN) with bound Mn^{2+} (instead of naturally occurring Mg^{2+}) and the substrate analogue 3,3-dichloro-2-phosphonomethyl-acrylic acid (DCO) bound in the active site.

Scheme 6. Catalytic Cycle of PEPC; Changes of the Oxidation State of Selected Carbons Are Given in Roman Numerals

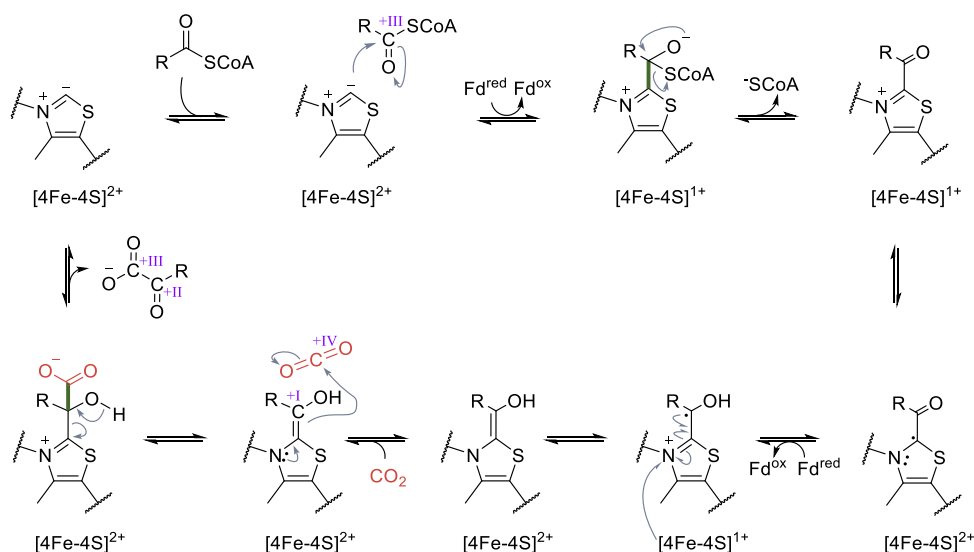
Scheme 7. Catalytic Cycle of Acetyl-CoA/Propionyl-CoA Carboxylases^a

^aChanges of the oxidation state of selected carbons are given in roman numerals. BC, biotin carboxylase; BCCP, biotin carboxyl carrier protein; CT, carboxytransferase.

Upon coordination of PEP to the Mg^{2+} as the first step in the catalytic cycle, three water molecules are released (Scheme 6). Next, bicarbonate enters the active site, triggering formation of a pyruvate enolate anion and carboxyphosphate via nucleophilic attack on the phosphate group of PEP. Carboxyphosphate is subsequently deprotonated by a conserved histidine, which is located on a flexible loop (Figure 2).^{33,51,108} Deprotonation causes elimination of the phosphate group producing CO_2 at the active site. As a last step, the enolate anion reacts with CO_2 , thereby forming oxaloacetate. During the reaction, CO_2 is located in a hydrophobic pocket excluding water from the active site and thereby suppressing unwanted protonation of the

reactive enolate.³³ Similarly, as in RuBisCO, the problem of reducing CO_2 without using external reductants is solved by oxidation of the substrate (Scheme 6). However, in contrast to RuBisCO, PEPC does not suffer from the competing oxygenation reaction due to the different mechanism of carboxylation, which requires bicarbonate to undergo a series of transformations before the carboxylation step occurs. Some of the required catalytic steps, such as the nucleophilic attack on the phosphate group of PEP, are impossible with O_2 as a substrate. As this step leads to formation of the reactive enolate while placing CO_2 in a hydrophobic pocket in close proximity to the reactive species, side reactions with oxygen and protons (from

Scheme 8. Catalytic Mechanism of Oxoacid:Ferredoxin Oxidoreductases; Oxidation States of Selected Carbons Are Highlighted in Roman Numerals



water) are strongly suppressed. The example of PEPC nicely illustrates how specificity for CO_2 can be achieved using enzyme mechanism as “gatekeeper”.

3.1.1.3. Acetyl-CoA Carboxylase (ACC) and Acetyl-CoA/Propionyl-CoA Carboxylase (ACPCC). Acetyl-CoA carboxylase (ACC) catalyzes the formation of malonyl-CoA, the first step in fatty acid biosynthesis and therefore ACC is found in many organisms.¹⁰⁹ ACC alone, however, is insufficient for autotrophic growth on CO_2 . A characteristic feature of organisms employing either the 3HP/4HB cycle or the 3HB bicycle (section 4.1.4) is that they express an acetyl-CoA/propionyl-CoA carboxylase (ACPCC), which shows similar activity with both acetyl-CoA and propionyl-CoA.^{54,110} While ACC in eukaryotes is a single polypeptide with three domains, ACC in prokaryotes is composed of two to four subunits.⁵⁶ The bifunctional ACPCC consists of three distinct subunits: the biotin carboxylase (BC), the carboxytransferase (CT), and the biotin carboxyl carrier protein (BCCP). In the first catalytic step, BC catalyzes formation of carboxyphosphate from bicarbonate and ATP (Scheme 7).⁵⁶ Carboxyphosphate is proposed to spontaneously decompose into CO_2 and phosphate. The phosphate then serves as a general base, deprotonating the biotin, which is subsequently carboxylated by reaction with CO_2 .³⁴ Therefore, by investing one ATP, the enzyme gains specificity by producing a high local concentration of CO_2 in the active site. This high local CO_2 concentration prevents unwanted side reactions such as protonation. The carboxylation of CoA esters occurs in the CT domain. Although the exact mechanism is unknown, it likely features an acetyl-CoA enolate or a carbanion, which attacks carboxybiotin to form malonyl-CoA or methylmalonyl-CoA as product. As in RuBisCO and PEPC, reduction of CO_2 is achieved by a formal oxidation of the substrate.

3.1.2. CO_2 -Converting Enzymes with External Reductant. **3.1.2.1. 2-Ketoglutarate:Ferredoxin Oxidoreductase (2KFOR) and Pyruvate:Ferredoxin Oxidoreductase (PFOR).** The enzymes 2-ketoglutarate:ferredoxin oxidoreductase (2KFOR) and pyruvate:ferredoxin oxidoreductase (PFOR) (also referred to as 2-ketoglutarate synthase and pyruvate synthase in literature) are very similar in many aspects and both belong to the family oxoacid:ferredoxin oxidoreductases.⁵⁸ Both

2KFOR and PFOR are thiamine pyrophosphate (TPP)-dependent enzymes that require ferredoxins as redox partners. They both use CoA esters as substrates and produce α -keto acids as products.

The first step in the reaction mechanism (Scheme 8) is the activation of TPP by deprotonation. After reduction of the enzyme's 4Fe-4S cluster by ferredoxin, TPP acts as nucleophile and attacks the CoA ester, forming a tetrahedral intermediate, which readily eliminates CoA. Concomitant electron transport from the 4Fe-4S cluster to the TPP intermediate results in formation of a TPP-centered radical intermediate. Reduction of the iron sulfur cluster by another ferredoxin triggers radical recombination resulting in formation of an intermediate, which can react with CO_2 . Deprotonation of the hydroxyl group leads to elimination of the product and regeneration of the resting state. The reaction mechanism of these TPP-dependent enzymes has been studied in detail, and intermediates along the reaction coordinate have been characterized spectroscopically^{36–38} and crystallographically (Figure 3).^{111,112} The reducing equivalents necessary to reduce CO_2 are transferred from ferredoxins.

3.1.2.2. Isocitrate Dehydrogenase (IDH). Isocitrate dehydrogenase (IDH) is a canonical enzyme of the TCA cycle. While all isocitrate dehydrogenases catalyze the oxidative decarboxylation of isocitrate, only some are able to catalyze the reductive carboxylation of 2-oxoglutarate.^{59,60} As an enzyme from core metabolism, IDH is present in all organisms and often several isoforms exist in the same host. In general, two classes of IDHs occur: the NAD^+ -dependent IDHs and the NADP^+ -dependent IDHs. While IDH is a well-studied enzyme, most reports focus on the decarboxylation reaction.

The mechanism of the reductive carboxylation catalyzed by IDH is shown in Scheme 9 and resembles to some extent the mechanism of RuBisCO. Similarly to RuBisCO, IDH contains a Mg^{2+} (or in some cases Mn^{2+}) ion in the active site which coordinates the enolate of 2-oxoglutarate in a bidentate fashion. The enolized substrate subsequently reacts with CO_2 to form the carboxylated 2-oxoacid oxalosuccinate. Finally, reduction of this intermediate by NAD(P)H yields isocitrate. Interestingly, the carboxylation step with concomitant formal reduction of the CO_2 occurs before the NAD(P)H is consumed. The external

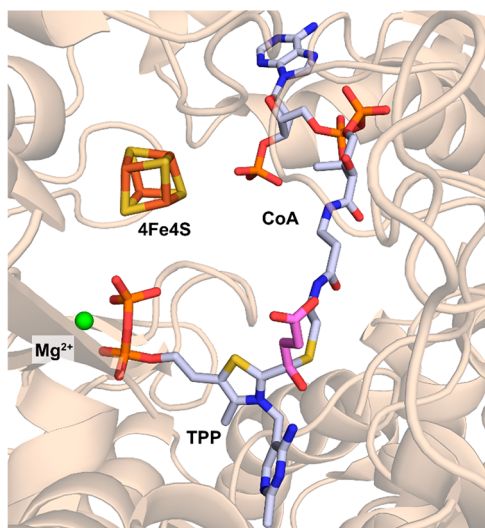
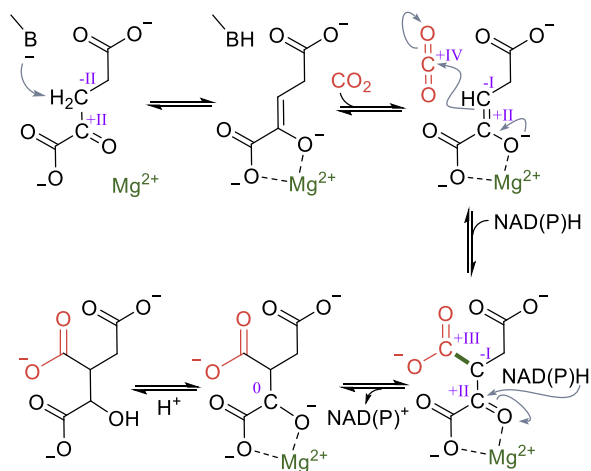


Figure 3. Active site of 2KFOR from *Magnetococcus marinus* with a TPP-bound succinyl-CoA intermediate present (PDB 6N2O). The carbon atoms of succinate are highlighted in pink.

Scheme 9. Catalytic Cycle of Isocitrate Dehydrogenase When Run in Reductive TCA Cycle; Changes of the Oxidation State of Selected Carbons Are Given in Roman Numerals



reductant is required for the final reduction of the α -keto acid functionality.

3.1.2.3. Glycine Cleavage System (GCS). The glycine cleavage system (GCS) catalyzes the reversible transformation of glycine, tetrahydrofolate (THF), and NAD^+ to the products 5,10-methylenetetrahydrofolate (5,10-mTHF), ammonia, NADH, and CO_2 .²⁴ When acting in the forward direction, the GCS generates NADH and 5,10-mTHF that is an essential intermediate in cellular C1 metabolism (section 5). In plants, the GCS is additionally involved in the recycling of 2PG, which is a side product produced by RuBisCO.⁹⁸ The GCS is a complex composed of four different proteins: the L-protein, the T-protein, the P-protein and the H-protein.²⁴ The H-protein is responsible for shuttling intermediates to the L-, T-, and P-protein and has a lipoic acid moiety that is covalently attached to a lysine residue (Figure 4). Besides its prevalent role in glycine and serine catabolism, natural⁶² and synthetic^{113–116} examples have recently highlighted that the GCS can operate in reverse to support autotrophic growth on C1 substrates.

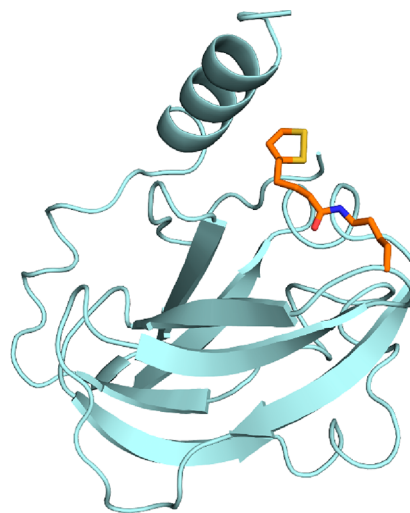


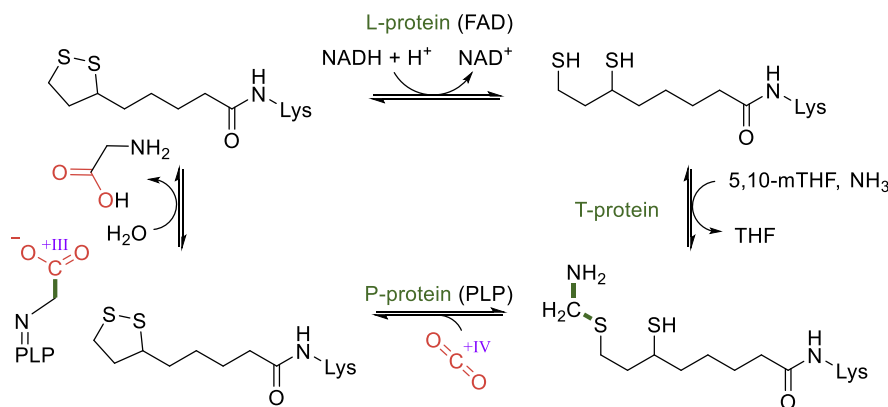
Figure 4. Crystal structure of the H-protein of the glycine cleavage system of *Pisum sativum* (PDB 1HPC) with the lipoic acid anchored to a lysine (highlighted in orange).

During autotrophic growth, the GCS needs to operate in the reverse direction.^{117–119} The catalytic cycle in this direction starts by the L-protein-catalyzed reduction of the H-protein's lipoic acid moiety using NADH (Scheme 10). Then, the T-protein catalyzes the reaction of the reduced lipoic acid with 5,10-mTHF and ammonia to form an aminomethyl lipoate intermediate.²⁴ Finally, the pyridoxal-5'-phosphate (PLP)-dependent P-protein catalyzes the reductive carboxylation step in which CO_2 is reduced, while the lipoic acid in the H-protein is reoxidized to form a disulfide. Recently, a detailed molecular dynamics-based study investigated the protection and T-protein-mediated release of the aminomethylation on the lipoate arm.¹²⁰ This provided crucial insights into the mechanisms responsible for guiding the reaction along the desired reaction trajectory and showed that aminomethylation release from the lipoate arm is the rate-limiting step of the GCS reaction.¹²⁰ Knowledge of the mechanisms and limitation of GCS can hopefully be leveraged for targeted engineering aiming to improve its carbon fixation potential.

3.1.2.4. Formate Dehydrogenase (FDH) and Formylmethanofuran Dehydrogenase (FMFDH). Formate dehydrogenase (FDH) and formylmethanofuran dehydrogenase (FMFDH) are the only known enzymes besides CO dehydrogenase (CODH, covered in the next section) that directly reduce CO_2 . While FDH catalyzes the reaction of CO_2 to formate, FMFDH first produces formate and then directly converts it to formylmethanofuran by channeling formate through a tunnel from one active site to the next.²⁷ FMFDH is found in methanogens, while FDH is found in acetogens. However, FDH is also present in other organisms, where it mainly catalyzes the oxidation of formate to CO_2 , thereby generating reducing equivalents. These can be used in formatotrophic growth using the reductive glycine pathway or the CBB cycle.

In general, two classes of FDHs exist: NAD^+ -dependent FDHs and metal-dependent FDHs. Under physiological conditions, NAD^+ -dependent FDHs can only operate in the oxidative direction, converting formate to CO_2 . Metal-dependent FDHs and FMFDHs contain molybdenum or tungsten metal centers.¹²¹ In metal-dependent FDH, the central molybdenum or tungsten atom is coordinated by six ligands: four sulfur atoms from two pyranopterin ligands, a sulfur or

Scheme 10. Mechanism of the Glycine Cleavage System; Changes of the Oxidation State of Selected Carbons Are Given in Roman Numerals.



selenium atom from a cysteine or selenocysteine, respectively, and another sulfido ligand (Figure 5).¹²² Although they usually

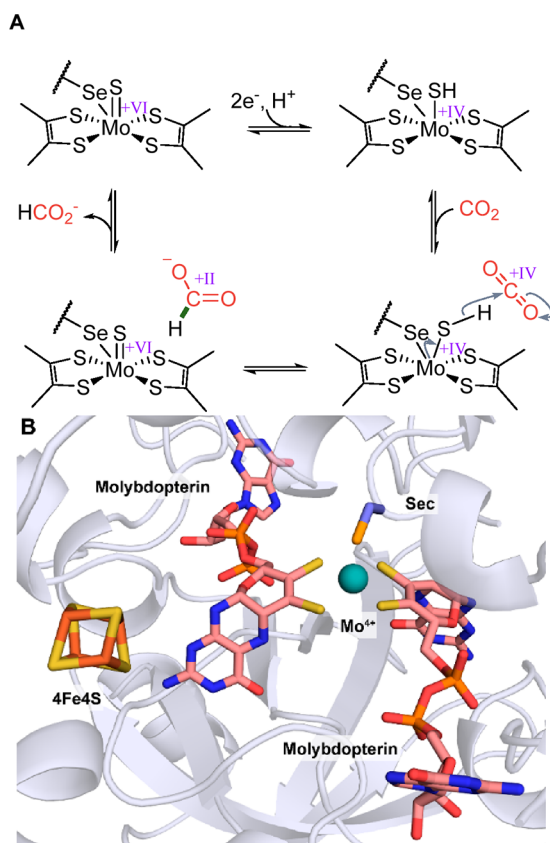


Figure 5. Molybdenum-dependent formate dehydrogenase (FDH). (A) Proposed catalytic cycle of molybdenum-dependent FDHs. (B) Active site of the reduced molybdenum-dependent FDH from *Escherichia coli* (PDB 1AA6).

more efficiently work in the oxidative direction, metal-dependent FDHs can reduce CO₂. Three options exist for metal-dependent FDHs to provide sufficient reducing power: they can either use ferredoxins only, ferredoxins in combination with NADPH using an electron bifurcation mechanism,^{123,124} or they directly use molecular hydrogen (hydrogen-dependent CO₂ reductases).^{125,126} Alternatively to using strong reducing agents, the enzymatic reaction can also be powered using electrochemical methods.^{127,128}

The currently proposed reaction mechanism for the CO₂ reduction catalyzed by the molybdenum-containing enzymes is shown representatively in Figure 5A and presumably works analogously in tungsten enzymes.^{129,130} First, the molybdenum center is reduced and the sulfido ligand is protonated forming a sulfohydride group. Next, CO₂ enters the active site. In a subsequent hydride transfer from the sulfohydride group to CO₂, formate is formed while the metal center is oxidized from Mo(IV) to Mo(VI). Although alternative mechanisms have been proposed, the mechanism shown in Figure 5A corroborates several important findings and therefore seems to be most plausible. First, it has been shown that the sulfido ligand is essential for activity,¹³¹ and *E. coli* has a dedicated cellular machinery composed of a cysteine desulfurase and a sulfur transferase to transfer the ligand into the active site.⁶⁵ Second, FDH efficiently catalyzes the oxidation of formate, however the C_α carbon of formate is not acidic. Therefore, mechanisms involving a proton transfer seem unlikely. Lastly, EPR studies have found that during formate oxidation the C_α hydrogen atom of formate is transferred to the coordination shell of molybdenum, as evidenced by a strong coupling of the hydrogen with the molybdenum metal center.^{64,66} These observations are consistent with formation of a sulfohydride intermediate.

3.1.2.5. CO Dehydrogenase (CODH). Two classes of CODHs are known: oxygen-sensitive nickel-iron [NiFe] CODHs and air-stable molybdenum-copper [MoCu] CODHs.²⁶ While both classes can oxidize CO, only [NiFe] CODHs are able to reduce CO₂, as the molybdenum-containing enzymes lack sufficient reducing power. The active site of the [NiFe] enzyme contains a modified 4Fe4S cluster where one iron atom is replaced with a nickel atom and an additional iron atom coordinates to a sulfur atom, forming a Ni4Fe4S complex as shown in Figure 6.⁶⁹

The catalytic cycle in the direction of CO₂ reduction starts with the transfer of two electrons from redox partners such as ferredoxins to the Ni4Fe4S cluster (Scheme 11). CO₂ subsequently binds to the active site nickel atom and the anionic species is stabilized via a hydrogen bond with a protonated histidine residue which is suggested to function as general acid/base.¹³² Next, water is eliminated and an intermediate bridging the iron and nickel is formed. Cleavage of a C–O bond results in formation of an intermediate, which has been determined to be a Ni(II) species. Upon dissociation of CO, the resting state is regenerated.²⁶

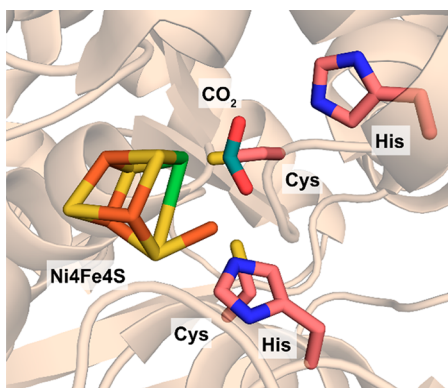
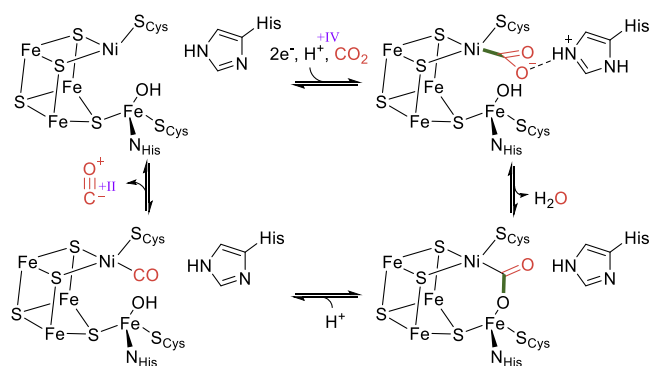


Figure 6. Active site of the [NiFe] CO dehydrogenase from *Carboxydotherrmus hydrogenoformans* with bound CO₂ (PDB 3B52).

Scheme 11. Catalytic Cycle of [NiFe] CO Dehydrogenases



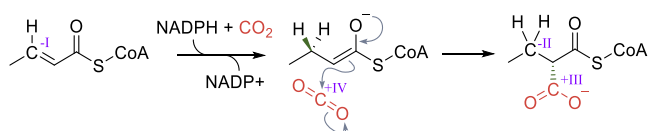
CODH directly reduces CO₂ using reducing equivalents supplied by the cell (e.g., ferredoxins). A major drawback of the direct reduction of CO₂ to CO is that CO itself is a very potent reducing agent. As a result, all CODHs catalyze the oxidation of CO more efficiently than the reverse reaction. For example, CODH from *Clostridium thermoaceticum* catalyzes CO oxidation with a k_{cat} of approximately 1500 s⁻¹, while the reduction of CO₂ is more than 2 orders of magnitude slower.⁶⁸ To circumvent this problem, CO production is tightly linked to production of acetyl-CoA by coupling CODH to acetyl-CoA synthase.^{133,134}

3.1.2.6. Enoyl-CoA Carboxylase/Reductase (ECR). Enoyl-CoA carboxylase/reductases (ECR) are not used in natural CO₂ fixation pathways but rather in a pathway that enables the carbon-positive assimilation of acetate, namely the ethylmalonyl-CoA pathway.⁶¹ Beyond their involvement in primary metabolism, members of the ECR family can additionally act in secondary metabolism for the production of unusual extender units for polyketide synthases.^{135,136}

Members of the ECR family are of interest, as they contain crotonyl-CoA carboxylase/reductase (CCR), the fastest known natural carboxylases (Table 1) and were used as the core enzymes for several non-natural CO₂ fixation cycles¹³⁷ (see section 4). CCRs catalyze the NADPH-dependent carboxylation of enoyl-CoA esters to produce alkyl-malonyl-CoA esters. In the absence of CO₂, CCRs catalyze the simple reduction of enoyl-CoA esters into the corresponding saturated CoA esters as a side reaction with up to 10% catalytic efficiency.

The first step in the reaction mechanism is a hydride transfer from pro-(4R)-NADPH to the *re*-face of the β -carbon of the enoyl-CoA ester, generating a nucleophilic enolate anion (Scheme 12).³² Thereafter, either CO₂ or a proton is added,

Scheme 12. Catalytic Cycle of Crotonyl-CoA Carboxylation by Crotonyl-CoA Carboxylase/Reductase



mainly in *anti*-fashion to the *re*-face at the α -carbon, to yield an alkyl-malonyl-CoA ester or a saturated CoA ester. Recent studies have shown in great detail that four amino acids: His, Asn, Glu, and Phe, form a CO₂-binding pocket in the active site of CCR, placing the gaseous substrate in close proximity to the enolate intermediate. The hydrophobic environment provided by the phenylalanine efficiently excludes water from the active site and therefore limits unwanted irreversible protonation of the enolate intermediate (Figure 7).¹³⁸ Furthermore, the active

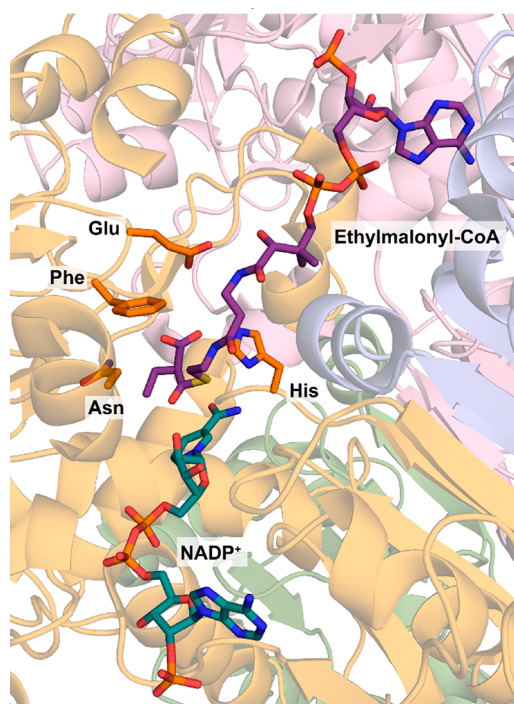
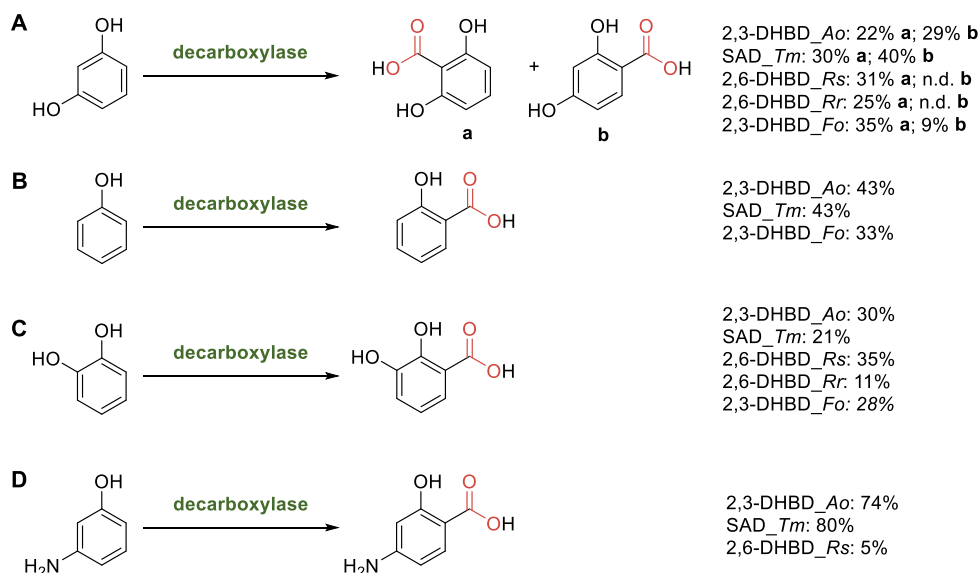


Figure 7. Active site of *Kitasatospora setae* crotonyl-CoA carboxylase/reductase (PDB 6OWE) with ethylmalonyl-CoA, the product of the carboxylation reaction, and NADP⁺ bound in the active site. Key active site residues necessary for accommodation of CO₂ (His, Asn, Phe, and Glu) are highlighted in orange.

sites of ECRs feature elements of “negative catalysis” that guide the reaction along a defined coordinate and prevent the formation of undesired side products.¹³⁹ In the enoyl-thioester reductase Etr1p, for example, a conserved threonine increases the energetic barrier to an alternative reaction coordinate and thus prevents the formation of an undesired covalent adduct between NADPH and the enoyl-CoA substrate.¹⁴⁰ Importantly, mutation of this conserved threonine only results in a minor loss of catalytic activity while the enzyme’s error rate is drastically increased. This suggests a role of this threonine as a catalytic gatekeeper that controls the accessibility of a given reaction coordinate with little influence on the energy barrier of the desired reaction.¹⁴²

Besides the mentioned inhibitory adduct, a different NADPH/enoyl-CoA thioester adduct has been observed when

Scheme 13. Enzymatic *ortho*-Carboxylation^a of (A) Resorcinol, (B) Phenol, (C) Catechol, and (D) *meta*-Aminophenol by Different Bivalent Metal-Dependent Decarboxylases^{142,152,158,164,167,170}



^aThe displayed numbers correspond to conversions to the respective product. n.d. = not determined or not found.

CO₂ was omitted from the reaction or when active site residues were mutated (so-called “C2-adduct”). This C2-adduct has been used extensively to probe the ECR’s catalytic cycle, and it was shown to be accepted by ECRs, where it directly serves as an activated species in carboxylation reactions.^{138,140,141} Thus, it was speculated that the C2-adduct serves as a storage form of the high-energy enolate when no resolving CO₂ electrophile is available. This mechanism could increase the overall reactivity of ECRs relative to other enolate-based carboxylases (such as RuBisCO), as it slows down the back-conversion of the activated enolate to the starting substrate.¹³⁸

3.2. Reversing Decarboxylases for CO₂ Fixation

Besides using natural carboxylases, another option to enzymatically incorporate CO₂ into molecules is by operating decarboxylases in the reverse direction.^{142–144} However, due to the lack of a strong thermodynamic driving force, decarboxylases require an excess of carboxylating source (CO₂ or bicarbonate) to shift the equilibrium toward the carboxylation side. Many of these biocatalysts operate in the secondary metabolism and/or detoxification. The robustness and broad substrate tolerance of several of these enzymes make them suitable for biocatalytic applications. Single enzyme systems have been developed for the enzymatic Kolbe–Schmitt reaction,^{12,145} among them prenylated flavin (prFMN) dependent (de)carboxylases,¹⁴⁶ bivalent metal-dependent (de)carboxylases, and cofactor-independent (de)carboxylases,¹⁰ including a new group of enzymes based on a catalytic dyad mechanism.¹⁴⁷ Furthermore, decarboxylases have been developed for the carboxylation of styrenes, polyaromatics, and heteroaromatic compounds. Recently, their synthetic applications have been reviewed by Leys et al.¹⁰ as well as Tomassi et al.¹¹ Here we focus on mechanistic and structural aspects. In addition, TPP-dependent keto acid decarboxylases have been applied in the reversed direction to produce α -keto acids from aldehydes and CO₂.^{39,148,149}

3.2.1. Bivalent Metal-Dependent (De)carboxylases.

Due to their broad substrate scope, dihydroxybenzoic acid decarboxylases (DHAD, also termed carboxyvanillate decar-

boxylases,¹⁵⁰ γ -resorcylic acid decarboxylases,¹⁵¹ salicylic acid decarboxylases,¹⁵² isoorotate decarboxylases,¹⁵³ or orsellinic acid decarboxylases¹⁵⁴) are a synthetically interesting class of catabolic decarboxylases.^{11,12,14} The enzyme family’s natural role is mostly the detoxification of phenolic acids via decarboxylation. However, native substrates have been identified in only a few cases.^{150,153} The intriguing feature of this enzyme class is that they also catalyze the carboxylation of phenols, forming phenolic acids, which represents a biochemical counterpart to the Kolbe–Schmitt reaction.¹⁴ In contrast to the Kolbe–Schmitt process, the enzyme class exhibits absolute selectivity for carboxylation at the *ortho*-position of phenolic substrates (and the reversed decarboxylation of the corresponding *o*-phenolic acid).^{11,12} An early example demonstrating the activity of a bivalent metal-dependent decarboxylase in the carboxylation direction was the formation of γ -resorcylic acid (2,6-dihydroxybenzoic acid) from resorcinol (1,3-dihydroxybenzene) applying 1 M KHCO₃[−], catalyzed by the 2,6-dihydroxybenzoic acid decarboxylase (2,6-DHBD_Rr) from *Rhizobium radiobacter* (cf. Scheme 13A).¹⁴²

The enzymes belong to the amidohydrolase family and share the superfamily’s characteristic (β/α)₈-TIM barrel fold. The catalytic activity of all characterized orthologues depends on a divalent metal ion, acting as a cofactor in the active site.^{11,12} Interestingly, the identity of this metal ion varies within the enzyme family and the individual enzymes tend to show high selectivity for their respective cofactor (Zn²⁺, Mn²⁺, and recently, Mg²⁺, have been described so far, compare Table 2).^{155,156}

Structural and mutational studies have identified a range of amino acids crucial for activity (Figure 8A). In all crystal structures, the metal cofactor is complexed by either three or four amino acids, as for example Glu8, His167, Asp293, and three water molecules in the case of the 2,3-DHBD_Ao from *Aspergillus oryzae*.¹⁵⁵ Mutation of these residues usually results in insoluble protein or diminished activity.^{165,170,172} Tight binding of the phenolic substrates is facilitated by hydrophobic interactions with amino acids such as phenylalanine or proline

Table 2. Bivalent Metal-Dependent (De)carboxylases

enzyme	source/organism	PDB	catalytic Asp	M ²⁺	substrate types	ref
2,3-dihydroxybenzoic acid decarboxylase (2,3-DHBD_Ao)	<i>Aspergillus oryzae</i>	7A19	Asp293	Mg ²⁺	phenols, resorcinols, catechols, naphthols, aminophenols, styrenes, coumaric acids and esters, phloretic acids, polyphenols	29,152,155,157–163
2,3-dihydroxybenzoic acid decarboxylase (2,3-DHBD_Fo)	<i>Fusarium oxysporum</i>	7BP1 (substrate bound)	Asp291	Zn ²⁺	phenols, resorcinols, catechols	164,165
2,6-dihydroxybenzoic acid decarboxylase (2,6-DHBD_Rs) ^c	<i>Rhizobium</i> sp. (MTP-10005)	2DVU (substrate bound)	Asp287	Zn ²⁺	phenols, resorcinols, catechols, naphthols, aminophenols, styrenes, coumaric esters, polyphenols	48,144,151,152,158,160,166
2,6-dihydroxybenzoic acid decarboxylase (2,6-DHBD_Ps)	<i>Polaromonas</i> sp. (JS666)	4QRO (inhibitor bound)	Asp287	Mn ²⁺	decarboxylation of γ -resorcylic acid and derivatives ^b	156
2,6-dihydroxybenzoic acid decarboxylase (2,6-DHBD_Rr) ^c	<i>Rhizobium radiobacter</i> WU-0108		Asp287 ^a	nd	phenols, resorcinols, catechols, polyphenols	142,167
salicylic acid decarboxylase (SAD_Tm)	<i>Trichosporon moniliforme</i>	6JQW	Asp298	Zn ²⁺	phenols, resorcinols, catechols, naphthols, aminophenols, styrenes, coumaric esters, polyphenols	152,158,160,168–170
5-carboxyvanillate decarboxylase (LigW_Sp)	<i>Sphingomonas paucimobilis</i> SYK-6	4ICM (substrate bound)	Asp296	Mn ²⁺	phenols, guaiacols, coumaric acids, phloretic acids	150,162,171,172
5-carboxyvanillate decarboxylase 2 (LigW2_Sp)	<i>Sphingomonas paucimobilis</i> SYK-6		Asp313 ^a	nd	phenols, guaiacols, coumaric acids, phloretic acids	150,162
5-carboxyvanillate decarboxylase (LigW_Na)	<i>Novosphingobium aromaticivorans</i>	4QRN (substrate bound)	Asp314	Mn ²⁺	decarboxylation of 5-carboxyvanillate ^b	172
iso-oroate decarboxylase (IDC_Cm)	<i>Corydopsis militaris</i> CM01	4HK5 (apo form)	Asp323	Mn ²⁺	decarboxylation of 5-carboxy-uracl ^b	153

^aBased on sequence alignment. ^bReaction in decarboxylation direction. ^cAlso: γ -resorcylic decarboxylase; nd = not determined.

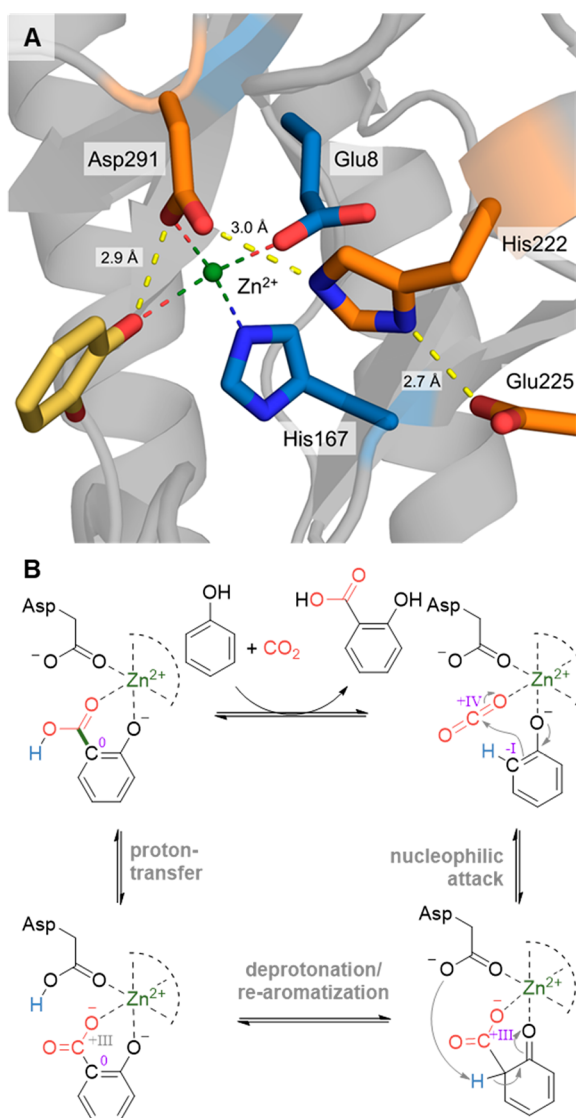


Figure 8. (A) View of the active site of the 2,3-DHBD_Fo from *Fusarium oxysporum*, bound substrate catechol (yellow). The catalytic Zn^{2+} is displayed as a green ball, and the complexing amino acids (Glu8, His167, and Asp291) and the catalytic triad (Asp291, His222, and Glu225) are displayed as sticks (PDB 7BP1).¹⁶⁵ (B) General mechanism of the (de)carboxylation of phenol by a bivalent metal-dependent decarboxylase (Zn^{2+} is shown as example and can be Mg^{2+} or Mn^{2+} in other enzymes).

(e.g., Phe27, Pro189, Phe193, and Phe294 in the case of 2,3-DHBD_Fo from *Fusarium oxysporum*),¹⁶⁵ and coordination of the hydroxy-group at the catalytic metal center. The residues, that perform the mechanistically crucial proton transfer (vide infra), are often arranged in a triad, consisting of asparagine, glutamine, and histidine (e.g., Asp293, His222, and Glu225 for 2,3-DHBD_Ao²⁹ or Asp291, His222, and Glu225 for DHBD_Fo¹⁶⁵). Mutation of these residues, for example in LigW_Sp (Asp296, His226, Glu229) lowered the enzyme's k_{cat} by several orders of magnitude.¹⁷²

While the mechanism of the decarboxylation reaction is well studied experimentally and by computational methods, the carboxylation reaction has only recently been investigated using quantum chemical calculations.^{29,30,155,172} In general, the steps resemble the electrophilic aromatic substitution mechanism of the Kolbe–Schmitt reaction: both CO_2 and the deprotonated

phenolic substrate bind to the bivalent metal in the active site (Figure 8B). The C–C bond is formed in a nucleophilic attack of the *ortho*-carbon onto CO_2 , resulting in a dearomatized intermediary cyclic dienone. Deprotonation of the *ortho*-position is performed by the catalytically-active Asp (Table 2) and accelerated by a His and Glu residue, which form a catalytic triad. This results in rearomatization of the intermediate, forming the deprotonated phenolic acid product bound as a chelate to the bivalent metal. Although in theory, the mechanism could feature first proton transfer followed by carboxylation, density functional theory (DFT) calculations (for both carboxylation and decarboxylation),^{29,156,173,174} and isotope labeling studies (for decarboxylation)¹⁷² suggest the displayed order of events.

The identity of the CO_2 -source that initially binds in the active site is still a matter of debate. While reactions under CO_2 -pressure point to bicarbonate (HCO_3^-),⁴⁸ recent quantum chemical investigations, paired with exact determinations of the CO_2 partial pressure in solution, came to the conclusion that CO_2 is the molecule that is utilized by the enzyme.²⁹ Furthermore, mass spectrometry provided evidence that the initial product of the decarboxylation reaction is CO_2 , rather than HCO_3^- .¹⁷⁴ However, the source of the carboxylate might be different for different enzymes.

Due to the uncomplicated setup, the majority of biocatalytic carboxylation reactions using this enzyme class are performed using bicarbonate salts (mostly the potassium salt but also others were evaluated¹⁶⁶) as a CO_2 source.^{152,162,164,166} High concentrations between 1 and 3 M are usually applied to drive the equilibrium. Note that such high bicarbonate concentrations either require exceptionally concentrated buffers, or are applied as unbuffered solution at its pH of 8.3.⁴⁸ Alternatively, the reaction is run by direct supply of CO_2 , either via bubbling¹⁷⁵ or at high pressure under CO_2 atmosphere.^{29,48,152,159,163} Note the addition of ascorbic acid allows suppression of spontaneous oxidation of resorcinol- and catechol-derivatives and therefore to run the reaction under air.⁴⁸

There is a small number of “classic” carboxylation substrates (Scheme 13) that most members of the enzyme family were characterized with, namely resorcinol (A), phenol (B), catechol (C), and *meta*-aminophenol (D).^{142,152,158,164,167,170} The second hydroxy group of the dihydroxybenzenes serves as additional handle, allowing better binding of the substrate in the active site. Due to its application as antituberculous agent, *para*-aminosalicylic acid (D), was identified early as a promising target compound.^{159,169,170}

The enzymes also carboxylate bulkier compounds such as naphthols, styrenes, *p*-coumaric acids, esters, and polyphenols.^{11,12} The minimal structural requirements for a substrate is a phenolic hydroxy group with an accessible *ortho*-position.¹² Table 2 gives a brief overview of generic substrate types that the individual enzymes have been characterized with.

Carboxylations catalyzed by metal dependent decarboxylases proceeded with absolute regioselectivity, with the exception of resorcinol, which is carboxylated at the two *ortho*-positions in roughly equal amounts (22% and 29%, respectively, Scheme 13A).¹⁵⁸

Although the enzymes are highly regiospecific, they accept a range of bulky substituents at the phenolic *ortho*- and *meta*-positions. A number of examples, including coumaric acid and ester, phloretic acid, the phenyl pyruvic ester, and even polyphenols such as resveratrol.^{160,162,167}

Table 3. Overview of Cofactor-Independent Decarboxylases

enzyme	source/organism	PDB	catalytic Glu	ref
phenolic acid decarboxylase (PAD_ <i>Lp</i>)	<i>Lactobacillus plantarium</i>	2W2A	Glu71	176,179,180
phenolic acid decarboxylase (PAD_ <i>Ba</i>)	<i>Bacillus amyloliquefaciens</i>			176,181
phenolic acid decarboxylase (PAD_ <i>Bl</i>)	<i>Bacillus licheniformis</i>			176
phenolic acid decarboxylase (PAD_ <i>Bs</i>)	<i>Bacillus subtilis</i>	2P8G (4ALB, Tyr19Ala)	Glu64	176,182,183
phenolic acid decarboxylase (PAD_ <i>Mc</i>)	<i>Mycobacterium colombiense</i>			176
phenolic acid decarboxylase (PAD_ <i>Ms</i>)	<i>Methylobacterium</i> sp.			176
phenolic acid decarboxylase (PAD_ <i>Ps</i>)	<i>Panteo</i> sp.			176
ferulic acid decarboxylase (FDC_ <i>Es</i>)	<i>Enterobacter</i> sp.	3NX1, 3NX2, 4UU3	Glu72	176,184

3.2.2. Cofactor-Independent (De)carboxylases. Phenolic acid decarboxylases (PADs) represent a further class of enzymes from secondary metabolism which have been successfully applied in biocatalytic carboxylation reactions.^{12,152,176} It is noteworthy that PADs do not require any cofactor or metal ion for catalysis. In nature, they are involved in the biodegradation of cinnamic acid derivatives such as ferulic, coumaric, and caffeic acids, the latter derived from the oxidative breakdown of lignin.^{177,178} Several enzymes from bacterial sources which share a sequence identity within a range of ~40–80% have been shown to be able to carboxylate *para*-hydroxystyrene derivatives regioselectively at the β -atom of the side chain to yield the corresponding cinnamic acid derivatives exclusively in (*E*)-configuration (Table 3).¹⁷⁶ In order to enable PADs to run the reaction in the reverse carboxylation direction, elevated concentrations of the CO₂ source such as bicarbonate are required.^{152,176}

In particular, the structure of the phenolic acid decarboxylase from *Bacillus subtilis* (Figure 9),¹⁸² combined with quantum

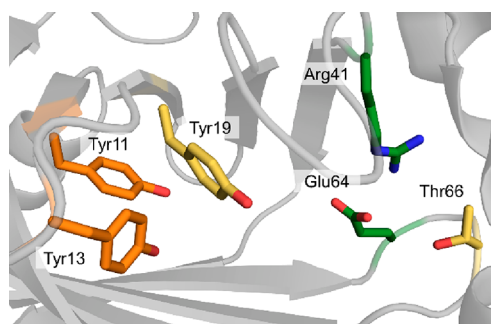


Figure 9. Active site of the phenolic acid decarboxylase from *Bacillus subtilis*. Amino acid residues involved in the hydrogen-bonding network of the substrate (Tyr11, Tyr13) and the carboxylating source (Tyr19, Tyr66) as well as the glutamate residue acting as the catalytically important general acid are displayed as sticks (PDB 2P8G).

chemical calculations using a large active site model (>300 atoms), has facilitated a detailed proposal of the reaction mechanism which proceeds via classical acid–base catalysis (Scheme 14).^{31,185} A highly conserved glutamate residue (e.g., Glu64 in PAD_*Bs*) acts as general acid, transferring a proton to bicarbonate to generate carbon dioxide as the actual carboxylating agent. Note that the reaction with CO₂ was calculated to be energetically much more feasible than the reaction with bicarbonate.³¹ The β -carbon atom of the styrene side chain then performs a nucleophilic attack on carbon dioxide to yield a quinone methide intermediate. This step is supported by two tyrosine residues (e.g., Tyr11, Tyr13 in PAD_*Bs*), which interact with the *para*-hydroxy group via hydrogen bonding. Reprotonation of the glutamate residue, which goes in hand with

the rearomatization, yields the final (*E*)-cinnamic acid derivatives.

Biocatalytic characterization studies (such as substrate scope, reaction conditions, etc.)^{166,176} were performed to evaluate the potential of phenolic acid decarboxylases as carboxylation tool. Compared to the regio-complementary *ortho*- and *para*-selective decarboxylases (see sections 3.2.1 and 3.2.3), PADs display a more limited substrate tolerance as well as a narrow operational window concerning the reaction parameters (substrate concentration, pH-, and temperature range). Their independence of a cofactor as well as the lack of alternative chemical methods for the side chain carboxylation of styrenes (except a Pd-catalyzed method for substituted 2-hydroxystyrenes)¹⁸⁶ are strong arguments for their consideration as biocatalytic carboxylation tool. However, potential styrene-type substrates need to fulfill various features in order to be accepted by enzyme candidates that have been characterized so far: A fully conjugated system along the substrate and a *para*-hydroxy group are both mandatory to facilitate the required resonance stabilization of the negative charge via the quinone methide intermediate (Figure 10).

Substituents in the position *ortho* to the hydroxy group are well tolerated independent of their electronic nature. Therefore, conversions up to 35%, in the case of the *ortho*-methoxy monosubstituted hydroxystyrene, were achieved.¹⁷⁶ Modification of the substitution pattern in the α - or β -position of the styrene side chain or replacing the catalytically relevant *para*-OH group (e.g., by H, Cl, OMe, NH₂), is not accepted and leads to a loss of enzymatic activity.

3.2.3. prFMN-Dependent (De)carboxylases. In the recent decades, a number of decarboxylases with intriguing reactivities have been characterized, catalyzing e.g., *para*-decarboxylation of phenolic carboxylic acids,¹⁸⁷ decarboxylations of polyaromatic hydrocarbons (PAHs),¹⁸⁸ and heteroaromatics.^{189,190} However, it took further research until these reactions and the underlying mechanisms were fully understood. After the discovery of prenylated FMN (prFMN) by Leys et al.¹⁹¹ in 2015, the cofactor was confirmed to be present in several other members of the UbiX-UbiD family and it was shown to be associated with decarboxylase function.^{35,146,192–194} The substrate scope of different subfamilies of prFMN-dependent decarboxylases is quite diverse (Scheme 15) and encompasses cinnamic acids (forming styrenes), phenolic carboxylic acids (forming phenols), and heteroaromatic carboxylic acids, (forming heteroaromatic molecules). Furthermore, these species are (de)carboxylated using distinct mechanisms, all involving covalent binding of the substrate to the cofactor. In order to provide a comparative overview of the action of these subclasses, this section is divided into further subsections, discussing the different enzymes side-by-side.

3.2.3.1. Prenylated FMN (prFMN) Biosynthesis and Maturation. In nature, the enzymes UbiX and UbiD are

Scheme 14. Catalytic Cycle of the Carboxylation, Catalyzed by Phenolic Acid Decarboxylases, Shown for *para*-Vinylphenol by a Cofactor-Independent Phenolic Acid Decarboxylase^{31,185}

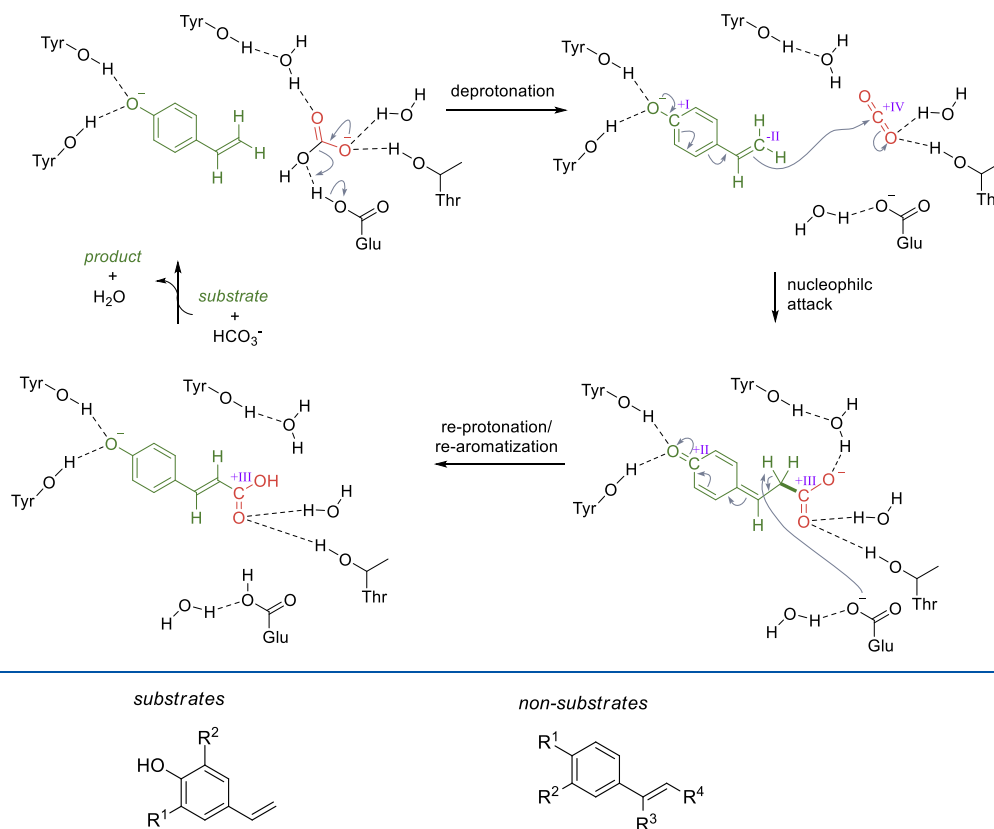
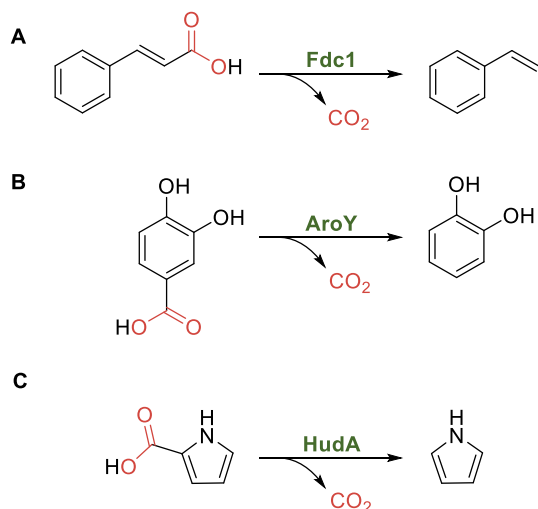


Figure 10. General substrate scope of the side chain carboxylation of styrene derivatives by phenolic acid decarboxylases.¹⁷⁶

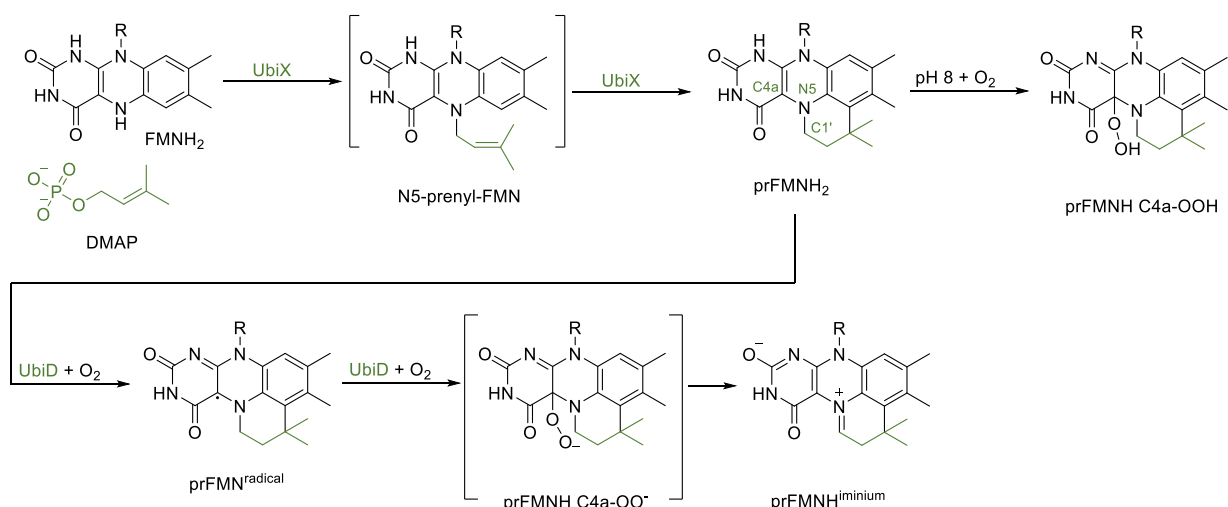
Scheme 15. Overview on prFMN-Dependent Decarboxylation Reactions: (A) Decarboxylation of Cinnamic Acids by Ferulic Acid Decarboxylases; (B) Decarboxylation of Phenolic Substrates by AroY Type Enzymes; (C) Decarboxylation of Heteroaromatic Substrates by Pyrrole-2-carboxylate Decarboxylase from *Pseudomonas aeruginosa*



involved in the biosynthesis of ubiquinone, a cofactor responsible for electron transport in proteobacteria and eukaryotes.¹⁹⁵ UbiX is a flavin prenyltransferase responsible for the prenylation of FMN by connecting a dimethylallyl moiety to FMN. This creates a fourth nonaromatic ring via a mechanism resembling class I terpene cyclases (Scheme 16).^{195–199} UbiD and its homologues in turn bind the prFMN cofactor in their active site, enabling reactions such as the decarboxylation of ferulic acid catalyzed by the UbiD homologue ferulic acid decarboxylase (Fdc).²⁰⁰ Note that PAD1 and Fdc are isofunctional to UbiX/UbiD.²⁰⁰

In detail, UbiX is a dodecameric metal-independent enzyme, with monomers that represent a typical Rossmann fold. FMN and two additional sulfate ions bind at the interface of two subunits.¹⁹⁷ UbiX utilizes either dimethylallyl monophosphate (DMAP) or dimethylallyl pyrophosphate (DMAPP) for the prenylation of N5, which is followed by an intramolecular Friedel–Crafts type alkylation of the flavin's C6.¹⁹⁸ Due to blocking of the cofactor's N5 position, the usual flavin chemistry as well as photocatalysis are not possible with prFMN.^{35,192}

The prFMNH₂ biosynthesized by UbiX binds to Fdc1, a fungal UbiD homologue.²⁰¹ In the enzyme, the cofactor is coordinated by the metal ions Mn²⁺ and K⁺ with its phosphate moiety.^{187,191} After binding, the cofactor requires oxidative maturation via a radical and a peroxo-species to produce the catalytically active iminium species (Scheme 16).^{194,198,199}

Scheme 16. Biosynthesis of the prFMN Cofactor (prFMNH₂) by the UbiX Enzyme^a

^aOxidative maturation of the bound cofactor is required to reach the catalytically active iminium form (prFMNH^{iminium}). Free prFMNH₂ in the presence of oxygen degrades to prFMN-hydroperoxide (prFMNH C4a-OOH).

Table 4. Selected prFMN Dependent Decarboxylases That Were Applied for Carboxylation

enzyme	source organism	PDB	substrate type	ref
ferulic acid decarboxylase (AnFdc)	<i>Aspergillus niger</i>	4ZA4 (prFMN in iminium form), 4ZA7 (with α -methyl cinnamic acid bound)	styrenes	191,211–213
phenolphosphate carboxylase ScFdc	<i>Thauera aromatica</i> <i>Saccharomyces cerevisiae</i>	4S13, 4ZAC (prFMN in iminium form)	phenolic compounds aryl and heteroaryl styrenes	18,80 212,214–217
HmfF	<i>Pelotomaculum thermopropionicum</i>	6H6X (with prFMN), 6H6V (with FMN)	heteroaromatic substrates	218
KpAroY AroY (3,4-dihydroxybenzoic acid/protocatechuic acid decarboxylase)	<i>Klebsiella pneumoniae</i> (<i>Aerobacter aerogenes</i>)	5O3M	catechols	187,219
EcAroY	<i>Enterobacter cloacae</i>	5O3N, 5NY5	catechols	187,220
VdcCD (vanillate and 4-hydroxybenzoate decarboxylases)	<i>Streptomyces</i> sp. D7		catechols	219
PYR2910	<i>Bacillus megaterium</i>		heteroaromatic substrates	190,221–224
PA0254 (HudA)	<i>Pseudomonas aeruginosa</i>	7ABN, 7ABO, 4IP2	heteroaromatic substrates	224,225
AnInD	<i>Arthrobacter nicotinanae</i> FI1612	7P9Q	heteroaromatic substrates	189,226
PhdA (phenazine decarboxylase)	<i>Mycobacterium fortuitum</i>		polyheteroaromatic substrates	227
PfFDDC	<i>Paraburkholderia fungorum</i> KK1		heteroaromatic substrates	228

Oxidation of unbound prFMNH₂ results in formation of prFMN-hydroperoxide, a dead-end species that does not assist in enzyme activity.²⁰² The catalytically active prFMNH^{iminium} cofactor is highly sensitive. For example, exposure to light causes tautomerization to the ketimine form inducing irreversible enzyme inactivation.²⁰³

In Fdc, Arg173 (*A. niger* nomenclature) is a key residue for cofactor maturation because mutation to alanine or lysine results in accumulation of a prFMN^{radical} species. Nevertheless, Arg173Ala displays low levels of activity, indicating that cofactor maturation still occurs, albeit significantly slower.²⁰³ As oxygen is required for prFMNH^{iminium} formation, its maturation mechanism for homologues active in anaerobic hosts needs to proceed via an alternative pathway that is independent of O₂. Fe²⁺ is suspected to play a pivotal role in anaerobic oxidative prFMN maturation.^{203–206}

Production of active UbiD requires either heterologous coexpression of UbiX and UbiD or reconstitution of apo-UbiD with prFMNH₂ and its subsequent activation. Several protocols for in vitro and in vivo FMN prenylation and maturation have been described.^{207–209}

3.2.3.2. Summary of Known prFMN-Dependent Decarboxylases with Confirmed Carboxylation Activity. In order to understand the evolutionary history of the prenylated cofactor, prFMN-dependent decarboxylases have been subjected to phylogenetic analysis.^{10,12,35,146,192} Shen et al. reported a phylogenetic tree containing more than 200 homologues of TtnD, a prFMN dependent decarboxylase acting in the tautomycin biosynthetic pathway. The analysis revealed three main clusters that fit to the enzyme's substrate specificities: decarboxylases acting on (i) aromatic carboxylic acids, (ii) cinnamic acids, and (iii) aliphatic α,β -unsaturated acids.²¹⁰ The

number of putative prFMN-dependent decarboxylases without confirmed prFMN cofactor is still immense. As this review focuses on CO₂ fixation, the following discussion will highlight enzymes, which not only perform decarboxylation reactions but also catalyze carboxylation reactions.

Table 4 presents a selection of characterized prFMN dependent decarboxylases that were tested for the reversible decarboxylation, along with their preferred substrate classes.

3.2.3.3. Structure and (De)carboxylation Mechanisms. UbiD and its homologues catalyze an impressive range of (de)carboxylation reactions with different mechanisms. The better described decarboxylation mechanisms are outlined in detail below, including, (i) the decarboxylation of cinnamic acids catalyzed by Fdc type enzymes, which proceeds via a 1,3-dipolar cycloaddition,^{25,191} (ii) the *para*-decarboxylation of phenolic substrates featuring an intermediate which covalently links the prFMN cofactor and the quinoid substrate,¹⁸⁷ and similarly, (iii) the decarboxylation of heteroaromatic carboxylic acids that proceeds via a substrate-prFMN intermediate formed in an electrophilic aromatic substitution, catalyzed by the HudA type enzymes.²²⁴

(i) **1,3-Dipolar Cycloaddition Catalyzed by Fdc Type Enzymes.** The (de)carboxylation of cinnamic acids catalyzed by Fdc type enzymes proceeds via a unique cycloaddition. First, the cinnamic acid substrate enters the active site with its carboxylic acid group pointing into the CO₂/Glu282 binding pocket. The substrate's C α is located 3.2 Å away from the prFMN C1' and the C β is in close proximity to the cofactor's C4a (3.4 Å) (Figure 11).²¹¹

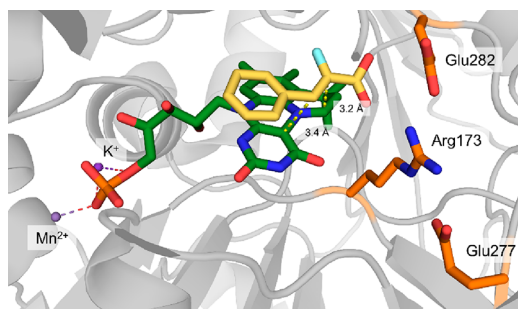


Figure 11. Crystal structure of the active site of Fdc1 from *A. niger* (PDB 4ZAB) with α -fluoro cinnamic acid (yellow). The substrate is positioned with its α -carbon near prFMN C1' and with its β -carbon on top of prFMN C4a. The residues Arg173, Glu277, and Glu282 (orange) constitute the catalytic triad.

After correct positioning of the substrate, a 1,3-dipolar cycloaddition of the substrate and the prFMN occurs, thereby forming a new cycle (Scheme 17).¹⁹¹ Subsequent decarboxylation leads to ring opening and strain release. CO₂ then leaves the active site and Glu282 can trigger protonation of the substrate leading to formation of another cyclic intermediate. Mutation of Glu282 to Gln causes loss of decarboxylation activity, while the Glu282Asp variant retains its activity. After protonation, the rate-limiting step, cycloelimination, happens using loss of ring strain as the driving force. Elimination results in product release and restoration of the prFMN cofactor.^{25,203,215,229} DFT calculations support the 1,3-dipolar cycloaddition mechanism and revealed α -hydroxycinnamic acid inhibition by keto–enol tautomerization.²¹³

The highly conserved RX_nEX₄(E/D) motif among UbiD family members, constituting the catalytic triad (e.g., Arg173,

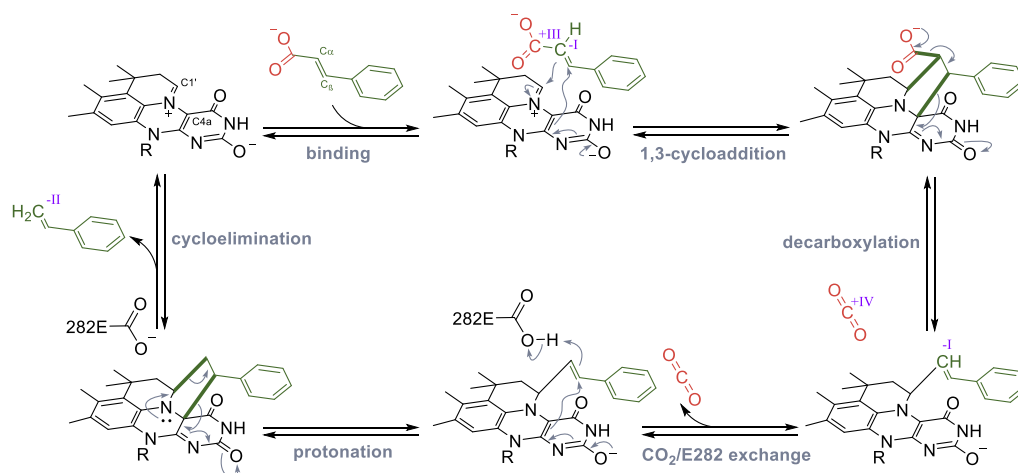
Glu277, and Glu282 in *A. niger*) is displayed in Figure 11. The active site of Fdc was found to be highly complementary to the substrate–prFMN^{iminium} complex, causing the cycloadduct products to experience considerable strain, which guarantees fast progress in the reaction. Reducing this strain by mutagenesis resulted in decreased reaction rates.^{25,203,229}

(ii) **Nucleophilic Attack of Phenolic Substrates, Forming a Covalent Bond between the Substrate Quinoid and prFMN by AroY-Type Enzymes.** In contrast to the dipolar cycloaddition, a distinct mechanism is proposed for AroY-type enzymes, involving a nucleophilic attack of the aromatic substrate on the C1' of the prFMN. In this group of enzymes, a cycloaddition mechanism is unlikely due to the high strain that would be generated in the intermediate.¹⁸⁷ In AroY, phenolic acid substrates are positioned in the active site with the substrate's nucleophilic α -carbon on top of the isoalloxazine's N5 atom. According to DFT calculations, Arg171 and Glu289 are in hydrogen bonding distance to the phenolic acid's carboxylate moiety. In addition, the residues Arg188, His327, Lys363, and His436 are involved in hydrogen bonding interactions with the hydroxy functional group of the catechol-type substrates. The additional hydroxy group on the substrate aids its correct orientation and plays a pivotal role in increasing the nucleophilicity of the substrate's α -carbon. After substrate binding, the reaction is proposed to proceed via nucleophilic attack to form a quinoid-like intermediate that is covalently bound to prFMN. This triggers decarboxylation, leading to a phenol intermediate that is covalently bound to the cofactor (Scheme 18). Finally, protonation, most likely mediated by Glu289 similar to the mechanism of Fdc from *A. niger*,¹⁸⁷ leads to elimination of the substrate from the cofactor. Besides mutation of the key amino acid residues highlighted in Figure 12, also substitution of Leu438, Glu223, His189, and Phe183 results in loss of decarboxylating activity, suggesting their involvement in catalysis. Overall, this mechanism closely resembles an electrophilic aromatic substitution with CO₂ being the leaving group.¹⁸⁷

(iii) **Nucleophilic Attack of Heteroaromatic Substrates on prFMN, via an Electrophilic Aromatic Substitution Catalyzed by the HudA Type Enzymes.** The pyrrole-2-carboxylate decarboxylase from *Pseudomonas aeruginosa* (HudA) accepts heteroaromatic compounds like pyrroles and furans as substrates. Decarboxylation is proposed to proceed via an electrophilic aromatic substitution on the pyrrole's C2 carbon, forming a Wheland-type intermediate with the pyrrole ring oriented parallel to the prFMN^{iminium} plane (Scheme 19).²²⁴

The enzyme was crystallized in two different conformations. While the apo-structure assumes an open conformation, cofactor and substrate binding induce structural changes leading to a more closed conformation. Similar results have been obtained in AnFdc.^{224,230} Imidazole is a competitive inhibitor, binding to residue Asn318 as seen in the crystal structure (Figure 13). Mutation of this residue to nonpolar amino acids causes a drop to very low conversions, which supposedly is a result of reduced cofactor binding.²³¹ Apart from the above-mentioned AnFdc and PaHudA crystal structures, most UbiD enzymes have been crystallized in the “open” state. In the case of AnInD, a hexameric light and oxygen sensitive indole-3-carboxylate decarboxylase from *Arthrobacter nicotinae*, small-angle X-ray scattering (SAXS) investigations revealed the existence of several open and closed conformations in solution.²²⁴

Scheme 17. Proposed Reaction Mechanism for Ferulic Acid Decarboxylases Decarboxylating Cinnamic Acid-Type Substrates Based on a Dipolar 1,3-Cycloaddition



Scheme 18. Proposed Reaction Mechanism for Decarboxylation of Phenolic Substrates by AroY-Type Enzymes

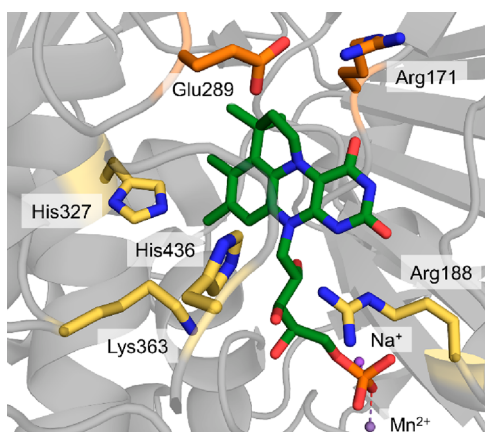
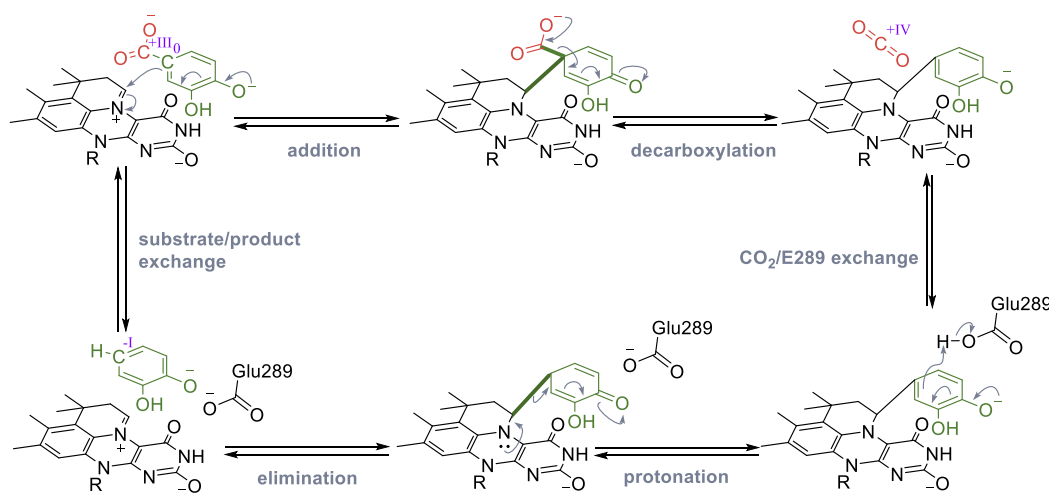


Figure 12. Crystal structure of EcAroY reconstituted with prFMN without substrate (PDB 5O3N). The amino acids marked in orange (Arg171, Glu289) contribute with hydrogen bonding to the substrate carboxylate moiety, and residues colored in yellow (Arg188, His327, Lys363, His436) are in hydrogen bonding proximity to the hydroxy group of the substrate according to DFT calculations.

3.2.3.4. Substrate Scope. The most studied prFMN-dependent enzymes are fungal ferulic acid decarboxylases,

namely the orthologue originating from *Aspergillus niger* (AnFdc) and its homologue from *Saccharomyces cerevisiae* (ScFdc), both able to catalyze the decarboxylation of structurally and electronically diverse styrenes. In contrast to phenolic acid decarboxylases (PADs), Fdcs do not require a *p*-hydroxy moiety, and substrates with weak electron-withdrawing and electron-donating substituents are generally well accepted. In addition to cinnamic acid derivatives, unsaturated aliphatic carboxylic acids are decarboxylated by Fdcs. Leys et al.²¹² summarized the structural substrate requirements to be an acrylic acid functionality connected to an expanded π -system, as for instance (hetero)aromatic moieties or further double bonds. In addition, the presence of strongly electron-donating groups decreases reaction rates and the (*E*)/(*Z*)-configuration of the unsaturated C=C bond has an influence on the outcome.²¹²

Several prFMN-dependent enzymes have been reported also to be able to run the reaction in the reverse carboxylation direction in the presence of an appropriate carbon dioxide source at elevated concentrations. A variety of aromatic compounds are accepted as substrates which are divided in: (A) styrene-type,^{211,212,214,217,232} (B) phenol-type,^{80,187,188,206,218,219,228,233–235} and (C) heteroaromatic substrates (Scheme 20).^{190,221,223,224,227} However, except for the carboxylation of the activated phenylphosphate substrate

Scheme 19. Proposed Electrophilic Aromatic Substitution for Decarboxylation via HudA-Type Enzymes

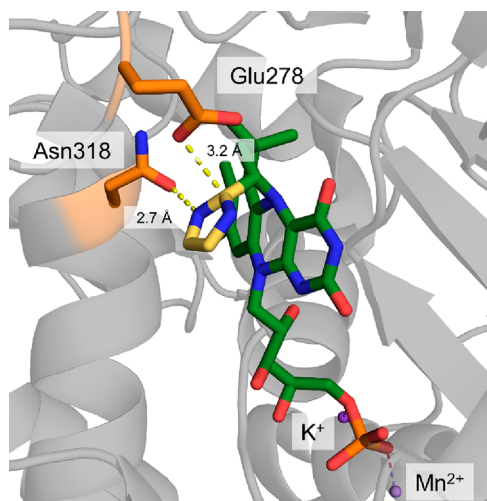
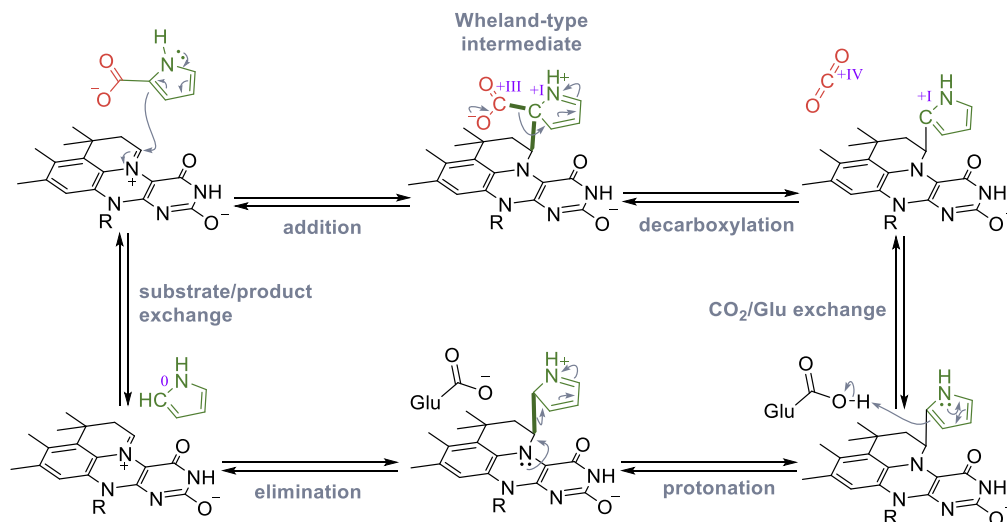


Figure 13. Crystal structure of pyrrole-2-carboxylic acid decarboxylase HudA from *Pseudomonas aeruginosa* with the reversible inhibitor imidazole bound in a covalent pFMN-imidazole adduct (PDB 7ABN). A key role is assigned to Glu278 and Asn318 in the decarboxylation of heteroaromatic compounds.

catalyzed by *T. aromatica* phenylphosphate carboxylase, which was well tolerated by the enzyme (99% conversion), only poor to moderate results in terms of carboxylation power were observed.

3.2.4. TPP-Dependent Keto Acid Decarboxylases. TPP-dependent keto acid decarboxylases such as pyruvate decarboxylase Pdc1 from *Saccharomyces cerevisiae*,^{148,236} phenylpyruvate decarboxylase Aro10 from *Saccharomyces cerevisiae*,²³⁷ and the branched-chain decarboxylase KdcA from *Lactococcus lactis*²³⁸ represent further examples of catabolic enzymes that are utilized as biocatalysts for the synthesis of valuable, industrially relevant products. By simply reversing the Ehrlich pathway, which in nature is responsible for the degradation of various amino acids,²³⁹ the latter are synthesized, starting from aldehydes. L-Methionine (L-Met) besides other amino acids (L-Leu, L-Ile) was obtained via a two-step enzymatic cascade.³⁹ In the case of L-Met, the cascade is initiated by the carboxylation of methional, to yield the corresponding α -keto acid intermediate, followed by a subsequent amination step catalyzed by either an amino acid

dehydrogenase or aminotransferase (Scheme 21A). The application of pressurized gaseous CO₂ (~2 bar) and the pull by the amine-forming enzyme are required to move the equilibrium of the energetically-unfavored carboxylation to the product side.³⁹ Scheme 21B displays the TPP-dependent mechanism for the natural decarboxylation reaction, involving an attack of the TPP on the keto acid, decarboxylation, protonation of the formed enol, and finally cleavage of the aldehyde from TPP. For details regarding the cascade, refer to section 4.3.³⁹

Furthermore, pyruvate decarboxylase from *Saccharomyces cerevisiae* was used for the carboxylation of acetaldehyde (100 μ M) to yield pyruvic acid (up to 81% conversion) using bicarbonate (500 mM, sodium carbonate buffer) as carboxylating source.¹⁴⁸

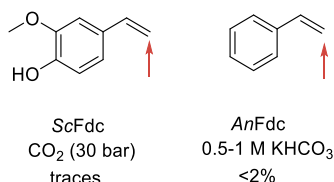
3.2.5. Decarboxylases from Tannin Degradation. Very recently, a new class of decarboxylases was discovered, which does not depend on a cofactor (compare the PADs discussed in section 3.2.2). The enzymes are involved in tannin degradation, converting gallic acid and protocatechuic acid to pyrogallol and catechol, respectively (Scheme 22).¹⁴⁷ AGDC1 from *Arxula adenivorans* and PPP2 from *Madurella mycetomatis* both form trimers and do not require any organic cofactor. Instead, the enzymes only rely on acid–base catalysis that facilitates the stabilization of the reaction's transition state. Each trimer contains one potassium ion, coordinated 3-fold by the Glu88-residue of each monomer, overall forming a distorted octahedral coordination.¹⁴⁷ Although this new group of nonoxidative decarboxylases remains to be investigated for carboxylation reactions, it holds great potential to further expand the substrate scope accessible to carboxylases.

3.3. Reaction Engineering of Enzymatic Carboxylation Reactions

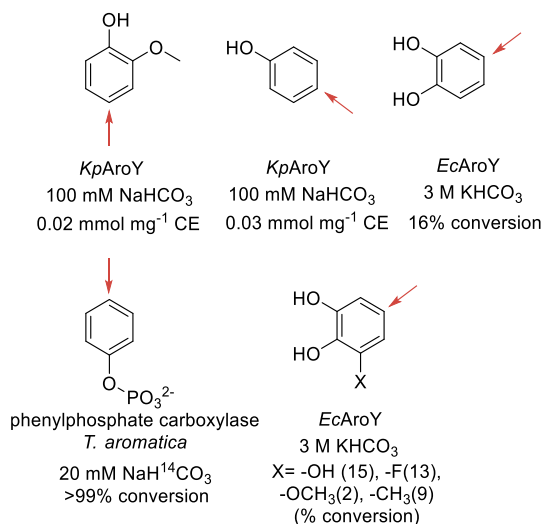
Many of the discussed enzymatic carboxylation reactions suffer from low productivities and incomplete conversions, mostly due to the high amount of energy that is required to utilize CO₂ (vide supra). Nature overcomes this issue by using cofactors to provide reaction energy, such as NAD(P)H and ATP (compare section 2).¹⁴ However, in case ATP- or NAD(P)H-dependent enzymes are applied in biotechnology or synthesis, recycling of the costly cofactors by dedicated cofactor regeneration systems, either in vivo or in vitro, becomes crucial to render the process

Scheme 20. Substrates That Were Accepted for Carboxylation by prFMN-Dependent Enzymes^a

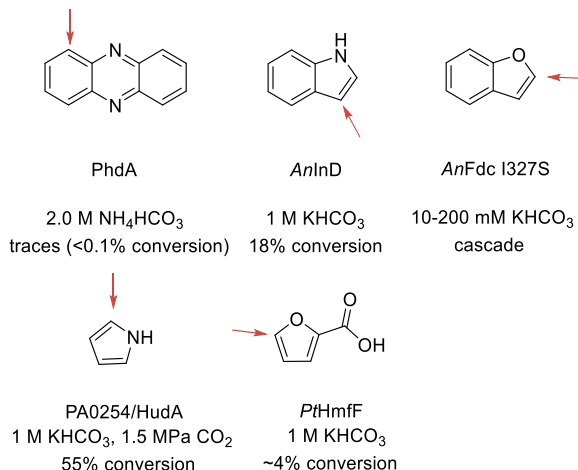
A) Styrenes



B) Phenolic substrates



C) (Poly)heteroaromatic substrates



^aRed arrows indicate the position of carboxylation.^{80,187,189,211,212,218,219,224,227} For each substrate the carboxylating enzyme, the carboxylating agent and the results in terms of carboxylation activity indicated by conversion are shown (see also Table 4).

to give a more general overview of such methods and puts them in the context of reaction engineering.

In general, enzymatic carboxylations offer several opportunities for reaction engineering (Scheme 23), including (i) supply of CO₂ in order to push the equilibrium, (ii) removal of the carboxylation product from the reaction (equilibrium) to exert a pull force onto the reaction, e.g., via the addition of further enzymes in a cascade reaction (compare section 4.1) or in situ product removal methods (ISPR), (iii) improving the catalyst itself via enzyme engineering or immobilization, and (iv) optimization of reaction conditions such as pH, temperature, buffer composition, and other related parameters, including the regeneration of cofactors.

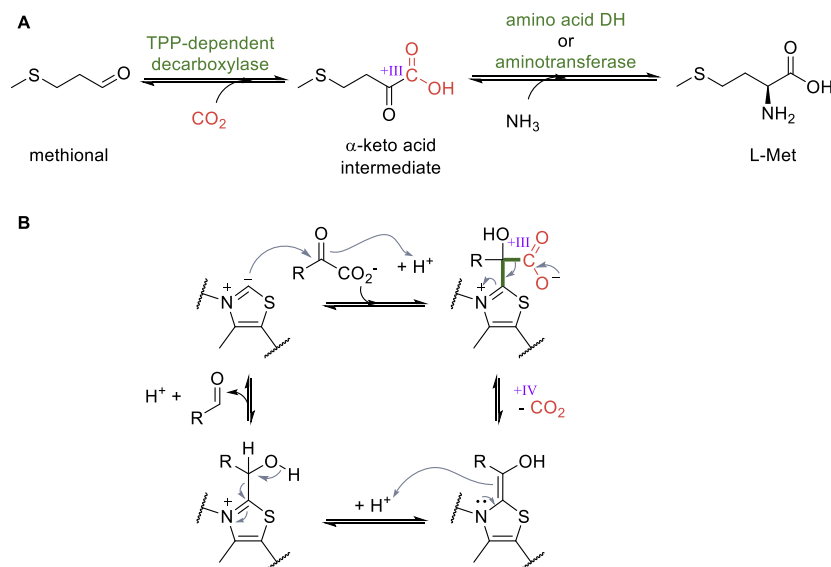
3.3.1. CO₂ Source. For many carboxylases and reversed decarboxylases, it is still unclear whether dissolved CO₂ (aq), or bicarbonate is utilized by the enzyme.^{9,12} As the different species contributing to the total CO₂ concentration (CO₂ (total)) are in equilibrium, the identification of the carboxylation cosubstrate is not straightforward and often computational methods in combination with kinetic measurements are used to investigate which species initially binds in the active site.^{29,30,48} For carboxylations, reaction rates are often measured at different bicarbonate concentrations and compared to results obtained under CO₂ atmosphere at different pressures.^{39,48,163} However, due to the fast interconversion of the different species contributing to CO₂ (total) (i.e., CO₂ (g), CO₂ (aq), HCO₃⁻, CO₃²⁻, cf. Scheme 23), such experiments often lead to ambiguous results. For reaction engineering, the spontaneous interconversion of the different CO₂ species is beneficial, as it enables both bicarbonate and CO₂ (g) to be used as carboxylation agent.

Bicarbonate is usually used in concentrations greater than 1 M (up to saturation at approximately 3 M) (refs 9, 148, 152, 162, 164, 166, and 187). Increasing the concentration of bicarbonate has been shown to improve the free energy of the transformation.²⁹ Evaluation of different bicarbonate sources revealed similar performance, as long as the counterion is not too chaotropic in the Hofmeister series. Following this trend, K⁺, Na⁺, Cs⁺, bicarbonate based ionic liquids, and quaternary amines such as NH₄⁺ or choline are well accepted by bivalent metal dependent decarboxylases and phenolic acid decarboxylases.^{159,166}

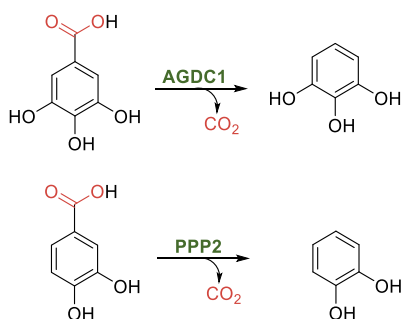
An attractive option to supply a carboxylation reaction with CO₂ is adding it directly as gas, either by applying pressure or a gas stream.^{9,10,12,39} Increasing CO₂ pressure goes in hand with an increased CO₂ solubility (e.g., 0.04 mol L⁻¹ at 1 bar, 0.7 mol L⁻¹ at 25 bar; 1.13 mol L⁻¹ at 50 bar, and 1.5 mol L⁻¹ at 100 bar, all at 20 °C),²⁴⁰ while higher temperatures lead to a decreased solubility (e.g., 0.9 mol L⁻¹ at 12.4 °C, 0.7 mol L⁻¹ at 20 °C, 0.6 mol L⁻¹ at 31.04 °C, 0.5 mol L⁻¹ at 40 °C, all at 25 bar).²⁴⁰ Note that different concentrations of CO₂ lead to varying concentrations of bicarbonate, resulting in a change of pH at different pressures. While some carboxylases have been reported to be irreversibly deactivated at higher pressure,¹⁶³ others tolerate pressures greater than 80 bar,^{159,187} which allows application of supercritical CO₂ for carboxylations.^{10,48,79,241–243}

Methods applied for CO₂ capture and storage can be used to increase the effective concentration of CO₂ in solution for biocatalytic applications. For example, aqueous medium can be exchanged or supplemented by solvents that dissolve higher concentrations of CO₂ (e.g., 2-(isopropylamino)ethanol and 2-amino-2-methyl-1-propanol).^{166,241} Alternatively, amines can be used to capture CO₂ in the form of ammonium bicarbonate

economically feasible. In contrast, the equilibrium of cofactor-independent carboxylases is often shifted to the product side by supplying the CO₂-source (often bicarbonate) in large excess (compare section 3.3.1).^{10,12} While the strategies for pushing the equilibrium of enzymatic carboxylation reactions are discussed in a recent review in great detail,¹⁰ this section aims

Scheme 21. Application of TPP-Dependent Decarboxylases for Carboxylations^a

^a(A) Two-step enzymatic cascade towards the synthesis of L-Met starting from methional via a carboxylation and subsequent amination step. (B) Catalytic cycle of the decarboxylation of keto acids by TPP-dependent decarboxylases.

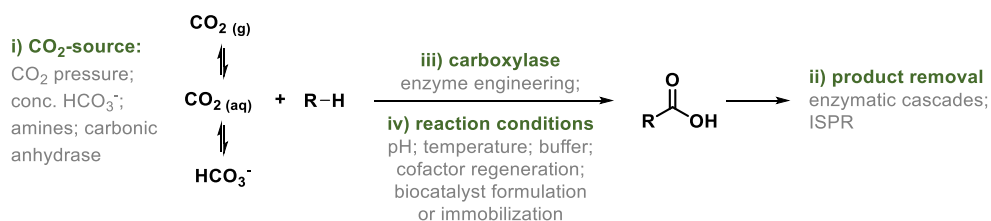
Scheme 22. Decarboxylation of Gallic Acid and Protocatechuic Acid by the Two Fungal Enzymes AGDC1 and PPP2¹⁴⁷

salts. A range of different primary-, secondary-, and tertiary amines have been applied to sequester $\text{CO}_{2(\text{g})}$ serving as substrate for 2,3-DHBD_Ao, a bivalent metal-dependent decarboxylase.¹⁵⁹ Carbon dioxide was provided either under pressure (50 bar) or at atmospheric pressure via bubbling aeration. In both cases, the sequestering amine was added in a concentration of up to 1 M.¹⁵⁹ In a follow up study, the system was further extended to supplying CO_2 as very fine bubbles using small diameter spargers in the presence of 3 M triethylamine for CO_2 sequestration. This method provides CO_2 with a high volume-specific surface area and therefore increases mass transfer, which allowed reaching of 26% conversion of catechol to the corresponding carboxylate, using the enzyme 2,6-

DHBD_Rs and a substrate loading of 80 mM.¹⁷⁵ An attractive alternative to batch carboxylation reactions, is running the reactions in continuous flow. Similar to batch, it is possible using this technology to provide CO_2 at high pressure. In an exemplary process, pyrrole was carboxylated to pyrrole-2-carboxylate at a pressure of 65 bar and a flow rate of 1.5 mL min^{-1} , using the immobilized carboxylase from *B. megaterium* (PYR2910). The final process achieved a space-time yield of $24 \pm 7 \mu\text{mol h}^{-1}$, which is a 25-fold improvement over the corresponding batch protocol.²²³ In another example, utilizing immobilized RuBisCO, HCO_3^- was applied as carbon source in continuous flow.²⁴⁴

Carbonic anhydrases (CAs) belong to the fastest known enzymes and accelerate the interconversion of bicarbonate and CO_2 from approximately 10^{-2} s^{-1} (spontaneous) to a turnover frequency of up to 10^6 s^{-1} .²³ This is beneficial for both enzymes utilizing CO_2 and enzymes utilizing bicarbonate, as the concentrations of the preferred carboxylation source is kept constant due the fast CA catalyzed equilibration. While CA is found in many organisms, functioning for example in pH regulation, CA has a particularly interesting function in photosynthetic bacteria. There, CA is colocalized in the carboxysome, a carbon concentration mechanism that evolved to increase the local CO_2 concentrations around RuBisCO, thereby effectively suppressing the oxygenase side reaction.²⁴⁵ For enzymatic applications, CAs have been used to improve the enzymatic reduction of CO_2 to formate using formate dehydrogenases,^{246,247} they improved the carboxylation activity of a phosphoenolpyruvate carboxylase,²⁴⁸ and they are even

Scheme 23. Reaction Engineering of Biocatalytic Carboxylation Processes



beneficial in multienzymatic systems that convert carbon dioxide to methanol.^{249,248} In contrast, only little effect was found, when CA was combined with bivalent metal-dependent decarboxylases, suggesting that the availability of the mechanistically relevant carboxylation source was not rate determining in this setup.^{10,152}

3.3.2. Product Removal. An efficient way to exert an external driving force onto an enzymatic reaction system is the removal of the formed product by an additional (irreversible) reaction. Owing to the fact that biocatalysts usually require similar reaction conditions, the addition of a subsequent enzymatic step to a carboxylation reaction is often straightforward and mirrors nature's CO₂ fixation strategies, where carboxylation reactions are part of biosynthetic pathways or cycles.^{10,12,15,137,250–256} The efficiency of a reaction can be evaluated from a thermodynamic point of view by estimating the Gibbs free energy demand of the individual reactions. Dedicated tools allow to calculate the ΔG of small cascades and even entire pathways at physiological or process conditions and therefore to evaluate their thermodynamic feasibility.⁴²

Enzymatic reactions that are applied for product removal either directly functionalize the newly formed carboxylate moiety or derivatize one of the product's substituents that is mechanistically relevant in the (de)carboxylation.^{10,137,253,255} An example for the first case is the application of carboxylic acid reductases and other enzymes for the further conversion of cinnamic acids or aromatic acids, that were produced via carboxylation reactions catalyzed by ferulic acid decarboxylase from *Aspergillus niger* (AnFdc) and its variants.²¹¹ The removal of the produced carboxylic acids from the equilibrium via this cascade allowed reduction of the required excess of bicarbonate and to overall increase the conversions from below 15%¹⁸⁷ (without the cascade) to conversions that are greater than 90%.²¹¹ An example for the latter case is methionine synthesis by a sequence of carboxylation and amination. Carboxylation is performed using a TPP-dependent branched-chain decarboxylase, and amination is catalyzed by a transaminase or an amino acid dehydrogenase. The amination of the α -keto moiety of the carboxylation product converts it into a nonsubstrate for the decarboxylase, making the reaction irreversible and yielding the desired methionine in 40% conversion.³⁹ Similar processes are further discussed in section 4.3.

Alternatives to the mentioned enzymatic systems are chemical derivatization or scavenging of the carboxylation products, i.e., by ISPR. One option is the use of dedicated adsorbents for binding/desorption cycles of the carboxylation products.¹⁶¹ Such a system has been developed using the anion exchange resin Dowex 1 \times 2 (Cl) for adsorption of 2,6-dihydroxy-4-methylbenzoic acid produced via carboxylation of orcinol, using the decarboxylase from *Aspergillus oryzae* (2,3-DHBD_Ao). The method was used at a 400 mL scale and produced 878 mg of highly pure product requiring no additional purification steps.¹⁶¹

Chemical modification of carboxylation products was required to assay the off-equilibrium acetyl-CoA carboxylation activity of the PFOR from *Desulfovibrio africanus* and *Sulfolobus acidocaldarius*.⁴⁷ The energetic barrier for carboxylation was overcome by derivatization of the generated pyruvate with semicarbazide, forming pyruvate semicarbazone.⁴⁷ The reduced ferredoxins required by PFOR as electron carrier, were regenerated using a photobiocatalytic system.

An alternative ISPR was developed by capitalizing on the fact that some benzoic acid derivatives form insoluble salts with quaternary ammonium counterions.²⁵⁷ Thus, these salts can be

used to precipitate the carboxylation products and therefore remove them from the reaction equilibrium. A systematic evaluation of different quaternary ammonium salts for the precipitation of 2,4-dihydroxybenzoic acid via carboxylation of resorcinol at 10 mM concentration, identified tetrabutylammonium bromide as an ideal supplement. Adding 50 mM of this salt, allowed increasing of the conversion from 37% (no salt) to 97% using the decarboxylase 2,6-DHBD_Rs. Interestingly, precipitation is selective for the target product acid and the regio-isomer was not found.²⁵⁷ However, choosing the precipitation agent is nontrivial, as different benzoic acids require different ammonium salts. For example, in contrast to 2,4-dihydroxybenzoic acid, precipitation of 1,2-dihydroxybenzoic acid required dodecyltrimethylbenzylammonium counterions.²⁵⁷ Importantly, product precipitation can also be combined with other methods to increase conversion. Combining tetrabutylammonium bromide as precipitation agent, together with trimethylamine for CO₂ sequestration, allowed increase the carboxylation yield of an 80 mM solution of resorcinol from 7% to 43%. However, elevated triethylamine concentrations also increased the solubility of the precipitated salts requiring further reaction optimization.^{257,258}

3.3.3. Engineering of the Biocatalyst. One of the most straightforward methods to improve a biocatalytic process is direct engineering of the catalyst itself. However, enzyme engineering can only change the kinetics of the catalyzed reaction and has no effect on the reaction's thermodynamics. Especially carboxylation reactions often reach equilibrium and enzyme engineering cannot influence conversion beyond this point, as the forward and reverse reactions are equally fast. However, generating variants of carboxylases allowed to increase their stability, activity, and to broaden their substrate scope. The most prominent example by far is RuBisCO, as a tremendous amount of mutational studies, including directed evolution approaches, have targeted the enzyme with the goal to increase its activity or its specificity toward CO₂.^{9,49,259,260} Besides acceleration of their catalytic function, the substrate scope of enzymes can be altered using enzyme engineering. In an impressive example, a minimal carboxylation activity of a biotin-independent propionyl-CoA carboxylase from *Methylobacterium extorquens* toward glycoyl-CoA was increased more than 50-fold by rational design paired with directed evolution.⁵⁵ Likewise, a double mutation of the enzyme SAD_Tm (Y64T-F195Y) fine-tuned the active site for better binding and higher activity toward the substrate *para*-aminosalicylic acid (cf. Scheme 13).^{169,170} In some cases, enzymes that previously exhibited completely different functions can be modified to perform carboxylation reactions. Recently, the latent carboxylation activity of the propionyl-CoA synthase from *Erythrobacter* sp. NAP1, as well as the promiscuous carboxylase activity of an acrylyl-CoA reductase from *Nitrosopumilus maritimus*, were improved to synthetically relevant levels using rational design.⁴⁶

Studies such as the latter one underline that rational engineering involving careful studies of the enzyme's mechanism and structure still is an efficient way to create beneficial variants. However, high-throughput and computational methods are on the verge of being broadly applicable and will solve many challenges in enzyme engineering.^{261–264} Note, that within this review, the most important variants of the individual enzyme classes are discussed in their respective subsections.

3.3.4. Optimization of the Reaction Conditions and the Formulation of the Biocatalyst. Identification of the ideal reaction conditions is crucial, especially for enzymatic

reactions, as the operational window of enzymes is usually quite narrow, i.e., biocatalysts often do not tolerate extreme temperatures, solvent concentrations, pH values, or pressure. In case several enzymes are combined into a reaction cascade, either a good compromise of the individual catalysts preferred reaction conditions has to be found, or the cascade is performed in a stepwise fashion, by sequential addition of catalysts (see section 4.2). Besides the obligatory checks for the ideal reaction temperature, pH, and buffer composition, some parameters are of special interest for carboxylases, including the supply and form of the carboxylation source (for details, see discussion in section 3.3.1).

As the formulation of the biocatalyst significantly affects the applicable reaction conditions, this parameter must be especially considered. Enzymes can be provided as living cells (in vivo), as purified enzymes, or in any formulation in between, including their application as resting cells, lyophilized whole cells and cell-free extracts. By using methods of immobilization, enzymes can be covalently or noncovalently attached to a solid support. These different formulations affect the catalyst's stability (total turnover numbers, e.g. at different temperatures or levels of cosolvent) and activity (turnover number).

Decarboxylases are often produced in *E. coli* and applied as cell-free lysates. If the cell's background does not interfere with the catalyzed reaction, purification is only required for mechanistic investigations and kinetic experiments.^{11,12} For more complex systems, such as artificial synthetic pathways, purified enzymes are used in most cases in order to minimize side reactivities and to allow for careful balancing of the individual enzymatic activities.^{137,253–255} As a special case, enzymes from the UbiD family depend on the prenylated FMN cofactor. Their heterologous expression requires a host that is able to catalyze formation and maturation of this cofactor (e.g., *E. coli*).¹⁸⁷

Whereas the immobilization of CA has been applied in larger scale,²³ only few carboxylases have been immobilized yet. Immobilization often increases enzyme stability, but more importantly, it also allows enzyme recovery and reuse by simple filtration. Immobilization strategies range from covalent immobilization over the use of adsorbents to encapsulation/entrapment methods.^{265–267} However, the outcome of a specific immobilization method is often unpredictable, and different immobilization conditions and methods need to be evaluated empirically. For example, for the immobilization of the Mn²⁺-dependent phenylphosphate carboxylase from *Thauera aromatica*, several supports, including zeolites, pumice, and polyacrylamide, were tried unsuccessfully. Finally, using low-melting agar as support yielded an active preparation that was stable for more than one week.¹⁸ The carboxylase from *B. megaterium* (PYR2910) was adsorbed onto a polyallylamine ion-exchange resin to allow its application as stationary phase in a continuous flow process.²²³ Another example is the immobilization of an acetyl-coenzyme A carboxylase on sepharose.²⁶⁸ RuBisCO from spinach leaves was covalently immobilized on a nylon membrane and on agarose²⁶⁹ or on polydopamine and further applied in a microfluidic reactor.²⁴⁴ Also, the coimmobilization of carboxylases, together with other enzymes forming an enzymatic cascade, has been explored. The cascade, catalyzing the formation of ribulose 1,5-bisphosphate either from ribose-5-phosphate or glucose, and its subsequent carboxylation by RuBisCO, was immobilized on self-assembled synthetic amphiphilic peptide nanostructures.²⁷⁰ In another example, CA and phosphoenolpyruvate decarboxylase covalently coim-

mobilized on microbeads were applied to produce oxaloacetate from PEP and could be reused up to 20 times without a reduction of activity.²⁷¹ Similar coimmobilization strategies have been repeatedly applied to entrap FDH together with other enzymes to form enzymatic cascades for converting CO₂ to methanol.^{272,273} Immobilization methods also allow the linkage of redox enzymes to electrodes, facilitating direct electron transfer. In one study, ferredoxin-NADP⁺ reductase from *Synechococcus* sp. and crotonyl-CoA carboxylase/reductase from *Methylobacterium extorquens* were coimmobilized on a glassy carbon electrode in a viologen-modified hydrogel.²⁷⁴ Viologen facilitates electron transfer from the electrode to the ferredoxin, which regenerates NADPH that in turn is consumed by the carboxylase. This system, producing ethylmalonyl-CoA from crotonyl-CoA, reached a total turnover number of 117.²⁷⁴

The supplementation of the reaction medium with cosolvents, such as organic solvents, ionic liquids, or other additives, can have a positive effect on the reaction rates and the enzyme stability.^{166,181,241,275} Interestingly, the use of dedicated CO₂-capture solvents is not necessarily beneficial.¹⁶⁶ Therefore, the identity and amount of the supplied solvent needs to be empirically optimized for individual enzymes.

Many classes of carboxylation enzymes require stoichiometric amounts of cofactors, such as ATP or NAD(P)H. For example, the activation of carboxylic acids as CoA thioesters is an ATP-dependent process that produces the substrates for enoyl-thioester reductases/carboxylases or glycolyl-CoA carboxylase.^{9,10,12,14} To avoid consumption of stoichiometric amounts of the costly cofactors, regeneration systems can be implemented.^{276,277} Besides traditional coupled enzyme systems, also whole cells, electrochemical methods, or even photosynthetic membranes encapsulated in microfluidic droplets were shown to drive regeneration of ATP and NADPH.^{274,278}

4. CO₂ FIXATION PATHWAYS AND CASCADES

CO₂ is freely diffusible in air and soluble in water. Therefore, its concentration is stable in most environments with very little diurnal or seasonal fluctuations. Its constant availability makes CO₂ an attractive carbon source, especially for sessile organisms such as plants. As a result, nature has developed several, evolutionarily independent ways to utilize CO₂ as a carbon source.

To date, seven natural autotrophic carbon fixation pathways have been elucidated in detail: the Calvin–Benson–Bassham (CBB) cycle,²⁷⁹ the reverse TCA (rTCA)/reverse oxidative TCA (roTCA) cycle,^{280–282} the Wood–Ljungdahl (WL) pathway,²⁸³ the reductive glycine pathway,^{62,284} the dicarboxylate 4-hydroxybutyrate (dicarboxylate) cycle,²⁸⁵ the 3-hydroxypropionate 4-hydroxybutyrate (3HP/4HB) cycle,²⁸⁶ and the 3-hydroxypropionate (3HP) bicycle.²⁸⁷ Although these pathways have been extensively reviewed,^{256,288,289} we want to give a concise overview serving as a starting point for subsequent discussions.

In addition to the naturally evolved carbon fixation pathways, several synthetic cascades have been developed that rely on carboxylases as key enzymes. Herein, we differentiate these systems into cascades that produce key cellular metabolites from CO₂ (section 4.2) and into cascades that in contrast utilize the synthetic potential of (de)carboxylases to produce fine chemicals (section 4.3).

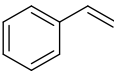
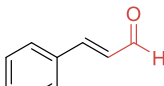
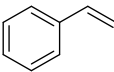
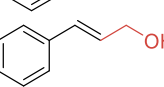
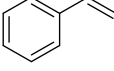
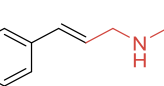
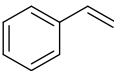
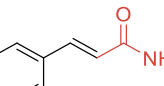
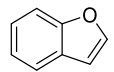
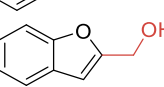
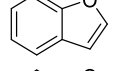
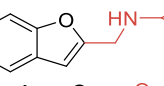
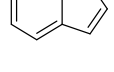
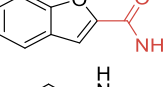
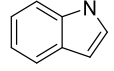
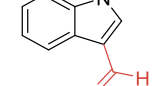
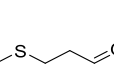
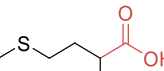
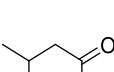
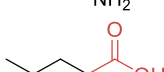
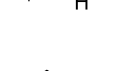
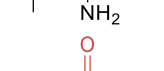
Synthetic carbon fixation pathways are designed as alternative to natural pathways. Very often, synthetic pathways aim to

Table 5. Overview of Natural and Synthetic CO₂ Fixation Cycles^a

pathway	primary product	normalized product	ATP	NAD(P)H	FADH ₂	Fdx ²⁻	ATP eq/CO ₂ (acetyl-CoA)	$\Delta_r G'^0$ (kJ/mol)/(CO ₂ (acetyl-CoA))	O ₂ sensitivity	status	ref
CBB cycle	glyceraldehyde-3P	acetyl-CoA	7	4	0	0	8.5	-102.8 ± 6.4	no, but side reactivity	natural	279
reverse (o)TCA	acetyl-CoA	acetyl-CoA	2(1)	2	1	1	5.5(5)	-34.3 ± 13.3 (-19.5 ± 13.3)	yes	natural	256,281,282,290
WL pathway (acetogens)	acetyl-CoA	acetyl-CoA	1	2	0	2	5.5	-27.2 ± 13.0	yes	natural	291
rGlycine ^b	pyruvate	acetyl-CoA	2	2	0	2	6	-42.0 ± 13.0	yes (if using Fdx for FDH)	natural	62,113,292
DC cycle	acetyl-CoA	acetyl-CoA	5	2	1 ^c	1	7	-72.4 ± 8.9	yes	natural	285
3HP/4HB cycle	acetyl-CoA	acetyl-CoA	4	4	0	0	7	-58.5 ± 6.2	no	natural	286
3HP bicycle	pyruvate	acetyl-CoA	5	5	-1	0	8	-81.3 ± 7.0	no	natural	287,293
CETCH 5.4	glyoxylate	acetyl-CoA	2	8	-4	0	8	-59.7 ± 13.5	no	synthetic (in vitro)	137,254,278
HOPAC	glyoxylate	acetyl-CoA	6	6	-2	0	9	-103.5 ± 8.8	no	synthetic (drafted)	137
rGPS-MCG	acetyl-CoA	acetyl-CoA	5	5	-1	0	8	-80.9 ± 7.0	no	synthetic (in vitro)	294
POAP	oxalate	acetyl-CoA	6	3	0	1	8	-94.6 ± 8.5	yes	synthetic (in vitro)	253
GED	glyceraldehyde-3P	acetyl-CoA	7	4	0	0	8.5	-102.8 ± 6.4	no	optimized in host	70

^aCBB, Calvin–Benson–Bassham; reverse (o)TCA cycle refers to both the reverse TCA cycle employing citrate-ATP lyase and the reverse oxidative TCA cycle employing citrate synthase in the reverse reaction. Values for the reverse oxidative TCA cycle are listed in parentheses. WL, Wood–Ljungdahl; rGlycine, reverse glycine; DC, dicarboxylate/4-hydroxybutyrate; 3HP/4HB, 3-hydroxypropionate/4-hydroxybutyrate; 3HP, 3-hydroxypropionate bicycle; CETCH 5.4, crotonyl-CoA/ethylmalonyl-CoA/hydroxybutyryl-CoA cycle version 5.4; HOPAC, hydroxypropionyl-CoA/acetyl-CoA cycle; rGPS-MCG, reductive glyoxylate and pyruvate synthesis and malyl-CoA-glycerate cycle; POAP, PYC-OAH-ACS-PFOR cycle; GED, Gnd–Entner–Doudoroff cycle. ^bFerredoxin is assumed to be the electron donor for formate dehydrogenase in this pathway. ^cFumarate reductase in the dicarboxylate cycle uses FADH₂ as electron donor. Fdx, ferredoxin; FDH, formate dehydrogenase. For ATP per CO₂ conversions, a P/O ratio of 2.5 for Fdx²⁻, 2.5 for NAD(P)H, and 1.5 for FADH₂ was assumed. Products were normalized for the production of acetyl-CoA via conversions presented in Schwander et al.¹³⁷ and in Supporting Information, Table 1. Fdx²⁻ refers to the use of two separate single electron-transferring ferredoxins (i.e., a 2-electron reduction).

Table 6. Overview of Biocatalytic Cascades for Synthetic CO₂ Utilization^a

Entry	Number of enzymes	Carboxylating enzyme	Functionalizing enzymes	Cofactors ^a	Substrate	Product	Ref.
1	2	AnFdc	TpCAR	1 ATP, 1 NADPH			211
2	3	AnFdc	CAR-EcADH	1 ATP, 2 NAD(P)H			211
3	3	AnFdc	CAR-CfIRE	1 ATP, 2 NADPH			211
4	2	AnFdc	TpCAR	1 ATP			211
5	3	AnFdc I327S	CAR-EcADH	1 ATP, 2 NAD(P)H			211
6	3	AnFdc I327S	CAR-AspRedAm	1 ATP, 2 NADPH			211
7	2	AnFdc I327S	TpCAR	1 ATP			211
8	2	ArInD	SrCAR	1 ATP, 1 NADPH			189,176
9	2	KdcA	YbdL	L-Gln ^b			39
10	2	KdcA	LeuDh	1 NADH			39
11	3	PyDC	ADH, LDH	1 NAD ⁺ , 1 NADH			149

^aAnFdc, ferulic acid decarboxylase from *Aspergillus niger*; CAR, carboxylic acid reductase; EcADH, alcohol dehydrogenase from *Escherichia coli*; CfIRE, imine reductase from *Cystobacter ferrugineus*; TpCAR, carboxylic acid reductase from *Tsukamurella paurometabola*; AspRedAm, reductive aminase from *Aspergillus oryzae*; SrCAR, carboxylic acid reductase from *Segniliparus rugosus*; ArInD, indole-3-carboxylic acid decarboxylase from *Arthrobacter nicotianae*; PyDC, pyruvate decarboxylase; LDH, lactate dehydrogenase; KdcA, decarboxylase from *Lactococcus lactis*; YbdL, methionine aminotransferase from *Escherichia coli* K12; LeuDh, leucine dehydrogenase from *Lysinibacillus sphaericus* ATCC 4525; PEPC, phosphoenolpyruvate carboxylase; CA, carbonic anhydrase. ^bAs none of the carboxylating enzymes in this table require either ADP, NAD(P)H, or Fdx, the cofactor equivalents required in the full cascade are given. ^cOne equivalent of L-glutamine is required as amino donor by the aminotransferase.

kinetically or thermodynamically outcompete natural pathways or provide other advantages such as ease of incorporation into host strains or oxygen tolerance. While some of them have been successfully demonstrated in vitro, they ultimately need to be transferred into in vivo systems to prove that they can sustain life. Like their natural counterparts, artificial CO₂ fixation pathways often have a cyclic topology, are typically complex, and consist of many enzymes (typically more than ten different enzymes). The successful realization of these systems therefore requires careful planning, selection, and characterization of the biocatalysts, as well as optimization of their interplay. Section 4.2 summarizes the current state of methodologies to overcome this

challenge. Synthetic cascades for CO₂ utilization in contrast focus on the addition of CO₂ as C1 building block to a target molecule and mostly consist of two to five enzymes. Because such systems are often linear and less complex, typically higher productivities and concentrations are achieved.

For a comprehensive overview, both natural and synthetic CO₂ fixation pathways are listed in Table 5 (further details can be found in the Supporting Information). Synthetic CO₂ utilization pathways are summarized in Table 6.

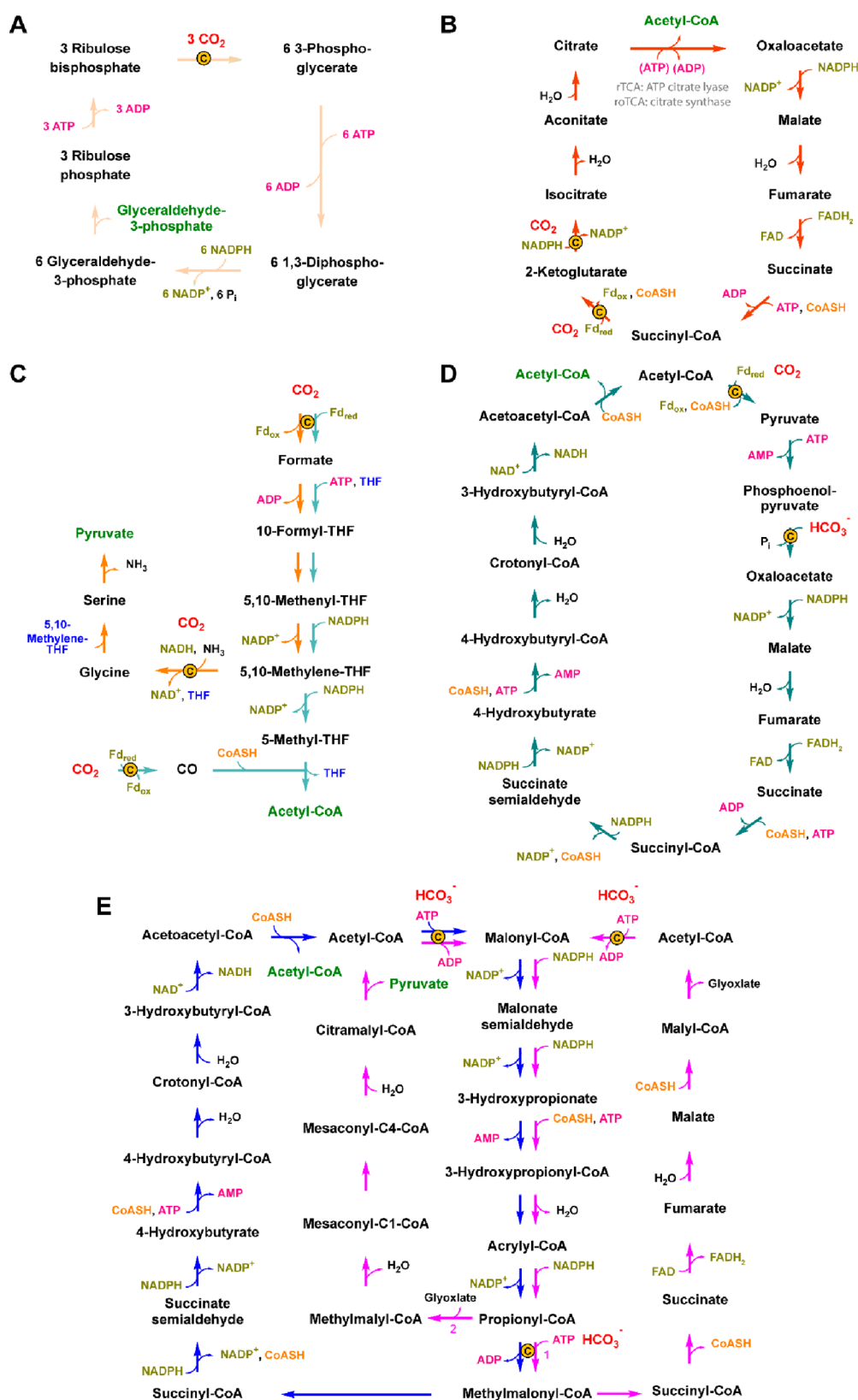


Figure 14. Natural carbon fixation cycles. (A) CBB cycle, (B) rTCA and roTCA cycle, (C) acetogenic WL pathway (turquoise) and reductive glycine pathway. (D) dicarboxylate cycle (orange). (E) 3HP/4HB cycle (blue) and 3HP bicycle (magenta). Carboxylation steps are highlighted.

4.1. Natural CO₂ Fixation Pathways

4.1.1.1. CBB Cycle. The CBB cycle (Figure 14A) is nature's predominant carbon fixation pathway. It occurs in plants, cyanobacteria, algae, and other photosynthetic bacteria.⁸⁶

Almost all organic matter existing today was once fixed by the CBB cycle. The central carbon-fixing enzyme in the CBB cycle is RuBisCO (see [section 3.1.1.1](#)) that catalyzes carboxylation of RuBP to form two molecules of 3PG. Via 1,3-bisphosphogly-

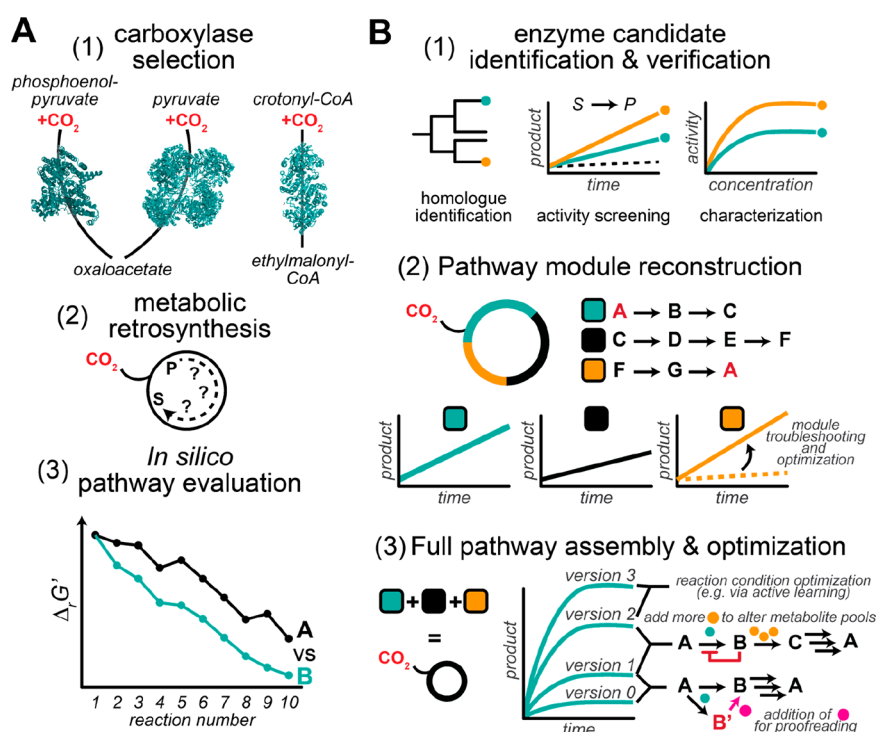


Figure 15. Design and realization of synthetic CO₂ fixation pathways. (A) The theoretical considerations for the creation of new-to-nature pathways are (1) selection of a suitable carboxylase, (2) design of a pathway around the chosen carboxylase, and (3) pathway evaluation. (B) The experimental workflow for the assessment and optimization of new-to-nature (carboxylation) pathways entails (1) characterization of single enzymes, (2) reconstruction of pathway modules, and (3) full in vitro pathway assembly and optimization.

cerate, glyceraldehyde-3-phosphate and a series of transaldolase reactions, 3PG is converted into ribulose-5-phosphate which is phosphorylated by phosphoribulokinase, forming RuBP and completing the cycle. Overall, three full turns of the cycle produce one molecule of glyceraldehyde-3-phosphate.

4.1.2. rTCA Cycle. The rTCA cycle (Figure 14B and Table 5) was first discovered in green sulfur bacteria and is also present in eubacteria.²⁵⁶ It is essentially the reverse reaction of the TCA cycle and hence produces acetyl-CoA as final product. The two CO₂-fixing steps are catalyzed by the enzymes 2-ketoglutarate synthase and isocitrate dehydrogenase (cf. section 3.1.2). It has long been thought that citrate synthesis from oxaloacetate and acetyl-CoA, the key step of the oxidative TCA cycle (oTCA), is irreversible. Therefore, the reverse reaction present in the rTCA is either catalyzed by the reversible ATP-dependent citrate lyase (ACL)²⁹⁵ or the step is separated into two steps catalyzed by citryl-CoA synthetase and citryl-CoA lyase.^{296,297} In 2018, two pioneering studies showed that citrate synthases can also operate in the reverse direction, thereby constituting the reverse oxidative TCA cycle (roTCA).^{281,290} Although it has long been put forward that the rTCA cycle is strictly anaerobic, it can operate under microaerobic conditions.²⁹⁸

4.1.3. WL and Reductive Glycine Pathway. Both the WL (Figure 14C, turquoise; Table 5) and the reductive glycine pathway (Figure 14D, orange) are linear pathways, which distinguishes them from all other CO₂-assimilation pathways. Two different variants of the WL pathway are known: the acetogenic²⁹¹ and the methanogenic.⁶⁷ Both pathways share the same intermediates, with the only difference being that methanogens use methanofuran-based cofactors, while acetogens use tetrahydrofolate (THF) as cofactor. The WL pathway is strictly anaerobic as both CO₂-fixing enzymes, CODH (see also section 3.1.2.5) and FDH/FMFDH (see also section

3.1.2.4), are highly sensitive to oxygen. The pathway fixes two molecules of CO₂ and produces acetyl-CoA as final product, but it can also be used to metabolize other C1 compounds (see section 5).

The reductive glycine pathway (Table 5) was initially proposed as a hypothetical carbon fixation pathway for growth on formate.^{117,119,299} However, recently it was proposed that the phosphite oxidizing deltaproteobacteria *Candidatus Phosphitovorax anaerolim* might use this pathway for carbon assimilation.²⁸⁴ In 2020, the pathway was demonstrated to sustain autotrophic growth in the sulfate-reducing bacterium *Desulfovibrio desulfuricans*.⁶² Although the glycine cleavage system, which is the pathway's key carbon-fixing enzyme, is insensitive to oxygen, for fully autotrophic growth on CO₂, 5,10-methylene tetrahydrofolate (5,10 mTHF) is required. Production of 5,10 mTHF can be achieved using formate as starting material, which in turn can be produced by the oxygen-sensitive enzyme FDH. Therefore, aerobic autotrophic growth on CO₂ using the reductive glycine pathway is not possible.

4.1.4. Dicarboxylate, 3HP/4HB Cycle, and 3HP Bicycle. The dicarboxylate cycle (Figure 14D and Table 5) is found in anaerobic archaea and, like the rTCA cycle, it includes oxygen-sensitive enzymes but tolerates microaerobic conditions.³⁰⁰ It fixes two molecules of CO₂ via PEPC and PFOR (see sections 3.1.1.2 and 3.1.2.1) and yields acetyl-CoA as final product.

The 3HP/4HB cycle (Figure 14E, blue; Table 5) and the 3HP bicycle (Figure 14E, magenta; Table 5) occur in aerobic *Sulfolobales* and green nonsulfur bacteria respectively,²⁵⁶ have common intermediates and share the same carboxylating enzyme, ACPCC (see also section 3.1.1.3), which catalyzes both carboxylation steps. Both pathways can operate under aerobic conditions. However, while the 3HP/4HB cycle fixes two molecules of CO₂ per round and produces acetyl-CoA as

output, the 3HP bicycle fixes three CO₂ molecules and produces the C3 compound pyruvate instead. A defining feature of the 3HP bicycle is that it is composed of two cycles which share several common steps (synthesis of propionyl-CoA from acetyl-CoA). One branch of the cycle produces glyoxylate, which the other branch uses as a substrate. All three pathways start from acetyl-CoA and produce succinyl-CoA as an intermediate. The 3HP/4HB cycle and the 3HP pathway use the same enzymatic transformations to produce succinyl-CoA from acetyl-CoA, while the dicarboxylate cycle is distinct. However, transformation of succinyl-CoA to acetyl-CoA is highly similar in the dicarboxylate and the 3HP/4HB cycle, while the 3HP bicycle is clearly different.

4.2. Development and Current State of Synthetic CO₂ Fixation Pathways

Moving beyond naturally occurring CO₂ fixation cycles, synthetic biologists have recently shifted their attention to the design, realization, and implementation of synthetic CO₂ fixation cycles and linear cascades.

4.2.1. Motivation. Although nature has evolved several different pathways for the capture of CO₂ (outlined above), it has only populated a very small fraction of the possible solution space.³⁰¹ Notably, many of the existing solutions represent only a local optimum and are still limited by the inefficiencies of the respective pathways and their enzymes. By designing, realizing, and implementing de novo CO₂ fixation cycles, scientists aim to harness the favorable properties of highly efficient carboxylases, while designing thermodynamically- and energy-efficient (i.e., low ATP investment) reaction networks that regenerate the CO₂ acceptor. Such synthetic CO₂ fixation cascades are designed with the goal of augmenting natural CO₂ fixation pathways in vivo, completely replacing natural CO₂ fixation pathways in vivo, or providing a platform for the synthesis of compounds from CO₂ in vitro or in vivo. Additionally, these synthetic CO₂ fixation pathways can find applications in synthetic biology for the creation of synthetic autotrophic cells. In the near future, the development of synthetic, self-regenerating CO₂ fixation pathways can provide an efficient solution for the synthesis of tailor-made fine chemicals for which nature has not evolved dedicated biosynthetic pathways from renewable resources. Overall, synthetic CO₂ fixation pathways hold promise to increase, optimize, and enable the conversion of the greenhouse gas CO₂ into valuable chemical compounds.

4.2.2. Design. Synthetic CO₂ fixation cycles or CO₂-utilizing cascades are generally designed around carboxylases that exhibit desired properties, such as high rates of carboxylation or high energy-efficiency. Prospective carboxylases are sourced from nature and often are members of the PEPC, pyruvate carboxylase, or ECR enzyme families (Figure 15A(1)).^{302,302} Carboxylases of these families exhibit catalytic efficiencies that are orders of magnitude higher than those of the average enzyme, as well as those of carboxylases found in natural CO₂ fixation cycles, such as RuBisCO.^{81,302,303} With the chosen carboxylase at hand, synthetic pathways are designed in a “metabolic retrosynthesis” phase,¹³⁷ the aim of which is to identify a set of chemical reactions that efficiently converts the product(s) of the CO₂-fixing reaction back to the substrate, while producing an organic output molecule that can be further metabolized (Figure 15A(2)). The efficiency and feasibility of drafted reaction cascades is then quantified based on a combination of (i) reaction cascade kinetics, (ii) energetic

efficiency, (iii) thermodynamic feasibility, and (iv) difficulty of implementation (Figure 15A(3)).^{137,255,294,299}

Reaction cascade kinetics (i) are most often evaluated using the rate-limiting step concept,³⁰⁴ where pathways are designed to contain fast rate-limiting steps, ensuring high flux. This is combined with a pathway specific activity metric, which describes the maximum theoretical rate of product formation by a given total protein mass of a pathway and thus quantifies the efficiency of all employed enzymes.²⁹⁹ In addition, recent studies have implemented Max–Min Driving Force (MDF) calculations to determine pathways that require low enzyme loadings to catalyze a unit of flux.^{294,305–307} While MDF evaluations contain no kinetic information, they can help to predict efficient pathways based on their thermodynamic driving force when comprehensive kinetic data is not available for all enzymes involved.³⁰⁵

Pathway energetic efficiencies (ii) are determined by how many reducing (e.g., NAD(P)H, FADH₂, ferredoxins) and energy carrier (e.g., NTPs, CoA esters, phosphate-esters) equivalents are consumed per assimilated CO₂ under physiologically relevant conditions (pH and ionic strength).²⁹⁹ Standardized energetic efficiencies are often directly compared between drafted and natural CO₂ fixation cycles and thus help select efficient reaction cascades.^{137,253}

Thermodynamic efficiencies (iii) are closely intertwined with a pathway's energetic efficiency (ATP/NADPH equivalent cost). Pathways are designed to be exergonic, free of high thermodynamic barriers, and composed of reactions with high thermodynamic driving force.^{305,308} Thermodynamic feasibilities are evaluated by either calculating a pathway's (or a pathway module's) Gibbs free energy profile ($\Delta rG'$) by, e.g., using eQuilibrator^{43,42} or by MDF analysis.^{294,305}

Lastly, implementation feasibilities (iv) are a key determinant of pathway selections. This metric aims to quantify practical considerations such as the number of required enzymes, their oxygen-tolerance, availability of catalysts for all desired reactions, compatibility with host–organism metabolism, and the specificity of the utilized catalysts.

Because these evaluation criteria are applied to highly diverse pathways with strongly varying implementation goals, no single quantitative metric can be derived to parametrize evaluation outcomes. Efficiency and feasibility thus have to be evaluated on a pathway-to-pathway basis. This is nicely highlighted by the PYC-OAH-ACS-PFOR (POAP) cycle (Table 5),²⁵³ which assimilates CO₂ in a four-enzyme cycle with the oxygen-sensitive and thermophilic PFOR (see section 3) at its core. The oxygen-sensitivity and high temperature optimum of PFOR immediately render this pathway unsuited for implementation into mesophilic, aerobic organisms, yet exactly these qualities, as well as its short nature, make it perfectly suited for an implementation as a(n) (auxiliary) CO₂ fixation pathway in anaerobic thermophiles.

Despite the flexible nature of the evaluation criteria, an end-goal specific evaluation step of the drafted CO₂ fixation cycle is highly important, which is nicely highlighted in the creation of the crotonyl-Coenzyme A (CoA)/ethylmalonyl-CoA/hydroxybutyryl-CoA (CETCH) cycle (Table 5).¹³⁷ Before realizing the CETCH cycle, Schwander et al. evaluated a total of seven drafted synthetic CO₂ fixation cycles built around the carboxylase crotonyl-CoA carboxylase/reductase. Not only was the CETCH cycle the most exergonic pathway among drafts with similar energetic efficiencies, but it also represented the shortest pathway (11 enzymes required) and enzyme

candidates were available for all desired reactions. This in-depth evaluation during the initial pathway design phase was crucial for the successful *in vitro* realization of the first completely synthetic CO₂ fixation cycle.

Beyond cyclic CO₂ fixation pathways, recent efforts also focused on the design of linear CO₂ fixation cascades to either augment natural metabolism⁵⁵ or to enable the synthesis of products directly from CO₂.²⁵⁵ The recently described three-enzyme tartronyl-CoA (TaCo) pathway,⁵⁵ for example, converts glycolate into glycerate, while assimilating one molecule of CO₂ in the process. In doing so, the TaCo pathway enables a carbon-positive conversion of 2PG, the product of photorespiration, into an intermediate of central metabolism. This enables the replacement of the naturally carbon-releasing photorespiration³⁰⁹ by a synthetic, carbon-positive alternative that augments natural metabolism. The TaCo pathway was designed to be short and efficient, yet it included a carboxylation step that is not catalyzed by any known enzyme (namely the carboxylation of glycolyl-CoA to (S)-tartronyl-CoA). However, chemically similar reactions, such as the carboxylation of propionyl-CoA to methylmalonyl-CoA, are catalyzed by naturally occurring biotin-dependent carboxylases, which is why Scheffen et al. deemed the re-engineering of a naturally occurring carboxylase into a glycolyl-CoA carboxylase possible.

Lastly, synthetic CO₂ fixation cascades have recently been combined with chemical catalysts which reduce CO₂ prior to further chemoenzymatic conversion.^{255,310} These hybrid systems increase the chemical and enzymatic reaction space available during pathway design phases, as enzymes for the conversion of reduced C1 species can be used (see section 5). Furthermore, initiating chemoenzymatic cascades using formate or methanol as starting material, increases the theoretical energetic efficiency of CO₂-to-product conversions, due to the high energy efficiency of chemical CO₂ reductions.^{311,312} Reaction cascades based on reduced C1 species will be reviewed in section 5, yet the design, evaluation, and realization principles closely resemble those used to create purely chemoenzymatic CO₂ fixation cascades.

4.2.3. Realization and Implementation. After designing a reaction cascade, enzyme activities for individual reactions or selected pathway modules are validated *in vitro* prior to full cascade assembly. This stepwise reconstitution and validation serves to break down the complex reaction cascade into smaller sections, which are easier to validate and troubleshoot. Synthetic CO₂ fixation cascades are generally first realized in controlled *in vitro* environments, prior to *in vivo* implementation attempts, because reaction conditions can be tightly defined, controlled, and adapted in *in vitro* systems.

This stepwise *in vitro* realization principle is nicely highlighted in the establishment of the reductive glyoxylate and pyruvate synthesis and malyl-CoA-glycerate (rGPS-MCG) cycle (Table 5).²⁹⁴ The rGPS-MCG cycle employs the highly efficient PEPC and CCR to synthesize acetyl-CoA from two CO₂ molecules while regenerating the carboxylase substrates in a multistep cascade. During its realization, Luo et al. first validated the activity of each enzyme individually or sequentially (depending on the availability of read-out modules). Thereafter, the cycle was split into three sections, each of which was assembled separately. Thereby, the feasibility the rGPS-MCG cycle could be demonstrated. Subsequently, the rGPS-MCG cycle was fully assembled *in vitro* and equipped with sensing modules for online monitoring of concentrations of NAD(P)H, ATP, and FAD, as well as other reductants. This extensive

sensing setup revealed inefficiencies in enzyme homologue choice, side reactivities, enzyme instabilities, and cofactor balance problems. After correcting for the identified limitations, the rGPS-MCG cycle was successfully realized *in vitro* and reached continuous quasi-steady state operation for up to 6 h (Figure 15B).

Similar inefficiencies were identified by continuously monitoring the ¹³CO₂ label incorporation during the realization of the CETCH cycle.¹³⁷ Despite initial validation of enzyme activities in a “modularized” fashion, product synthesis in the fully assembled cycle halted prematurely. Eventually, methylsuccinyl-CoA dehydrogenase (mcd) was pinpointed as problematic as it was operated using the artificial electron acceptor ferrocenium. High concentrations of ferrocenium prevented effective cycling of CETCH, which is why Schwander et al. re-engineered mcd to accept O₂ as an alternative, noninterfering, electron acceptor.^{137,313} The same issue was encountered during the design of the rGPS-MCG cycle (described above) and circumvented by carefully fine-tuning the employed concentrations of ferrocenium.²⁹⁴ The stepwise establishment of the CETCH cycle further highlighted the need for fine-tuned reaction conditions, cofactor regeneration systems, and most importantly proof-reading enzymes that facilitate a re-entry of dead-end metabolites into the cycle. Such proof-reading reactions were used to prevent, e.g., the unwanted build-up of malyl-CoA in the CETCH cycle,¹³⁷ or to minimize the build-up of methylsuccinate in the rGPS-MCG cycle.²⁹⁴

While cyclic pathways are especially susceptible to premature arrest due to intermediate drainage, the recent realization of the artificial starch anabolic pathway (ASAP), a linear pathway for the synthesis of starch from CO₂, also required extensive fine-tuning efforts in order to balance enzyme reactivities and prevent inhibitory effects exerted by pathway intermediates.²⁵⁵ In ASAP, CO₂ is chemically reduced to formaldehyde and subsequently converted to starch in a chemoenzymatic reaction cascade. Enzymes of ASAP that were allosterically inhibited by cycle intermediates had to be re-engineered to be less susceptible to inhibition and enzymes exhibiting high cofactor competition had to be engineered to be more efficient, in order to successfully realize ASAP *in vitro*.

Although the highlighted monitoring and optimization efforts were successful in creating *in vitro* CO₂ fixation cascades, the final pathway efficiency is often still far from optimal. This is largely because the individual parts used to reconstruct these systems are derived from drastically different biological backgrounds, which makes their interactions hard to predict. Recent efforts have therefore implemented a machine learning-guided workflow called METIS²⁵⁴ to explore the vast combinatorial space of reaction conditions. By screening the efficiency of only ~1000 different pathway variants over a total of eight rounds of active learning, the productivity of the CETCH cycle could be improved roughly 10-fold compared to the previously best pathway combination.^{137,254} In theory, workflows like METIS can be used from the get-go to identify and optimize reaction conditions for efficient realization of CO₂ fixation cascades. These reaction condition optimizations can be paired with a novel computational tool (MEMO) developed to identify the smallest possible metabolic modules with a defined stoichiometry.³⁰⁷ MEMO can, e.g., predict short metabolic modules to regenerate the 4 NADPH, 1 ATP, and 1 acetyl-CoA consumed during operation of the CETCH cycle and thus predicts cofactor regeneration as well as carbon assimilation modules that can be tested in the realization phase. Such

computational workflows have already proven to be highly useful for in vitro optimization of pathways. These in vitro realizations and optimizations are crucial steps for downstream in vivo pathway implementation or for the use as in vitro production platforms.^{255,310,314,315}

Recently, Erb et al. defined five levels of metabolic engineering. Levels 1 and 2 encompass the optimization of natural pathways and the transplantation of naturally occurring pathways, whereas levels 3, 4, and 5 encompass the creation of new-to-nature pathways by recombining enzymes that catalyze their native reaction, novel reactions based on known mechanisms, or novel reactions based on novel enzymatic mechanisms, respectively.³⁰⁸ The CO₂ fixation cascades highlighted in section 4.2.2 and 4.2.3 all represent level 3 or 4 pathways, as they are (per current knowledge) truly new-to-nature. No new-to-nature pathway (level 3 or higher) for the fixation of CO₂ has successfully been implemented into host organisms yet. However, computational research predicts that successful implementations carry the potential to improve both natural CO₂ fixation^{137,316} and photorespiration.³¹⁷ Although not representing a full in vivo implementation, first steps toward integrating the CETCH cycle into complex biological systems were realized by linking the artificial CO₂ fixation cascade to the natural photosynthetic machinery, capable of replenishing energy- and reducing-equivalents from light.²⁷⁸ These artificial chloroplast mimics are functionally equivalent to their natural counterparts and even exceed the latter in CO₂ fixation efficiency.

To harness their full potential for biotechnology and agriculture, synthetic CO₂ fixation cycles will need to be successfully implemented into living systems. This implementation currently poses several technical and biological challenges. First, it requires methods to encode and assemble the necessary genetic information in a compact and tunable fashion. Second, these synthetic pathways need to be integrated into the native genetic and metabolic background of the host. To this end, the current strategy of choice is the utilization of selection strains that are designed to require the output molecule of a given CO₂ fixation cascade for growth.⁷⁰ Such selection strains can be fine-tuned to derive different percentages of their total biomass from the output molecule that is being selected for, which results in varying degrees of selection pressure for the non-natural pathway.

While not successfully applied for synthetic CO₂ fixation cycles yet, selection strains have been vital for the improvement and implementation of several level 1 and 2 pathways focused on establishing the ability to assimilate CO₂ or other C1 compounds in model organisms.

Satanowski et al., for example, improved a latent carboxylation cycle, the Gnd–Entner–Doudoroff (GED) cycle, via laboratory evolution of *E. coli* selection strains (Table 5).⁷⁰ The GED cycle is composed solely of enzymes native to the heterotrophic *E. coli*, which form a pathway that was able to supply selection strains with CO₂-derived biomass after short-term laboratory evolution. This *E. coli*-native CO₂ fixation pathway shows similar pathway specific activity to the CBB cycle and has the potential to improve CO₂ fixation if better enzyme homologues for the key reaction are engineered or identified in nature.⁵¹⁶

Similarly, recent efforts saw the introduction of a functional CBB cycle into *E. coli* strains that derived either all sugars³¹⁸ or all biomass from CO₂.^{319,320} Autotrophic growth was achieved after long-term evolution under selection for CO₂ fixation via the CBB cycle. These efforts nicely highlight that even trans-

plantation of natural CO₂ fixation cycles into heterologous hosts is associated with difficulties. Many mutations, most of which were difficult to predict, were required to rebalance intracellular fluxes and enable autotrophic growth. Equally complex rewiring efforts are expected to be required for the successful implementation of truly new-to-nature CO₂ fixation cascades.

Recently, the first “level 3” pathway, a new-to-nature pathway composed of enzymes catalyzing their native reactions, was realized in acetogenic bacteria.³²¹ This pathway, the so-called acetyl-CoA bicycle, fixes carbon via PFOR,⁵⁸ converts the produced pyruvate into hexose phosphates via gluconeogenesis and subsequently converts the hexose phosphate into the acceptor compound acetyl-CoA, while producing a surplus acetyl-CoA, via nonoxidative glycolysis. Implementation of the acetyl-CoA bicycle made use of 15 native enzyme activities of the clostridial host bacterium and required the introduction of only a single heterologous phosphoketolase to initiate the nonoxidative glycolysis part of the pathway.

Lastly, multiple natural C1 fixation pathways were recently transplanted into heterologous hosts and shown to be responsible for the assimilation of most to all biomass in specialized selection strains. These efforts include the successful introduction of the ribulose monophosphate shunt into *E. coli* strains that end up deriving either all³²² or most^{323,324} of their biomass from methanol or formaldehyde, respectively. Similarly, growth of *E. coli* on formate and methanol as the sole carbon sources was recently established via a similar strategy that involved short-term laboratory evolution of tailor-made selection strains carrying the reductive glycine pathway.¹¹³ Importantly, these successful pathway examples all have reduced C1 compounds as substrates, which can also be utilized as an energy source. This arguably facilitates their implementation into heterologous hosts, as the need for an external energy source is alleviated.

Together, these successful implementations of level 1 and 2 C1-assimilation pathways highlight the challenges, requirements, and strategies associated with introduction of truly new-to-nature CO₂ fixation cascades into living organisms.

4.3. Biocatalytic Cascades Using CO₂ as C1 Building Block for Fine Chemicals

Natural and synthetic CO₂ fixation systems usually produce compounds from central carbon metabolism, as those can in turn be used to biosynthesize all other biomolecules required by the cell. However, for purely synthetic applications, other target molecules are more attractive. To this end, decarboxylases represent an attractive enzyme class for application in biocatalytic cascades to produce synthetically relevant target molecules.²³² Although several examples of cascade reactions involving a decarboxylation step exist, only a limited number of CO₂ utilization cascades are reported.¹⁰ However, such processes hold great potential, as they allow the application of CO₂ as C1 building block in synthesis. Furthermore, as outlined in sections 2 and 4.2, the combination of carboxylases and decarboxylases with other enzymes promises to overcome the thermodynamic limitations of the challenging carboxylation reaction.

An efficient method to drive the carboxylation reaction of prFMN dependent decarboxylases and to modify the formed carboxylic acids is combining it with carboxylic acid reductases (CAR) to transform the carboxylic acid to an aldehyde (Table 6, entry 1).²¹¹ The aldehyde moiety opens many possibilities for further functionalization and valorization. For example, *A. niger*

Table 7. Overview of Natural and Synthetic C1 Fixation Pathways^a

pathway	starting material	primary product	ATP	NAD(P)H	ATP eq (acetyl-CoA)	status	ref
serine	FALD	acetyl-CoA	3	2	8.00	natural	334
mod. serine	FALD	acetyl-CoA	4	2	9.00	synthetic (in vivo)	337
homoserine	FALD	acetyl-CoA	1	0	1.00	synthetic (in vivo)	338
RuMP	FOR	GA3P	3	0	−4.00	natural	332
XuMP	MeOH	DHA	0	0	−6.00	natural	333
FORCE	MeOH	glycolate	0	0	0	synthetic (in vivo)	339
HWLS	FOR	DHAP	4	3	4.50	synthetic (in vivo)	340
ASAP ^b	MeOH	starch	2	0		synthetic (cell-free)	255
SACA	FALD	acetyl-CoA	0	0	0.00	synthetic (in vivo)	341
SMGF ^c	FOR	pyruvate	2	2	4.50	synthetic (in vivo)	342
lin Met	MeOH	DHAP	1	−3	−13.50	synthetic (in vivo)	343

^aRuMP, ribulose monophosphate pathway; XuMP, xylulose monophosphate pathway; FORCE, formyl-CoA elongation pathway; HWLS, Half-Wood–Ljungdahl–Formolase pathway; ASAP, artificial starch anabolic pathway; SACA, synthetic acetyl-CoA pathway; SMGF, synergistic metabolism of glucose and formate pathway; lin Met, linear methanol assimilation pathway; DHA, dihydroxyacetone; DHAP, dihydroxyacetone phosphate; FOR, formate; FALD, formaldehyde; MeOH, methanol; ^bNormalized against incorporation of one C6 sugar to starch; ^cOnly C1 branch;

decarboxylase was coupled to CARs and the alcohol dehydrogenase (ADH) from *E. coli* to produce cinnamyl alcohol (Table 6, entry 2). Using the same prFMN-CAR system in the presence of amines and an imine reductase allowed production of secondary amines, while employing a reductive aminase allowed production of amides (Table 6, entries 3 and 4). By replacing Ile327 with Ser, the substrate scope of AnFdc was extended for carboxylation of the heteroaromatic substrate benzofuran. This allowed production of various benzofuran derivatives (Table 6, entries 5–7).²¹¹ The heteroaromatic substrate scope was further expanded by application of the indole-3-carboxylic acid decarboxylase from *Arthrobacter nicotianae* for the carboxylation of indole and coupling it to CAR (Table 6, entry 8). The aldehyde product is a valuable building block for the synthesis of anticancer active pharmaceutical ingredients (APIs) like indole phytoalexins brassinin or 1-methoxyspirobrassinol methyl ether.¹⁸⁹ Furthermore, the CAR from *Tsukamurella paurometabola* was exploited for NADPH-free amidation, subsequent to prFMN-dependent styrene carboxylation to yield cinnamamide.²¹¹

Reverse decarboxylation, i.e., carboxylation was applied in the production of the amino acids L-methionine, L-leucine, and L-isoleucine by reversing the Ehrlich pathway (see also section 3.2.4).³⁹ Methional was carboxylated by KdcA, yielding an α -keto acid, which is then converted to L-methionine or L-leucine using a methionine aminotransferase or leucine dehydrogenase, respectively (Table 6, entries 9 and 10). The production of L-methionine by applying YbdL is quite costly, as it requires L-Gln as amino donor. The utilization of LeuDH is therefore advantageous, as it accepts inorganic ammonia and consumes NADH, which can easily be recycled via established methods. Applying 2-methylbutanal as a substrate results in L-isoleucine after transformation by the cascade.³⁹

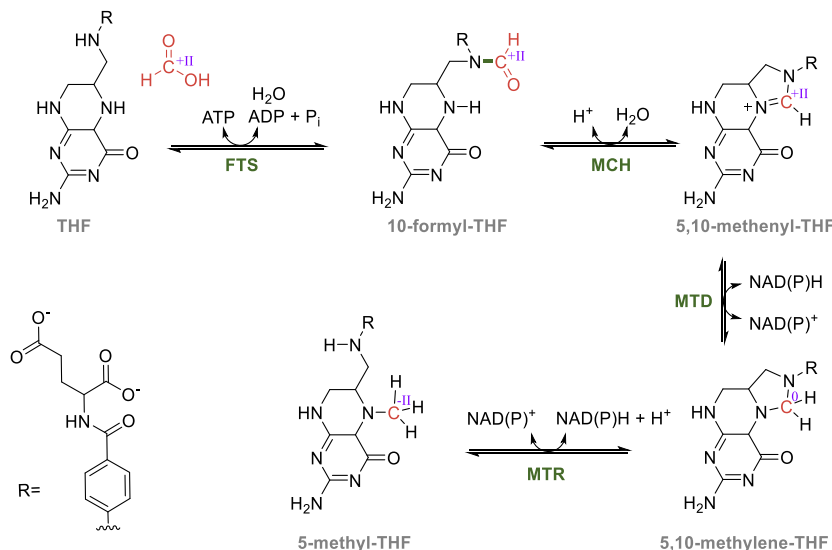
In another example, ethanol was converted to L-lactic acid using a three-enzyme catalytic system involving an ADH for alcohol oxidation, a pyruvate decarboxylase for the carboxylation of acetaldehyde and a lactate dehydrogenase to reduce the pyruvate to L-lactate (Table 6, entry 12). This multi-enzymatic system involves an internal cofactor regeneration system known as borrowing hydrogen, as the NAD⁺ that is consumed by the ADH is recycled within the cascade by the LDH, which makes the system overall redox neutral.¹⁴⁹ Note, that pyruvate is a core metabolite of central carbon metabolism.

Therefore, this system might be further utilized in (artificial) metabolic pathways (compare section 4.2)

5. APPROACHES TO USE CO₂ DERIVATIVES

5.1. Benefits to a Bioeconomy Based on Soluble One-Carbon Compounds

As discussed above, CO₂ is the most oxidized C1 species available in nature. Biological carbon assimilation requires its reduction to hydrocarbons, consuming energy. A comprehensive study of the conversion of C1 substrates showed that more reduced C1 compounds are assimilated at higher energetic efficiency than CO₂, both aerobically and anaerobically (Table 7).³²⁵ In particular, the water-soluble C1 species formate, formaldehyde, and methanol are promising C1 compounds for a circular bioeconomy as potential mass transfer barriers are eliminated. While these molecules can be produced enzymatically by the reduction of CO₂,^{326–329} this requires either expensive redox equivalents, usually ferredoxins and/or NAD(P)H^{326–328} or molecular hydrogen.^{125,126} Alternatively, electrochemical hydrogenation can be used for the direct production of these compounds with off-peak renewable energy as reductive power. While this approach requires high CO₂ concentration and can suffer from low efficiency and selectivity toward the desired product, it provides carbon-neutral energy and hydrogen storage^{330,331} and allows biotechnological generation of more complex products from reduced C1 compounds. Although soluble C1 compounds are easy to store and can be made available to platform organisms at high titers, they also pose challenges: some of them are toxic to both the cultured organisms as well as humans, and they can pose fire hazards if stored in bulk. Additionally, only a limited number of organisms can naturally metabolize them, most of which are not genetically tractable or difficult to cultivate. Therefore, new strategies are developed that include on the one hand the realization of in vitro cascades, where substrate toxicity is less limiting, and on the other hand the engineering of common platform organisms toward growth on C1 compounds. Note that the assimilation of reduced C1 compounds is less dependent on carboxylases, but mainly relies on carbonylases that show distinct cofactor requirements and mechanisms.

Scheme 24. Reductive THF Cascade^a

^aThe carbon of formate is reduced in a stepwise fashion from oxidative state +II to −II. The oxidative state of the relevant carbon atom is indicated in roman numerals. FTS = formyl-THF synthase, MCH = methenyl-THF cyclohydrolase, MTD = methylene-THF dehydrogenase, MTR = methylene-THF reductase.

5.2. The Diversity of Natural C1 Assimilation

Natural formate and methanol assimilation pathways demonstrate a surprising amount of variety. Six natural pathways have been described so far: the ribulose monophosphate (RuMP) pathway,³³² xylulose monophosphate (XuMP) pathway,³³³ the serine cycle,³³⁴ the reductive glycine pathway,¹¹⁹ the WL pathway,³³⁵ and the CBB cycle (compare also Table 7).³³⁶ The latter three pathways are also CO₂-fixing and were already discussed in sections 4.1.3 and 4.1.1.^{119,335} The reductive glycine pathway in particular has been implemented into different platform organisms, which was summarized in a recent review.²⁹² In each pathway, the carbon assimilation steps are distinct from each other with respect to their mechanisms and cofactor requirements. In the following, we will discuss these natural pathways and mechanisms and the synthetic solutions in context.

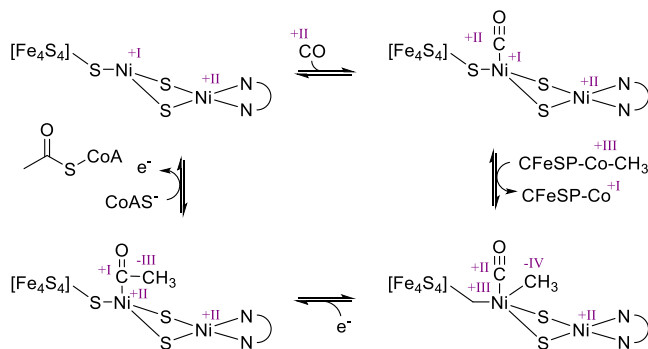
5.3. Tetrahydrofolate (THF) Cascade

A common feature of methanol, formate, and formaldehyde assimilation is that these C1 compounds often enter the central carbon metabolism via THF- (bacteria) or H₄MPT- (archaea)-bound intermediates.³⁴⁴ As they fulfill a similar function, we will only discuss THF here. THF serves as a chemical handle to activate the C1 compound, to facilitate binding to enzymes, and to reduce substrate toxicity. The full cascade shown in Scheme 24 starts by reaction of formate with THF to formyl-THF, followed by dehydration to the circularized methenyl-THF, reduction to methylene-THF, and finally reduction to methyl-THF. Incorporation into pathways usually occurs via methylene- or methyl-THF. Notably, formaldehyde is able to spontaneously react with THF to form methylene-THF, permitting an entry into the cascade.³⁴⁵ Introduction of the partial or full THF cascade has been used to enable synthetic formate assimilation in platform organisms.^{340,346}

5.4. WL Pathway and Metal Cofactors

The WL pathway is found in archaea and is one of the most versatile carbon assimilation pathways, able to assimilate multiple C1 sources, including CO₂, CO, and formate.^{291,347}

Reduction of CO₂ by FDH and CODH have been discussed in previous sections (see sections 3.1.2.4 and 3.1.2.5). Here, we will focus on the pathway's core enzyme acetyl-CoA synthase (ACS) (Scheme 25).²⁶

Scheme 25. Reaction Mechanism at the NiFeS Cluster of ACS^a

^aNote that the shown mechanism represents only one possibility. Alternative mechanisms involving Ni(0) species have also been proposed.²⁶

The WL pathway is split into a methyl and a carbonyl branch. ACS is the enzyme linking the two branches. CO generated in the carbonyl-branch can bind to the NiFeS-cluster of ACS. Within the methyl branch of the WL pathway, formate is reduced to methyl-THF via the THF cascade (Scheme 24). This methyl group is transferred to the cobalt cofactor of corrinoid iron-sulfur protein (CFESP). ACS can accept the methyl group from CFESP and transfer it to its nickel-iron-sulfur (NiFeS) cluster (Scheme 25). Acetyl-CoA is synthesized at the NiFeS cluster by linking the methyl group to the CO. Finally, acetyl-CoA is released from the cofactor by the transfer of the acetyl group to CoA and the cofactor is regenerated. Due to the specific cofactor requirements of its core enzymes (FDH, CODH, and

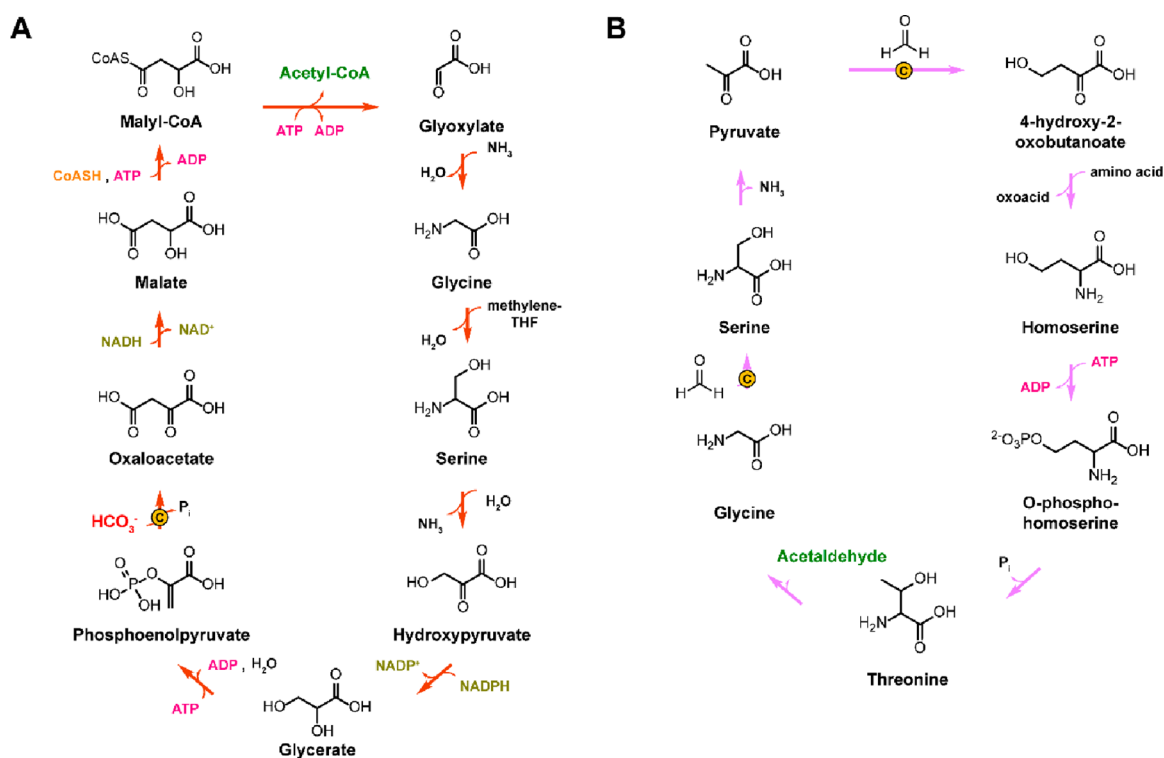
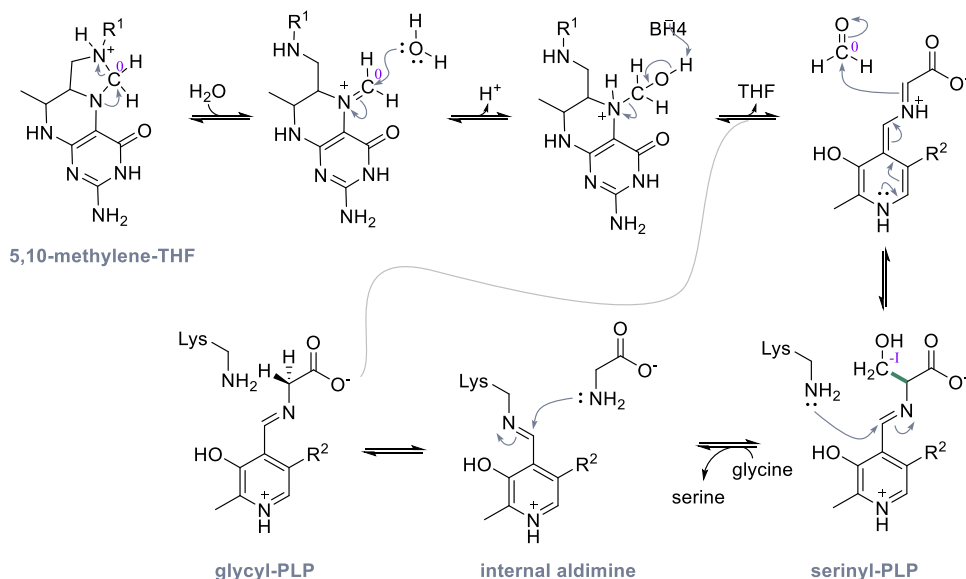


Figure 16. (A) Serine cycle and (B) homoserine cycle. Carboxylation/ C_1 elongation steps are highlighted.

Scheme 26. Reaction Mechanism of SHMT^{4a}



^{4a}Mechanism for the hydrolysis of 5,10-methylene tetrahydrofolate to formaldehyde and THF followed by the aldol condensation of glycine with formaldehyde to serine.³⁴⁸ The oxidative state of the relevant carbon atoms is indicated in roman numerals.

ACS), transfer of the WL pathway to non-native hosts is expected to be rather challenging.

5.5. Serine Cycle and Pyridoxal Phosphate Dependent Enzymes

The serine cycle naturally occurs in aerobic methylotrophic organisms, where it incorporates the two C_1 units, methylene-THF (which can be derived from formate or formaldehyde) and bicarbonate to form acetyl-CoA (Figure 16). In the pathway, serine is produced from glycine and methylene-THF. Via a series of enzymatic steps, serine is converted to PEP, which is

carboxylated by PEPC, thereby assimilating bicarbonate and forming oxaloacetate. Oxaloacetate is transformed to malyl-CoA by reduction and CoA ester formation. Then, malyl-CoA is cleaved, forming acetyl-CoA and glyoxylate, which is converted to glycine by serine glyoxylate aminotransferase.

Serine hydroxymethyltransferase (SHMT) is the serine cycle's key enzyme and catalyzes the PLP-dependent reaction of methylene-THF and glycine to serine (Scheme 26). While the exact mechanism and intermediates of the reaction are debated, recent studies suggest that the addition occurs as an aldol

reaction with formaldehyde as proposed intermediate.^{348–351} As SHMT also accepts formaldehyde as substrate, the assumption that free formaldehyde is involved in the enzymatic mechanism seems plausible.³⁵² Two computational studies investigated the reaction in the retro-aldol direction, giving insights into the enzyme mechanism.^{348,351} While both studies agree on the general mechanism, they find slightly different lowest-energy reaction paths and disagree on the identity of the general base, which has been suggested to be either a glutamate³⁵¹ or a histidine³⁴⁸ (Figure 17). The SHMT mechanism can be

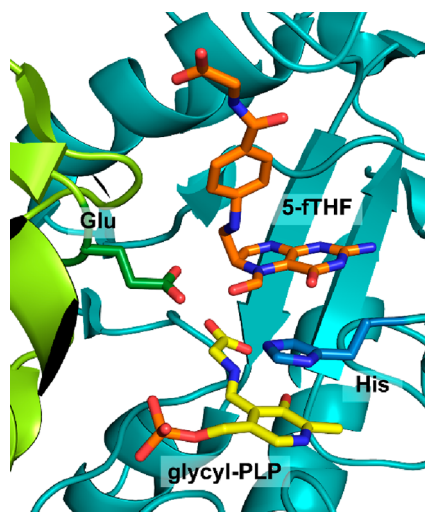


Figure 17. Crystal structure of *G. stearothermophilus* SHMT (PDB 1KL2³⁴⁹) with 5-formyl-tetrahydrofolate (5-fTHF; orange) and glycyl-PLP adduct (yellow). The two subunits that create the active site are indicated in different colors. The postulated general bases glutamate (green) and histidine (blue) are shown as sticks.

separated into two half-reactions: first, the hydrolysis of methylene-THF to formaldehyde and THF, and second, the PLP-dependent aldol reaction of formaldehyde with glycine to form serine (Scheme 26). The glycyl-PLP species required for the reaction is generated via an enzyme-bound internal aldimine intermediate.

Individual steps of the serine cycle, including SHMT, have been introduced into *E. coli* to enable formate assimilation,³⁵³ and a modified version of the full cycle has been implemented in *E. coli* (Table 7).³³⁷ A more derived variant, the homoserine cycle (Figure 16B),³³⁸ utilizes PLP-dependent aldolases for both of its C1-assimilating steps, with both of them incorporating formaldehyde instead of methylene-THF. In the homoserine cycle, a promiscuous serine-threonine aldolase, replaces SHMT and catalyzes the C1 elongation of glycine to serine. In contrast to the serine cycle, serine is subsequently not converted to PEP

but to pyruvate instead. Then, 4-hydroxy-2-butanate aldolase catalyzes the C1 elongation of pyruvate to 4-hydroxy-2-butanate. This metabolite is converted to threonine via homoserine and phosphohomoserine. In the last step, threonine is cleaved to form glycine and acetaldehyde, which can be converted to acetyl-CoA. Although both the modified serine cycle as well as the homoserine cycle are functional in vivo, neither is able to sustain growth of *E. coli* on formaldehyde (or methanol) as the sole carbon source thus far.^{337,338}

5.6. RuMP Pathway and RuBisCO-like Reactions

The RuMP pathway is an aerotolerant pathway present in methylotrophic bacteria (Table 7). Its core enzyme, 3-hexulose-6-phosphate synthase (HPS; Scheme 27), catalyzes the reaction of formaldehyde with RuMP to hexulose-6-phosphate. Hexulose-6-phosphate can be further converted to fructose-6-phosphate, thereby entering glycolysis. Similar to RuBisCO, HPS forms an enolate intermediate by abstraction of a proton and stabilizes it with a Mg^{2+} (Figure 18). The charged intermediate then performs a simple nucleophilic attack on formaldehyde, followed by protonation and release of 3-hexulose-6-phosphate.³⁵⁴

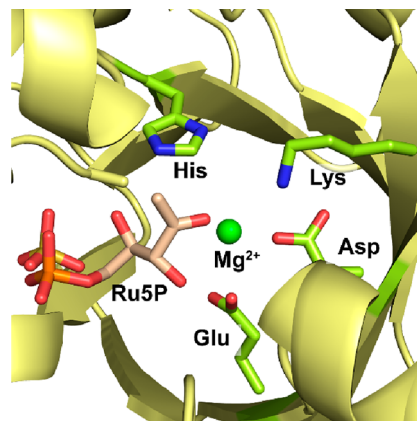
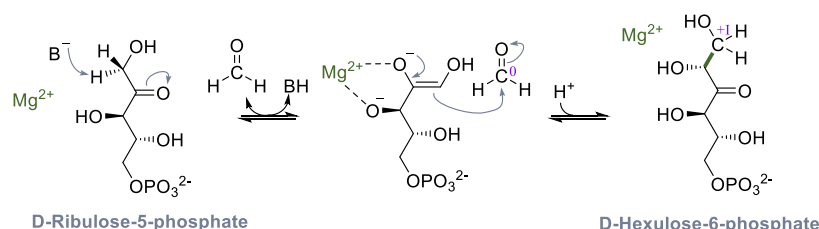


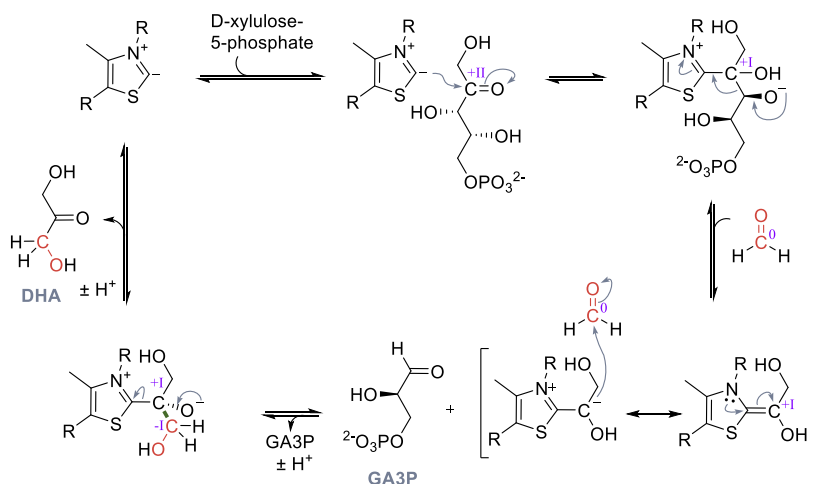
Figure 18. Crystal structure of *M. gastris* HPS (PDB 3AJX)³⁵⁵ with ribulose-5-phosphate (Ru5P) modeled from *E. coli* 3-keto-L-gulonate-6-phosphate decarboxylase structure (PDB 1XBV).³⁵⁴ The Mg^{2+} -coordinating charged residues, as well as the histidine base, are shown as sticks.

The transfer of the RuMP pathway into different host organisms has been extensively reviewed.³⁵⁶ Recently, the RuMP pathway was also combined with nonoxidative glycolysis to enable the biosynthesis of higher alcohols from methanol without requiring ATP,³⁵⁷ and the pathway was used to confer synthetic methylotrophy in *E. coli*.³²²

Scheme 27. Reaction Mechanism of HPS Showing Ru5P Condensation with Formaldehyde;³⁵⁴ The Oxidation States of Relevant Carbon Atoms Are Given in Roman Numeral



Scheme 28. Postulated TPP-Dependent Mechanism of DAS; The Oxidation State of Relevant Carbon Atoms Are Given in Roman Numerals



5.7. XuMP Pathway and Thiamine Pyrophosphate Dependent Reactions

The XuMP pathway is an aerotolerant pathway present in methylotrophic yeasts (Table 7). Its core enzyme is dihydroxyacetone synthase (DAS), a TPP-dependent enzyme converting xylulose-5-phosphate to glyceraldehyde 3-phosphate (GA3P) and dihydroxyacetone. While the mechanism of DAS has not been studied in detail, it is very likely that it uses a mechanism similar to that of other TPP-dependent lyases (Scheme 28).^{358–360} Deprotonated TPP performs a nucleophilic attack on the keto group of XuMP. Next, GA3P is eliminated, producing a reactive enolate/carbanion intermediate. The carbanion then acts as nucleophile, attacking formaldehyde, yielding an adduct which further reacts to form dihydroxyacetone (DHA) and TPP.

The XuMP pathway has been introduced into *Saccharomyces cerevisiae*.³⁶¹ While DAS is a key enzyme in natural C1 assimilation, it has not been extensively used in synthetic C1 assimilation pathways. However, other TPP-dependent enzymes have been explored in synthetic C1 assimilation due to their ability to perform Umpolung reactions of C1 compounds, which are mostly electrophilic. Notably, Umpolung allows direct coupling of two C1 building blocks. In recent years, this idea has gained considerable attention, and multiple enzymes have been engineered to directly link C1 units. The first of these was formolase (FLS),^{358,362} a benzaldehyde lyase which was engineered with the help of computational protein design. FLS condenses three molecules of formaldehyde to one molecule of DHA, making it the only known enzyme to catalyze a C1-to-C3 conversion. Mechanistically, it first performs an Umpolung of one formaldehyde molecule, which allows a nucleophilic attack on the second formaldehyde molecule. The resulting glycolaldehyde-TPP intermediate acts again as a nucleophile and attacks a third molecule of formaldehyde to produce DHA as the final product.³⁵⁸ As DHA can be incorporated into glycolysis via phosphorylation, formolase can be readily integrated into metabolism. Formate assimilation via formolase has been integrated into *E. coli* using the linear methanol assimilation pathway,³⁴³ the Half-Wood–Ljungdahl–Formolase (HWLS)³⁴⁰ pathway and the synergistic metabolism of glucose and formate (SMGF) pathway (Table 7).³⁴² In addition, a cell-free system, the artificial starch anabolic pathway (ASAP),²⁵⁵ uses formolase in the conversion of methanol to

starch. In another in vitro cascade, formolase was used to link two molecules of glycolaldehyde to produce the C4 sugar erythrulose.³¹⁵ However, pathways utilizing FLS are strongly limited by the enzyme's low efficiency. Additionally, in vivo realization of pathways involving formolase are expected to suffer from formaldehyde's toxicity.

Higher reaction rates are achieved in TPP-dependent additions of C1 compounds to C2 molecules. For example, benzoylformate decarboxylase (BFD) was evolved toward the production of glycolaldehyde from two molecules of formaldehyde and subsequently enabled methanol assimilation in *E. coli* via the synthetic acetyl-CoA (SACA) pathway (Table 7).³⁴¹ The same reaction, catalyzed by glyoxylate carboligase (GCL), was used to produce ethylene glycol in a short whole-cell biocatalytic cascade.³⁶³

Other examples of C1–C1 bond forming enzymes include members of the enzyme families 2-hydroxyl-CoA lyase (HACL) and oxalyl-CoA decarboxylase (OXC), which were shown to catalyze the reaction of formaldehyde with formyl-CoA.^{339,360,364} HACL was implemented in *E. coli* in the formyl-CoA elongation (FORCE) pathway for the conversion of methanol to glycolate (Table 7).³³⁹ Meanwhile, OXC was shown to catalyze C1-elongation of a range of aldehydes, yielding the CoA esters of chemicals like lactic or mandelic acid.^{359,360}

5.8. Pyruvate Formate-lyase: Exploiting Reverse Reactions

Pyruvate formate-lyase (PFL) is not part of any natural C1 fixation pathway, but is involved in the anaerobic glucose metabolism of bacteria. In its reverse reaction, it was shown to enable growth of *E. coli* on formate and acetate.³⁶⁵ PFL is the only known enzyme to assimilate unactivated formate. It performs this challenging task by employing a radical mechanism. However, PFL is sensitive to oxygen. To reduce the enzyme's exposure to oxygen, it was recently successfully encapsulated in a bacterial microcompartment to create a microaerobic environment under aerobic growth conditions.³⁶⁶

The radical mechanism of PFL is initiated by PFL-activating enzyme, generating a 5'-deoxyadenosine radical from S-adenosyl methionine. The radical is then transferred to an active site glycine of PFL (Figure 19). This glycy radical abstracts a hydrogen atom from an adjacent cysteine residue, forming a cysteinyl radical. The radical subsequently reacts with

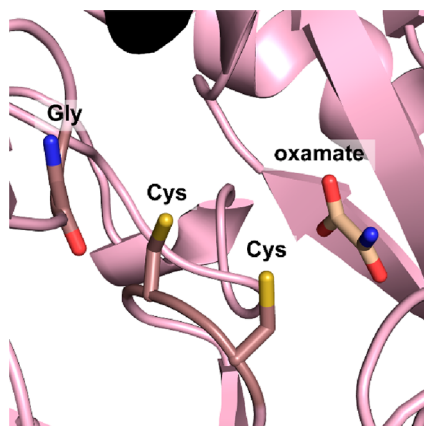


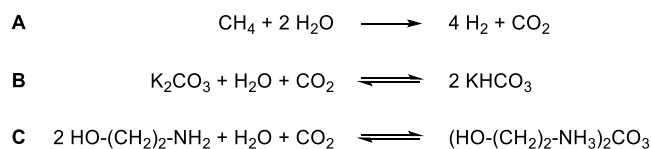
Figure 19. Crystal structure of *E. coli* PFL (PDB 3PFL).³⁶⁷ The relevant active site residues are shown as sticks. Oxamate (beige) is used as a substrate analogue in place of the natural substrate pyruvate.

acetyl-CoA, forming an enzyme bound acetyl-thioester and releasing a CoA radical, which is quenched by a second cysteine residue in the active site (Scheme 29). A hydrogen atom transfer from formate to this cysteinyl radical produces another radical species, which forms a bond with the enzyme-thioester, yielding a carboxyacetyl radical bound to the cysteine residue. Finally, pyruvate is released from the cysteine and the radical is transferred back to the initial glycine residue.³⁶⁷

6. TECHNO-ECONOMIC PERSPECTIVE

Today, the majority of the industrially used CO₂ is generated as a side product of ammonia production. The hydrogen required for ammonia synthesis is obtained by steam methane reforming, resulting in 5.5 tons of CO₂ for every ton of hydrogen produced (Scheme 30). The mixture of CO₂ and hydrogen, containing approximately 18% CO₂, is passed through a solution in which CO₂ is absorbed with the help of either potassium carbonate or ethanolamine. The absorbed CO₂ is released as concentrated gas upon heating the solution and subsequently liquified for storage and transport, if it is not directly used in a downstream process. Following CO₂ release, the absorption solution must be cooled to restore its CO₂-uptake capacity.³⁶⁸

Scheme 30. Industrial CO₂ Production^a

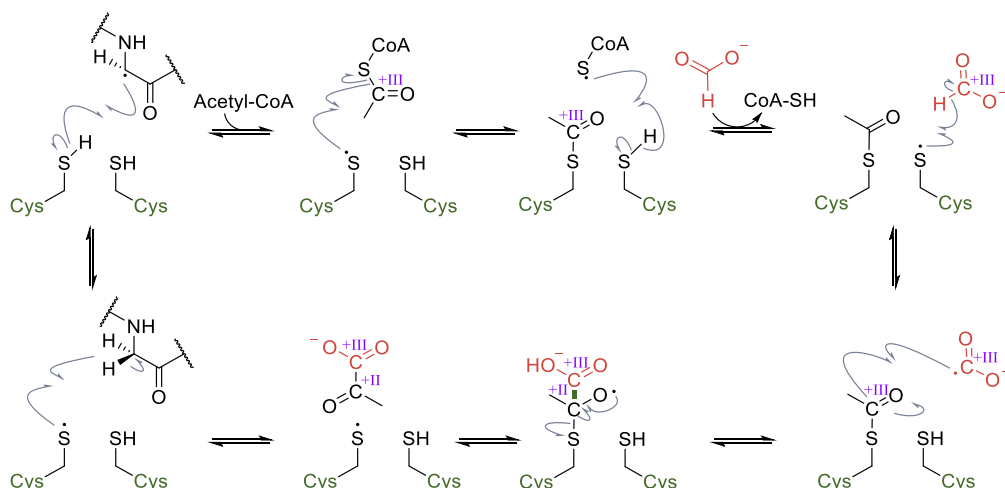


^a(A) CO₂ is a byproduct of hydrogen production by steam reforming. The CO₂ is removed from the product mixture by absorption in an aqueous solution of (B) potassium carbonate or (C) ethanolamine at high pressure and low temperature, and subsequently released by raising the temperature and lowering the pressure.

CO₂ capture from flue gases produced in fossil fuel-driven power plants and CO₂ sequestration from the atmosphere operate with the same principle: selective CO₂ absorption to a liquid or solid phase from a mixture of gases with CO₂ concentrations between 0.04% (atmosphere) and 20% (flue gases) followed by CO₂ release upon temperature increase. However, even considering state-of-the-art amine scrubbing technology, it is estimated that 20–30% of the power that is produced in a fossil-fuel driven power plant would be required to capture all the generated CO₂, thereby reducing the overall efficiency.^{369,370} Capturing atmospheric CO₂ is even more energy-intensive because absorbent materials must provide higher absorption enthalpies to efficiently capture the CO₂ from the more dilute mixture and consequently require a proportionally higher energy input for subsequent release. In order to generate a significant reduction in atmospheric CO₂ concentrations by way of carbon capture, the required energy must come from renewable sources.³⁷¹ Once ample electricity produced by CO₂-neutral processes is available, direct air capture of CO₂ may become one of several technologies suitable to extract CO₂ from the atmosphere.³⁷² The availability of efficient processes to convert sequestered CO₂ to industrial chemicals may increase the attractiveness of direct air CO₂ capture.

Technologies that allow the direct use of scrubbed industrial off-gases with a CO₂ content of up to 20% as carbon source are advantageous as enrichment and purification steps are not required. Consequently, carbon fixation reactions that can operate at low concentrations of dissolved CO₂ or bicarbonate

Scheme 29. Radical Mechanism for the Condensation of Formate and Acetyl-CoA Forming Pyruvate, Catalyzed by PFL;³⁶⁷ The Oxidation State of Relevant Carbon Atoms Are Given in Roman Numerals



are techno-economically preferred. Such integrated CO₂ capture and direct conversion processes are currently only possible with chemical reactions.³⁶⁹ The implication for biological processes is that the enzyme's K_m value for dissolved CO₂ or bicarbonate should be taken into consideration when designing CO₂-utilizing biocatalysts or CO₂ fixation pathways. Note that the K_m value for CO₂ in plant RuBisCO homologues is on average slightly higher than the concentration of dissolved atmospheric CO₂ in water under physiological conditions (14 μ M at 400 pm).^{373–375} Therefore, when using feedstock gases with enriched CO₂, RuBisCO enzymes would be easily substrate-saturated with respect to CO₂. For other CO₂-fixing enzymes such as reversed decarboxylases, the case is less clear because their K_m values for CO₂ are not known. It would be worthwhile to determine these values to evaluate whether they are already saturated by the 6.8 mM dissolved CO₂, resulting from using industrial exhaust gas mixtures with 20% CO₂ content at ambient pressure, or whether a pure CO₂ atmosphere would be required to efficiently drive the carboxylation.

The process parameters that must be met for a process to be commercially viable depend on the value of the product. For building the structural complexity of valuable active pharmaceutical ingredients (APIs), or other fine chemicals, biocatalytic reactions are particularly attractive because their innate chemo- and regioselectivity allows for shorter synthetic routes and a higher atom efficiency through the omission of activating reagents and protective groups.³⁷⁶ These advantages offset the typically higher catalyst and asset utilization costs caused by often longer reaction times and lower product concentrations compared to classical processes.² Nevertheless, even for API-syntheses, product concentrations up to 100 g/L are the standard for biocatalytic reactions nowadays.³⁷⁶ It is well conceivable that with a highly active catalyst and proper reaction engineering, an enzymatic carboxylation step employing a reversed decarboxylase can contribute to the synthesis of an API or other chemicals. A promising example is the biocatalytic *ortho*-carboxylation of *meta*-aminophenol to *para*-aminosalicylic acid, which is a tuberculostatic agent using salicylic acid decarboxylase from *Trichosporon moniliiforme* (SAD_Tm; see also section 3.2.1 and Table 2); the latter was further improved by enzyme engineering (200 mM scale).¹⁷⁰ Furthermore, the *ortho*-carboxylation of polyphenols such as resveratrol was used to enhance its polarity and water solubility, which are assumed to be beneficial for bioavailability.^{160,158,169}

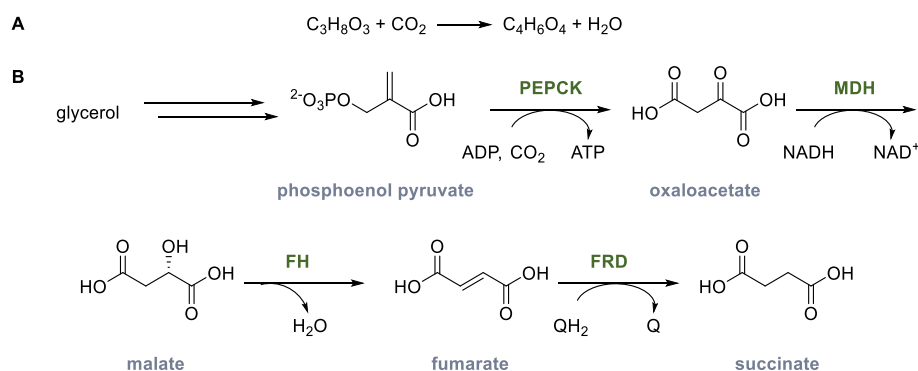
Overall, as biocatalytic reactions generally run at ambient conditions, biocatalysis can reduce a process carbon footprint, even if no carboxylation step is involved. Still, while biocatalysis is increasingly applied in industry, the number of large-scale processes is limited and therefore its impact on CO₂ sequestration or the reduction of its emission is of minor impact on a global scale.

CO₂ fixation on global scale hinges on the notoriously inefficient enzyme RuBisCO and is performed by algae and plants, which annually fix 10¹⁴ kg C.³⁷⁷ RuBisCO's inefficiency results from its comparatively low k_{cat} and its poor discrimination between CO₂ and O₂. One hypothesis is that RuBisCO emerged during times in which the earth's atmosphere contained very little oxygen. Once the oxygen levels had risen, the carbon-assimilation pathways involving RuBisCOs likely already had evolved, and fundamentally different molecular mechanisms could no longer evolve from scratch because they would be outcompeted by the established RuBisCO and the CBB. These arguments motivated and paved the way for the

design of *de novo*, artificial carbon fixation pathways and their subsequent *in vivo* realization. Note that increasing the carbon fixation efficiency in crops even by only a few percent would have a huge impact on global CO₂ fixation rates and also improve agricultural yields. Currently, 12 million km² (3.1 billion acres) cropland are in use that capture together almost 5.5 \times 10¹² kg C annually.³⁷⁸ Although agricultural efficiency has already substantially increased in the past century (e.g., between 1961 and 2005 global land productivity increased by a factor of 2.4³⁷⁹), further developments are necessary to provide food for a growing global population to supply feedstocks for a renewable-based chemical production,³⁸⁰ and to contribute to reducing atmospheric CO₂ concentrations through bioenergy with carbon capture and storage (BECCS).³⁸¹ The introduction of artificial carbon fixation pathways in plants provides an exciting approach to further increase plant productivity. Although genetic engineering of plants is much more laborious than microorganisms, fundamental advances in engineering crop plants were achieved in the past few decades. While previously being limited to only one or two heterologously expressed genes (e.g., conferring tolerance to insects, diseases, or herbicides), the genetic engineering capabilities have strongly improved. Recently, a cassette containing 10 different genes constituting a metabolic pathway for the biosynthesis of polyunsaturated fatty acids and one additional gene conferring herbicide resistance were introduced into canola.³⁸² The resulting canola variety has been approved for commercial use in the U.S., illustrating the technical and regulatory feasibility of introducing heterologous pathways with a size comparable to that of an average carbon fixation pathway into crop plants.

While the ultimate goal is the enhancement of crops for food and biofeedstock production, genetically accessible microalgae such as *Chlamydomonas reinhardtii* may be the primary choice for addressing fundamental questions and pathway optimization.³⁸³ For industrial production of biomass and chemicals, however, microalgae are challenging microorganisms because they grow slowly and to low cell densities. Their large-scale cultivation requires complicated reactor designs that provide high surface-to-volume ratios to maximize light influx while allowing good mass transfer to supply CO₂ and nutrients to the cells. In the very long-term, cultivation of genetically engineered microalgae in open ponds is conceivable, with saltwater lagoons being particularly attractive from a sustainability perspective. However, such open cultivation is not reconcilable with current policies on containment of genetically modified microorganisms.³⁸⁴

With light-driven carbon fixation being unattainable at large scale in industrial reactors in the short term, the required energy for CO₂ and water splitting could come from renewably generated electric energy that is provided to microorganisms or cell-free systems through electrodes. Such reactors would similarly need an extremely high surface-to-volume ratio because the range for electron transfer in an aqueous environment is so short that only the first few layers of cells colonizing an electrode could be supplied with the electrons required for CO₂ reduction.^{325,385} Such complex reactors will not only be capital intensive but also expensive to operate, as they are difficult to clean and maintain and have poor volumetric productivities. These limitations could be overcome by separating the CO₂ reduction step from the build-up of larger molecules.³¹² CO₂ reduction to formic acid, formaldehyde, or methanol could be driven by chemical catalysis operating at high efficiency and volumetric productivity. These water-soluble intermediates

Scheme 31. Fermentative Production of Succinic Acid from Glycerol and CO₂^a

^a(A) Overall reaction equation. (B) Metabolic pathway of *Mannheimia succiniciproducens*.³⁸⁸ Glycerol is converted to phosphoenolpyruvate, PEP, via dihydroxyacetone. PEP, carboxykinase; PEPCK, carboxylates PEP to oxaloacetate and transfers the phosphate group to ADP to produce ATP. Malate dehydrogenase, MDH, reduces the α -keto-acid to the α -hydroxy-acid malate, which is dehydrated by fumarate hydratase, FH, to fumarate. Fumarate reductase, FRD, reduces fumarate to succinate, using quinol as hydrogen donor.

could then be fed as carbon source to microorganisms in conventional aerobic or anaerobic fermentation setups and converted to more complex chemicals.

Including CO₂ fixation steps into biosynthetic pathways can contribute to the sustainability of microbial fermentations, even beyond usage of renewable feedstocks.³⁸⁶ A prominent example is the fermentative production of succinic acid, an important building block for the synthesis of polyesters (Scheme 31). While the current global market size for succinic acid is relatively small, with 15 kt annually, it may grow substantially when the demand for biobased polymer building blocks increases.^{386,387} The key step of the most efficient metabolic route, the reductive TCA route, is carboxylation of phosphoenolpyruvate (PEP) by either PEP carboxylase or PEP carboxykinase, resulting in one equivalent of CO₂ fixed per molecule succinic acid produced.³⁸⁸ The overall reaction is redox neutral when using glycerol as carbon source,³⁸⁹ but even if a process is not redox-neutral, a CO₂ fixation step can contribute to a net CO₂ consumption in fermentation.

In summary, enzymatic CO₂ fixation steps can contribute already in the short term to improving the sustainability profile of chemicals production. The contribution can be especially favorable if the process does not require purified CO₂, and the specific energy input needed to drive the fixation is low. The latter is particularly true for redox-neutral processes such as succinic acid production, which unfortunately are not common. In all other cases, the large amounts of energy required for attaining any of the reduced carbon oxidation states must not only be generated but also supplied at a rate that matches the rate of CO₂ fixation. Sunlight is ubiquitous and free, but the rate of energy transfer through photosynthesis is too slow to achieve the conversion rates expected for high density cell cultures in conventional industrial bioreactors. Conversely, plants have matched the rate of light harvesting to CO₂ fixation and subsequent reduction, even though CO₂ fixation remains limiting. Whether the carbon sequestration capacity of crop plants can be increased by the introduction of additional CO₂ fixation cycles remains to be seen, but given the recent advances in constructing such pathways and the expanding toolbox for genetic modification of crop plants, progress can be expected. As an alternative to light, the energy required for CO₂ reduction can be supplied as electrical energy through electrodes. However, the distances required for electron transfer are so short that cells would need to attach directly to the electrodes, requiring

intricate reactor designs that are difficult to upscale to the dimensions necessary for generating a global impact. Here, multistep processes consisting of electrochemical CO₂ conversion of C1 molecules, followed by fermentative conversion, are much more conceivable in the near future. The gas fermentative production of ethanol from synthesis gas, a mixture of CO, CO₂, H₂, and N₂, by acetogenic *Clostridium* cultures highlights the potential of utilizing microbes to build up larger molecules from C1 compounds, in this case CO and CO₂, at industrial scale.³⁹⁰

7. OUTLOOK AND OPPORTUNITIES

The previous sections have highlighted that CO₂ is not only a waste product harmful to the climate. It can also serve as an enzymatic substrate for the production of chemicals and is even required for the growth of many organisms, including plants. Although recent advances have shown that a range of products can be enzymatically synthesized from CO₂, some inherent limitations remain. For example, due to the low potential energy of CO₂, it is often necessary to employ high concentrations of CO₂ (or bicarbonate) to shift the equilibrium to the product side and achieve acceptable yields in carboxylation reactions involving only a single enzyme. Although implementation of product removal techniques, as well as coupling the carboxylation steps to thermodynamically favorable downstream reactions, have shown to significantly improve reaction efficiencies, further improvements in this area are desirable.

Carboxylation reactions are challenging, and therefore only few reactions directly employ CO₂ as starting material in organic synthesis. While the carboxylation reaction scope of enzymes is broader, still only a small range of compounds can be biosynthesized from CO₂ directly. Besides broadening the substrate scope of existing enzymes by protein engineering, identification of new carbon-fixing enzymes is an attractive way to tackle this problem. Driven by the rapid increase in available sequence data and the development of ever more efficient genome mining techniques, the discovery of novel carbon-fixing enzymes can be anticipated. Another approach is repurposing existing enzymes to reduce CO₂. The nitrogen gas-reducing enzyme nitrogenase is particularly interesting in this regard as it has been shown to accept both CO and CO₂ as substrates to produce reduced hydrocarbons such as methane, ethylene, and propane.^{391–396} However, hydrocarbon production by nitrogenase is currently limited by low turnover numbers.

Furthermore, the enzyme's oxygen sensitivity and its dependence on complex cofactor maturation systems has further complicated the study of nitrogenases. An alternative to using natural systems is complementing enzymes with chemically-synthesized cofactors. Such systems have produced promising results. For example, by incorporation of photosensitizers, proteins with extremely high reducing power have been generated. The reduction potential of these photosensitizer proteins could be tuned by enzyme engineering, which allowed production of CO³⁹⁶ and formate³⁹⁷ from CO₂ using NADPH as electron donor.

It is also possible to increase the palette of products accessible from CO₂ by using carboxylation products as substrates in downstream reactions. Nature already very successfully applies this principle, as almost all biomass can be produced from only three products of naturally occurring carbon fixation cycles: acetyl-CoA, pyruvate, or glyceraldehyde-3-phosphate. The same idea can be applied to synthetic CO₂ fixation cascades for sustainable production of chemicals without using any commodity chemicals derived from fossil feedstocks. A proof-of-principle study that such systems can function has been established for the synthesis of terpenes and polyketides from CO₂.³¹⁴ However, much more work needs to be done to improve this system beyond the proof-of-principle phase. One important challenge will be to increase the longevity and robustness of synthetic in vitro systems, e.g., by balancing fluxes and cofactor regeneration. Furthermore, higher flux through pathways is expected if it were possible to selectively remove the products of a given transformation, e.g., within engineered physical structures. Multicompartment engineered physical structures could mimic natural photosynthesis, in which fixed carbon is constantly pumped out of the chloroplast to create a strong source–sink relationship. The use of structures with selective transport capabilities would allow scientists to optimize reaction conditions between different compartments and implement different maintenance regimes, some of which would be impossible in living cells.

The ultimate challenge of synthetic biology is building novel living systems, often called synthetic cells. The central part of every living organism is carbon metabolism. In this regard, the in vivo implementation of artificial carbon fixation pathways is highly interesting as it would lay the foundation for artificial metabolism with no precedent in nature. At the same time, in vivo implementation of carbon fixation pathways into microorganisms is an interesting approach to validate their performance. Once the most efficient pathways have been identified, crops will be particularly attractive targets for engineering. As currently carbon fixation is a limiting factor in plant growth, improvements of carbon fixation efficiency are predicted to directly translate to increased photosynthetic yields. Opportunities thus arise in creating plants that feature new-to-nature CO₂-fixing capabilities either in the context of improving CO₂ fixation directly or by improving photorespiratory metabolism. Precedent shows that even introducing carbon-neutral photorespiratory bypasses can already stimulate plant growth in the field,³⁹⁸ which strongly incentivizes continuation of such efforts to expand the capabilities of plant metabolism beyond the constraints of natural evolution. With all the recent progress and enthusiasm around CO₂ sequestration and fixation technologies, it should not be forgotten that the technologies discussed in this review will only provide an impact in the future. However, slowing down the rise in atmospheric greenhouse gas concentrations warrants immediate action and we must address

the issue with today's toolbox focusing on reducing global carbon emissions.

ASSOCIATED CONTENT

Supporting Information

The Supporting Information is available free of charge at <https://pubs.acs.org/doi/10.1021/acs.chemrev.2c00581>.

Extended version of Table 5 (XLSX)

AUTHOR INFORMATION

Corresponding Authors

Silvia M. Glueck – Institute of Chemistry, University of Graz, NAWI Graz, 8010 Graz, Austria; orcid.org/0000-0003-2154-7585; Email: si.glueck@uni-graz.at

Matthias Tinzl – Department of Biochemistry and Synthetic Metabolism, Max Planck Institute for Terrestrial Microbiology, 35043 Marburg, Germany; Email: matthias.tinzl@mpi-marburg.mpg.de

Christoph K. Winkler – Institute of Chemistry, University of Graz, NAWI Graz, 8010 Graz, Austria; orcid.org/0000-0003-3068-9817; Email: christoph.winkler@uni-graz.at

Authors

Sarah Bierbaumer – Institute of Chemistry, University of Graz, NAWI Graz, 8010 Graz, Austria; orcid.org/0000-0003-3883-7108

Maren Nattermann – Department of Biochemistry and Synthetic Metabolism, Max Planck Institute for Terrestrial Microbiology, 35043 Marburg, Germany

Luca Schulz – Department of Biochemistry and Synthetic Metabolism, Max Planck Institute for Terrestrial Microbiology, 35043 Marburg, Germany

Reinhard Zschoche – BASF SE, 67056 Ludwigshafen am Rhein, Germany

Tobias J. Erb – Department of Biochemistry and Synthetic Metabolism, Max Planck Institute for Terrestrial Microbiology, 35043 Marburg, Germany; orcid.org/0000-0003-3685-0894

Complete contact information is available at: <https://pubs.acs.org/10.1021/acs.chemrev.2c00581>

Author Contributions

^{||}M.N. and L.S. contributed equally and are listed in alphabetical order. CRediT: **Sarah Bierbaumer** conceptualization, visualization, writing-original draft, writing-review & editing; **Maren Nattermann** conceptualization, visualization, writing-original draft, writing-review & editing; **Luca Schulz** conceptualization, visualization, writing-original draft, writing-review & editing; **Reinhard Zschoche** writing-original draft, writing-review & editing; **Tobias J. Erb** conceptualization, funding acquisition, writing-review & editing; **Christoph K. Winkler** conceptualization, visualization, writing-original draft, writing-review & editing; **Matthias Tinzl** conceptualization, funding acquisition, visualization, writing-original draft, writing-review & editing; **Silvia Maria Glueck** conceptualization, funding acquisition, writing-original draft, writing-review & editing.

Funding

APC Funding Statement: Open Access is funded by the Austrian Science Fund (FWF).

Notes

The authors declare no competing financial interest.

Biographies

Sarah Bierbaumer, born in 1996 in Gröbming, Austria, studied Chemistry at Graz University of Technology within the framework of the joint venture with University of Graz "NAWI Graz". For her Master's thesis, she investigated a deracemization system for secondary alcohols under the supervision of Prof. Wolfgang Kroutil. In 2019, she started her Ph.D. in the same research group at University of Graz under the supervision of Dr. Silvia M. Glueck, focusing on the combination of biocatalysis and photocatalysis in one pot by establishing a cyclic photobiocatalytic deracemization process for sulfoxides.

Maren Nattermann studied Biochemistry at the Ruprecht Karl University, Heidelberg, Germany. Since 2019, she is a doctoral candidate at the Department of Biochemistry and Synthetic Metabolism of the MPI for Terrestrial Microbiology, Marburg, Germany. Her research focusses on synthetic formate assimilation.

Luca Schulz studied Biology at the Philipps University, Marburg, and Biological Chemistry at ETH Zurich, Switzerland. He now works as a Ph.D. student in the lab of Prof. Tobias Erb at the Max Planck Institute for Terrestrial Microbiology in Marburg, Germany. His research focusses on deciphering the evolution of nature's most prominent carboxylase, RuBisCO.

Reinhard Zschoche works as Senior Specialist for New Business Development of Biotech Products at BASF in Ludwigshafen. After studying chemistry and biology at ETH Zurich in Switzerland, he did his Ph.D. work on mechanistic enzymology and artificial protein cages with Prof. Donald Hilvert. In 2016, Reinhard joined the White Biotechnology Research department at BASF to work on biocatalyst discovery and enzyme engineering for small molecule syntheses and crop trait development. Since 2021, he manages BASF's innovation projects for biotechnologically produced aroma ingredients. Reinhard's interest is to translate advances in the field of biotechnology to the sustainable production of chemicals.

Tobias Erb studied Chemistry and Biology and did his Ph.D. at the University of Freiburg, Germany, and The Ohio State University, USA. After a postdoctoral stay at the University of Illinois in Urbana–Champaign, USA, he started his career as junior group leader at ETH Zurich, Switzerland, in 2011. In 2014, he relocated to the Max Planck Institute for Terrestrial Microbiology, where he was promoted Director in 2017. His research focuses on the discovery, function, and engineering of novel CO₂ converting enzymes and their use in artificial photosynthesis, as well as the bottom-up design of synthetic chloroplasts and cells.

Christoph K. Winkler works as Senior Scientist and PI in the group of Prof. Wolfgang Kroutil at the University of Graz. He did his undergraduate and graduate studies at the University of Graz, Austria, with Prof. Kurt Faber. After spending some time in industry at Genericon GmbH, he returned to academia as University Assistant in the group of Prof. Faber at the University of Graz and later as Scientist and Project Leader at ACIB GmbH, before moving to his current position at the University of Graz. His research focusses on the application of enzymes in synthesis as well as on the use of light as reagent in biocatalysis.

After completing his undergraduate studies in Interdisciplinary Sciences at ETH Zurich in Switzerland, Matthias Tinzl carried out his doctoral research in the group of Prof. Donald Hilvert at ETH Zurich. There, he worked on mechanistic enzymology and biocatalysis. After finishing his Ph.D. in late 2020, he joined the lab of Prof. Tobias

Erb at the Max Planck Institute for terrestrial Microbiology in Marburg, Germany, where he currently works as a SNSF Postdoctoral Fellow. His research focuses on discovery of novel biocatalytic reactions, RuBisCO, and directed evolution of enzymes.

Silvia M. Glueck, born 1973, studied Chemistry at the University of Graz, Austria, where she received her Ph.D. degree under the supervision of Prof. Kurt Faber in 2004. After a postdoctoral stay at the University of Edinburgh and Manchester (2005–2007) with Prof. Nicholas J. Turner, she returned to Graz as Scientist and later appointed as Senior Scientist within the Austrian Centre of Industrial Biotechnology (ACIB) and the University of Graz. She currently holds a position as University Assistant at the Department of Chemistry at the University of Graz. Her research interests focus on biocatalytic synthesis as alternative to chemical systems.

ACKNOWLEDGMENTS

S.B. acknowledges the Austrian Science Fund (FWF) for funding within the project CATALOX (DOC 46-B21). M.T. is thankful for an individual SNSF Postdoctoral Fellowship (grant P500PB_203136). M.N. was supported by the German Ministry of Education and Research grant 031B0850B (MetAFor). The University of Graz and the Field of Excellence BioHealth are acknowledged for financial support. L.S. is supported by the Max Planck Society.

ABBREVIATIONS

2,3-DHBH = 2,3-dihydroxybenzoic acid decarboxylase
2KFOR = 2-ketoglutarate:ferredoxin oxidoreductase
3HP/4HB = 3-hydroxypropionate/4-hydroxybutyrate
3-PG = 3-phosphoglycerate
5,10 mTHF = 5,10-methylene tetrahydrofolate
ACC = acetyl-CoA carboxylase
ACPCC = acetyl-CoA/propionyl-CoA carboxylase
API = active pharmaceutical ingredient
ASAP = artificial starch anabolic pathway
BC = biotin carboxylase
BCCP = biotin carboxyl carrier protein
BFD = benzoylformate decarboxylase
CA = carbonic anhydrase
CABP = 2-carboxyarabinitol biphosphate
CAM = Crassulacean acid metabolism
CBB = Calvin–Benson–Bassham
CCM = carbon concentrating mechanism
CCR = crotonyl-CoA carboxylase/reductase
CETCH = crotonyl-coenzyme A (CoA)/ethylmalonyl-CoA/hydroxybutyryl-CoA
CODH = CO dehydrogenase
CT = carboxytransferase
DAS = dihydroxyacetone synthase
DFT = density functional theory
DHA = dihydroxyacetone
FDH = formate dehydrogenase
FLS = formolase
FMFDH = formylmethanofuran dehydrogenase
FORCE = formyl-CoA elongation
GCL = glyoxylate carboligase
GCS = glycine cleavage system
GED = Gnd–Entner–Doudoroff
H4MPT = tetrahydromethanopterin
HACL = 2-hydroxyl-CoA lyase
HPS = 3-hexulose-6-phosphate synthase
HWLS = Half–Wood–Ljungdal–Formolase

IDC = iso-orotate decarboxylase
IDH = isocitrate dehydrogenase
ISPR = in situ product removal
LigW = 5-carboxyvanillate decarboxylase
mcd = methylsuccinyl-CoA dehydrogenase
MDF = max–min driving force
MIMS = membrane inlet mass spectrometry
OXC = oxalyl-CoA decarboxylase
PEP = phosphoenolpyruvate
PEPC = phosphoenolpyruvate carboxylase
PFL = pyruvate formate-lyase
PFOR = pyruvate:ferredoxin oxidoreductase
PLP = pyridoxal-5-phosphate
POAP = PYC-OAH-ACS-PFOR
prFMN = prenylated flavin mononucleotide
PRI = phosphoriboseisomerase
PRK = phosphoribulokinase
rGlycine = reductive glycine
rGPS-MCG = reductive glyoxylate and pyruvate synthesis cycle and malyl-CoA-glycerate pathway
RLP = RuBisCO-like enzymes
rTCA = reverse tricarboxylic acid cycle
RuBisCO = ribulose-1,5-bisphosphate carboxylase/oxygenase
RuBP = ribulose-1,5-phosphate
RuMP = ribulose monophosphate
SACA = synthetic acetyl-CoA
SAD = salicylic acid decarboxylase
SHMT = serine hydroxymethyltransferase
SMGF = synergistic metabolism of glucose and formate
TaCo = tartronyl-CoA
TCA = tricarboxylic acid
THF = tetrahydrofolate
TPP = thiamine pyrophosphate
WL = Wood Ljungdahl
XuMP = xylulose monophosphate

REFERENCES

- (1) Woodley, J. M. Ensuring the Sustainability of Biocatalysis. *ChemSusChem* **2022**, *15*, No. e202102683.
- (2) Wu, S.; Snajdrova, R.; Moore, J. C.; Baldenius, K.; Bornscheuer, U. T. Biocatalysis: Enzymatic Synthesis for Industrial Applications. *Angew. Chem., Int. Ed.* **2021**, *60*, 88–119.
- (3) Winkler, C. K.; Schrittwieser, J. H.; Kroutil, W. Power of Biocatalysis for Organic Synthesis. *ACS Cent. Sci.* **2021**, *7*, 55–71.
- (4) Wiltschi, B.; Cernava, T.; Dennig, A.; Galindo Casas, M.; Geier, M.; Gruber, S.; Haberbauer, M.; Heidinger, P.; Herrero Acero, E.; Kratzer, R.; et al. Enzymes Revolutionize the Bioproduction of Value-Added Compounds: From Enzyme Discovery to Special Applications. *Biotechnol. Adv.* **2020**, *40*, 107520.
- (5) Sheldon, R. A.; Brady, D.; Bode, M. L. The Hitchhiker's Guide to Biocatalysis: Recent Advances in the Use of Enzymes in Organic Synthesis. *Chem. Sci.* **2020**, *11*, 2587–2605.
- (6) Unlu, A.; Duman-Ozdamar, Z. E.; Caloglu, B.; Binay, B. Enzymes for Efficient CO₂ Conversion. *Protein J.* **2021**, *40*, 489–503.
- (7) Nisar, A.; Khan, S.; Hameed, M.; Nisar, A.; Ahmad, H.; Mehmood, S. A. Bio-Conversion of CO₂ into Biofuels and Other Value-Added Chemicals Via Metabolic Engineering. *Microbiol. Res.* **2021**, *251*, 126813.
- (8) Giri, A.; Chauhan, S.; Sharma, T.; Nadda, A.; Pant, D. Recent Advances in Enzymatic Conversion of Carbon Dioxide into Value-Added Product In *Energy, Environment, and Sustainability*; Springer: Singapore, 2021; pp 313–326.
- (9) Bernhardsgrutter, I.; Stoffel, G. M.; Miller, T. E.; Erb, T. J. CO₂-Converting Enzymes for Sustainable Biotechnology: From Mechanisms to Application. *Curr. Opin. Biotechnol.* **2021**, *67*, 80–87.
- (10) Aleku, G. A.; Roberts, G. W.; Titchiner, G. R.; Leys, D. Synthetic Enzyme-Catalyzed CO₂ Fixation Reactions. *ChemSusChem* **2021**, *14*, 1781–1804.
- (11) Tommasi, I. C. Carboxylation of Hydroxyaromatic Compounds with HCO₃[−] by Enzyme Catalysis: Recent Advances Open the Perspective for Valorization of Lignin-Derived Aromatics. *Catalysts* **2019**, *9*, 37.
- (12) Payer, S. E.; Faber, K.; Glueck, S. M. Non-Oxidative Enzymatic (De)Carboxylation of (Hetero)Aromatics and Acrylic Acid Derivatives. *Adv. Synth. Catal.* **2019**, *361*, 2402–2420.
- (13) Schada von Borzyskowski, L.; Rosenthal, R. G.; Erb, T. J. Evolutionary History and Biotechnological Future of Carboxylases. *J. Biotechnol.* **2013**, *168*, 243–251.
- (14) Glueck, S. M.; Gumus, S.; Fabian, W. M. F.; Faber, K. Biocatalytic Carboxylation. *Chem. Soc. Rev.* **2010**, *39*, 313–328.
- (15) Erb, T. J. Carboxylases in Natural and Synthetic Microbial Pathways. *Appl. Environ. Microbiol.* **2011**, *77*, 8466–8477.
- (16) Zhao, T.; Li, Y.; Zhang, Y. Biological Carbon Fixation: A Thermodynamic Perspective. *Green Chem.* **2021**, *23*, 7852–7864.
- (17) Tsuji, Y.; Fujihara, T. Carbon Dioxide as a Carbon Source in Organic Transformation: Carbon-Carbon Bond Forming Reactions by Transition-Metal Catalysts. *Chem. Commun.* **2012**, *48*, 9956–9964.
- (18) Aresta, M.; Quaranta, E.; Liberio, R.; Dileo, C.; Tommasi, I. Enzymatic Synthesis of 4-OH-Benzic Acid from Phenol and CO₂: The First Example of a Biotechnological Application of a Carboxylase Enzyme. *Tetrahedron* **1998**, *54*, 8841–8846.
- (19) CRC Handbook of Chemistry and Physics; 84th ed.; CRC Press LLC: Boca Raton, FL, 2003; pp 5–4.
- (20) Bar-Even, A.; Flamholz, A.; Noor, E.; Milo, R. Thermodynamic Constraints Shape the Structure of Carbon Fixation Pathways. *Biochim. Biophys. Acta, Bioenerg.* **2012**, *1817*, 1646–1659.
- (21) Lindsey, R. Climate Change: Atmospheric Carbon Dioxide. *Climate.gov*; National Oceanic and Atmospheric Administration, 2022; <https://www.climate.gov/news-features/understanding-climate/climate-change-atmospheric-carbon-dioxide> (accessed 2022-04-21).
- (22) Hall, M. Enzymatic Strategies for Asymmetric Synthesis. *RSC Chem. Biol.* **2021**, *2*, 958–989.
- (23) Talekar, S.; Jo, B. H.; Dordick, J. S.; Kim, J. Carbonic Anhydrase for CO₂ Capture, Conversion and Utilization. *Curr. Opin. Biotechnol.* **2022**, *74*, 230–240.
- (24) Kikuchi, G.; Motokawa, Y.; Yoshida, T.; Hiraga, K. Glycine Cleavage System: Reaction Mechanism, Physiological Significance, and Hyperglycemia. *Proc. Jpn. Acad., Ser. B* **2008**, *84*, 246–263.
- (25) Bailey, S. S.; Payne, K. A. P.; Saaret, A.; Marshall, S. A.; Gostimskaya, I.; Kosov, I.; Fisher, K.; Hay, S.; Leys, D. Enzymatic Control of Cycloadduct Conformation Ensures Reversible 1,3-Dipolar Cycloaddition in a prFMN-Dependent Decarboxylase. *Nat. Chem.* **2019**, *11*, 1049–1057.
- (26) Can, M.; Armstrong, F. A.; Ragsdale, S. W. Structure, Function, and Mechanism of the Nickel Metalloenzymes, CO Dehydrogenase, and Acetyl-CoA Synthase. *Chem. Rev.* **2014**, *114*, 4149–4174.
- (27) Wagner, T.; Ermler, U.; Shima, S. The Methanogenic CO₂ Reducing-and-Fixing Enzyme Is Bifunctional and Contains 46 [4Fe-4S] Clusters. *Science* **2016**, *354*, 114–117.
- (28) Tommasi, I. C. The Mechanism of Rubisco Catalyzed Carboxylation Reaction: Chemical Aspects Involving Acid-Base Chemistry and Functioning of the Molecular Machine. *Catalysts* **2021**, *11*, 813.
- (29) Fan, Y.; Feng, J.; Yang, M.; Tan, X.; Fan, H.; Guo, M.; Wang, B.; Xue, S. CO₂(aq) Concentration-Dependent CO₂ Fixation Via Carboxylation by Decarboxylase. *Green Chem.* **2021**, *23*, 4403–4409.
- (30) Sheng, X.; Himo, F. Mechanisms of Metal-Dependent Non-Redox Decarboxylases from Quantum Chemical Calculations. *Comput. Struct. Biotechnol. J.* **2021**, *19*, 3176–3186.

- (31) Sheng, X.; Himo, F. Theoretical Study of Enzyme Promiscuity: Mechanisms of Hydration and Carboxylation Activities of Phenolic Acid Decarboxylase. *ACS Catal.* **2017**, *7*, 1733–1741.
- (32) Erb, T. J.; Brecht, V.; Fuchs, G.; Müller, M.; Alber, B. E. Carboxylation Mechanism and Stereochemistry of Crotonyl-CoA Carboxylase/Reductase, a Carboxylating Enoyl-Thioester Reductase. *Proc. Natl. Acad. Sci. U. S. A.* **2009**, *106*, 8871–8876.
- (33) Kai, Y.; Matsumura, H.; Izui, K. Phosphoenolpyruvate Carboxylase: Three-Dimensional Structure and Molecular Mechanisms. *Arch. Biochem. Biophys.* **2003**, *414*, 170–179.
- (34) Knowles, J. R. The Mechanism of Biotin-Dependent Enzymes. *Annu. Rev. Biochem.* **1989**, *58*, 195–221.
- (35) Bloor, S.; Michurin, I.; Titchiner, G. R.; Leys, D. Prenylated Flavins: Structures and Mechanisms. *FEBS J.* **2022**, DOI: 10.1111/febs.16371.
- (36) Menon, S.; Ragsdale, S. W. Mechanism of the *Clostridium Thermoaceticum* Pyruvate: Ferredoxin Oxidoreductase: Evidence for the Common Catalytic Intermediacy of the Hydroxyethylthiamine Pyropyrrophosphate Radical. *Biochemistry* **1997**, *36*, 8484–8494.
- (37) Furdul, C.; Ragsdale, S. W. The Roles of Coenzyme a in the Pyruvate: Ferredoxin Oxidoreductase Reaction Mechanism: Rate Enhancement of Electron Transfer from a Radical Intermediate to an Iron-Sulfur Cluster. *Biochemistry* **2002**, *41*, 9921–9937.
- (38) Smith, E. T.; Blamey, J. M.; Adams, M. W. Pyruvate Ferredoxin Oxidoreductases of the Hyperthermophilic Archaeon, *Pyrococcus Furiosus*, and the Hyperthermophilic Bacterium, *Thermotoga Maritima*, Have Different Catalytic Mechanisms. *Biochemistry* **1994**, *33*, 1008–1016.
- (39) Martin, J.; Eisoldt, L.; Skerra, A. Fixation of Gaseous CO₂ by Reversing a Decarboxylase for the Biocatalytic Synthesis of the Essential Amino Acid L-Methionine. *Nat. Catal.* **2018**, *1*, 555–561.
- (40) Marsden, S. R.; Mestrom, L.; McMillan, D. G. G.; Hanefeld, U. Thermodynamically and Kinetically Controlled Reactions in Biocatalysis - from Concepts to Perspectives. *ChemCatChem* **2020**, *12*, 426–437.
- (41) Note that the presented free energies are calculated using the eQuilibrator tool (<https://equilibrator.weizmann.ac.il/>) at the standard conditions (1 mM concentration) and using CO₂(tot). The free energies under physiologic conditions or under reaction conditions of biotransformations might differ. Furthermore, solvating energies and phase transfer are not considered.
- (42) Beber, M. E.; Gollub, M. G.; Mozaffari, D.; Shebek, K. M.; Flamholz, A. I.; Milo, R.; Noor, E. eQuilibrator 3.0: A Database Solution for Thermodynamic Constant Estimation. *Nucleic Acids Res.* **2022**, *50*, D603–D609.
- (43) Flamholz, A.; Noor, E.; Bar-Even, A.; Milo, R. eQuilibrator-the Biochemical Thermodynamics Calculator. *Nucleic Acids Res.* **2012**, *40*, D770–775.
- (44) Tcherkez, G. The Mechanism of Rubisco-Catalysed Oxygenation. *Plant, Cell Environ.* **2016**, *39*, 983–997.
- (45) Izui, K.; Matsumura, H.; Furumoto, T.; Kai, Y. Phosphoenolpyruvate Carboxylase: A New Era of Structural Biology. *Annu. Rev. Plant Biol.* **2004**, *55*, 69–84.
- (46) Bernhardsgrutter, I.; Schell, K.; Peter, D. M.; Borjian, F.; Saez, D. A.; Vohringer-Martinez, E.; Erb, T. J. Awakening the Sleeping Carboxylase Function of Enzymes: Engineering the Natural CO₂-Binding Potential of Reductases. *J. Am. Chem. Soc.* **2019**, *141*, 9778–9782.
- (47) Witt, A.; Pozzi, R.; Diesch, S.; Hadicke, O.; Grammel, H. New Light on Ancient Enzymes - in Vitro CO₂ Fixation by Pyruvate Synthase of *Desulfovibrio Africanus* and *Sulfolobus Acidocaldarius*. *FEBS J.* **2019**, *286*, 4494–4508.
- (48) Pesci, L.; Glueck, S. M.; Gurikov, P.; Smirnova, I.; Faber, K.; Liese, A. Biocatalytic Carboxylation of Phenol Derivatives: Kinetics and Thermodynamics of the Biological Kolbe-Schmitt Synthesis. *FEBS J.* **2015**, *282*, 1334–1345.
- (49) Spreitzer, R. J.; Salvucci, M. E. Rubisco: Structure, Regulatory Interactions, and Possibilities for a Better Enzyme. *Annu Rev Plant Biol* **2002**, *53*, 449–475.
- (50) Cleland, W. W.; Andrews, T. J.; Gutteridge, S.; Hartman, F. C.; Lorimer, G. H. Mechanism of Rubisco: The Carbamate as General Base. *Chem. Rev.* **1998**, *98*, 549–562.
- (51) Terada, K.; IZUI, K. Site-Directed Mutagenesis of the Conserved Histidine Residue of Phosphoenolpyruvate Carboxylase: His 138 Is Essential for the Second Partial Reaction. *Eur. J. Biochem.* **1991**, *202*, 797–803.
- (52) Cronan, J. E., Jr.; Waldrop, G. L. Multi-Subunit Acetyl-CoA Carboxylases. *Prog. Lipid Res.* **2002**, *41*, 407–435.
- (53) Wongkittichote, P.; Ah Mew, N.; Chapman, K. A. Propionyl-CoA Carboxylase - a Review. *Mol. Genet. Metab.* **2017**, *122*, 145–152.
- (54) Hügl, M.; Krieger, R. S.; Jahn, M.; Fuchs, G. Characterization of Acetyl-CoA/Propionyl-CoA Carboxylase in *Metallosphaera Sedula*: Carboxylating Enzyme in the 3-Hydroxypropionate Cycle for Autotrophic Carbon Fixation. *Eur. J. Biochem.* **2003**, *270*, 736–744.
- (55) Scheffen, M.; Marchal, D. G.; Beneyton, T.; Schuller, S. K.; Klose, M.; Diehl, C.; Lehmann, J.; Pfister, P.; Carrillo, M.; He, H.; et al. A New-to-Nature Carboxylation Module to Improve Natural and Synthetic CO₂ Fixation. *Nat. Catal.* **2021**, *4*, 105–115.
- (56) Tong, L. Structure and Function of Biotin-Dependent Carboxylases. *Cell. Mol. Life Sci.* **2013**, *70*, 863–891.
- (57) Baughn, A. D.; Garforth, S. J.; Vilcheze, C.; Jacobs, W. R., Jr. An Anaerobic-Type Alpha-Ketoglutarate Ferredoxin Oxidoreductase Completes the Oxidative Tricarboxylic Acid Cycle of *Mycobacterium Tuberculosis*. *PLoS Pathog.* **2009**, *5*, No. e1000662.
- (58) Ragsdale, S. W. Pyruvate Ferredoxin Oxidoreductase and Its Radical Intermediate. *Chem. Rev.* **2003**, *103*, 2333–2346.
- (59) Kanao, T.; Kawamura, M.; Fukui, T.; Atomi, H.; Imanaka, T. Characterization of Isocitrate Dehydrogenase from the Green Sulfur Bacterium *Chlorobium Limicola*: A Carbon Dioxide-Fixing Enzyme in the Reductive Tricarboxylic Acid Cycle. *Eur. J. Biochem.* **2002**, *269*, 1926–1931.
- (60) Aoshima, M.; Igarashi, Y. Nondecarboxylating and Decarboxylating Isocitrate Dehydrogenases: Oxalosuccinate Reductase as an Ancestral Form of Isocitrate Dehydrogenase. *J. Bacteriol.* **2008**, *190*, 2050–2055.
- (61) Erb, T. J.; Berg, I. A.; Brecht, V.; Müller, M.; Fuchs, G.; Alber, B. E. Synthesis of C5-Dicarboxylic Acids from C2-Units Involving Crotonyl-CoA Carboxylase/Reductase: The Ethylmalonyl-CoA Pathway. *Proc. Natl. Acad. Sci. U. S. A.* **2007**, *104*, 10631–10636.
- (62) Sanchez-Andrea, I.; Guedes, I. A.; Hornung, B.; Boeren, S.; Lawson, C. E.; Sousa, D. Z.; Bar-Even, A.; Claessens, N. J.; Stams, A. J. M. The Reductive Glycine Pathway Allows Autotrophic Growth of *Desulfovibrio Desulfuricans*. *Nat. Commun.* **2020**, *11*, 5090.
- (63) Rosenthal, R. G.; Ebert, M. O.; Kiefer, P.; Peter, D. M.; Vorholt, J. A.; Erb, T. J. Direct Evidence for a Covalent Ene Adduct Intermediate in NAD(P)H-Dependent Enzymes. *Nat. Chem. Biol.* **2014**, *10*, 50–55.
- (64) Khangulov, S. V.; Gladyshev, V. N.; Dismukes, G. C.; Stadtman, T. C. Selenium-Containing Formate Dehydrogenase H from *Escherichia Coli*: A Molybdopterin Enzyme That Catalyzes Formate Oxidation without Oxygen Transfer. *Biochemistry* **1998**, *37*, 3518–3528.
- (65) Thomé, R.; Gust, A.; Toci, R.; Mendel, R.; Bittner, F.; Magalon, A.; Walburger, A. A Sulfurtransferase Is Essential for Activity of Formate Dehydrogenases in *Escherichia Coli*. *J. Biol. Chem.* **2012**, *287*, 4671–4678.
- (66) Niks, D.; Duvvuru, J.; Escalona, M.; Hille, R. Spectroscopic and Kinetic Properties of the Molybdenum-Containing, NAD⁺-Dependent Formate Dehydrogenase from *Ralstonia Eutropha*. *J. Biol. Chem.* **2016**, *291*, 1162–1174.
- (67) Daniels, L.; Fuchs, G.; Thauer, R.; Zeikus, J. Carbon Monoxide Oxidation by Methanogenic Bacteria. *J. Bacteriol.* **1977**, *132*, 118–126.
- (68) Kumar, M.; Lu, W.-P.; Ragsdale, S. W. Binding of Carbon Disulfide to the Site of Acetyl-CoA Synthesis by the Nickel-Iron-Sulfur Protein, Carbon Monoxide Dehydrogenase, from *Clostridium Thermoaceticum*. *Biochemistry* **1994**, *33*, 9769–9777.
- (69) Jeoung, J.-H.; Dobbek, H. Carbon Dioxide Activation at the Ni, Fe-Cluster of Anaerobic Carbon Monoxide Dehydrogenase. *Science* **2007**, *318*, 1461–1464.

- (70) Satanowski, A.; Dronsella, B.; Noor, E.; Vogeli, B.; He, H.; Wichmann, P.; Erb, T. J.; Lindner, S. N.; Bar-Even, A. Awakening a Latent Carbon Fixation Cycle in *Escherichia Coli*. *Nat. Commun.* **2020**, *11*, 1812.
- (71) Attwood, P. V. The Structure and the Mechanism of Action of Pyruvate Carboxylase. *Int. J. Biochem. Cell Biol.* **1995**, *27*, 231–249.
- (72) Jitrapakdee, S.; St Maurice, M.; Rayment, I.; Cleland, W. W.; Wallace, J. C.; Attwood, P. V. Structure, Mechanism and Regulation of Pyruvate Carboxylase. *Biochem. J.* **2008**, *413*, 369–387.
- (73) Mus, F.; Eilers, B. J.; Alleman, A. B.; Kabasakal, B. V.; Wells, J. N.; Murray, J. W.; Nocek, B. P.; DuBois, J. L.; Peters, J. W. Structural Basis for the Mechanism of ATP-Dependent Acetone Carboxylation. *Sci. Rep.* **2017**, *7*, 7234.
- (74) Sluis, M. K.; Ensign, S. A. Purification and Characterization of Acetone Carboxylase from Xanthobacter Strain Py2. *Proc. Natl. Acad. Sci. U. S. A.* **1997**, *94*, 8456–8461.
- (75) Fan, C.; Chou, C. Y.; Tong, L.; Xiang, S. Crystal Structure of Urea Carboxylase Provides Insights into the Carboxyltransfer Reaction. *J. Biol. Chem.* **2012**, *287*, 9389–9398.
- (76) Kanamori, T.; Kanou, N.; Atomi, H.; Imanaka, T. Enzymatic Characterization of a Prokaryotic Urea Carboxylase. *J. Bacteriol.* **2004**, *186*, 2532–2539.
- (77) Furie, B.; Furie, B. C. Molecular Basis of Vitamin K-Dependent Gamma-Carboxylation. *Blood* **1990**, *75*, 1753–1762.
- (78) Esmon, C. T.; Sadowski, J. A.; Suttie, J. W. A New Carboxylation Reaction. The Vitamin K-Dependent Incorporation of H-14-CO₃²⁻ into Prothrombin. *J. Biol. Chem.* **1975**, *250*, 4744–4748.
- (79) Dibenedetto, A.; Lo Noce, R.; Pastore, C.; Aresta, M.; Fragale, C. First in Vitro Use of the Phenylphosphate Carboxylase Enzyme in Supercritical CO₂ for the Selective Carboxylation of Phenol to 4-Hydroxybenzoic Acid. *Environ. Chem. Lett.* **2006**, *3*, 145–148.
- (80) Schühle, K.; Fuchs, G. Phenylphosphate Carboxylase: A New C-C Lyase Involved in Anaerobic Phenol Metabolism in *Thauera Aromatica*. *J. Bacteriol.* **2004**, *186*, 4556–4567.
- (81) Bar-On, Y. M.; Milo, R. The Global Mass and Average Rate of Rubisco. *Proc. Natl. Acad. Sci. U. S. A.* **2019**, *116*, 4738–4743.
- (82) Bar-On, Y. M.; Phillips, R.; Milo, R. The Biomass Distribution on Earth. *Proc. Natl. Acad. Sci. U. S. A.* **2018**, *115*, 6506–6511.
- (83) Tabita, F. R.; Hanson, T. E.; Li, H.; Satagopan, S.; Singh, J.; Chan, S. Function, Structure, and Evolution of the Rubisco-Like Proteins and Their Rubisco Homologs. *Microbiol. Mol. Biol. Rev.* **2007**, *71*, 576–599.
- (84) Andersson, I.; Backlund, A. Structure and Function of Rubisco. *Plant Physiol. Biochem.* **2008**, *46*, 275–291.
- (85) Erb, T. J.; Zarzycki, J. A Short History of Rubisco: The Rise and Fall (?) of Nature's Predominant CO₂ Fixing Enzyme. *Curr. Opin. Biotechnol.* **2018**, *49*, 100–107.
- (86) Andersson, I. Catalysis and Regulation in Rubisco. *J. Exp. Bot.* **2007**, *59*, 1555–1568.
- (87) Schulz, L.; Guo, Z.; Zarzycki, J.; Steinchen, W.; Schuller, J. M.; Heimerl, T.; Prinz, S.; Mueller-Cajar, O.; Erb, T. J.; Hochberg, G. K. A. Evolution of Increased Complexity and Specificity at the Dawn of Form I Rubiscos. *Science* **2022**, *378*, 155–160.
- (88) Frolov, E. N.; Kublanov, I. V.; Toshchakov, S. V.; Lunev, E. A.; Pimenov, N. V.; Bonch-Osmolovskaya, E. A.; Lebedinsky, A. V.; Chernyh, N. A. Form III Rubisco-Mediated Transaldolase Variant of the Calvin Cycle in a Chemolithoautotrophic Bacterium. *Proc. Natl. Acad. Sci. U. S. A.* **2019**, *116*, 18638–18646.
- (89) Satagopan, S.; Chan, S.; Perry, L. J.; Tabita, F. R. Structure-Function Studies with the Unique Hexameric Form II Ribulose-1, 5-Bisphosphate Carboxylase/Oxygenase (Rubisco) from *Rhodospseudomonas Palustris*. *J. Biol. Chem.* **2014**, *289*, 21433–21450.
- (90) Kitano, K.; Maeda, N.; Fukui, T.; Atomi, H.; Imanaka, T.; Miki, K. Crystal Structure of a Novel-Type Archaeal Rubisco with Pentagonal Symmetry. *Structure* **2001**, *9*, 473–481.
- (91) Hanson, T. E.; Tabita, F. R. A Ribulose-1, 5-Bisphosphate Carboxylase/Oxygenase (Rubisco)-Like Protein from *Chlorobium Tepidum* That Is Involved with Sulfur Metabolism and the Response to Oxidative Stress. *Proc. Natl. Acad. Sci. U. S. A.* **2001**, *98*, 4397–4402.
- (92) Imker, H. J.; Fedorov, A. A.; Fedorov, E. V.; Almo, S. C.; Gerlt, J. A. Mechanistic Diversity in the Rubisco Superfamily: The “Enolase” in the Methionine Salvage Pathway in *Geobacillus Kaustophilus*. *Biochemistry* **2007**, *46*, 4077–4089.
- (93) Imker, H. J.; Singh, J.; Warlick, B. P.; Tabita, F. R.; Gerlt, J. A. Mechanistic Diversity in the Rubisco Superfamily: A Novel Isomerization Reaction Catalyzed by the Rubisco-Like Protein from *Rhodospirillum Rubrum*. *Biochemistry* **2008**, *47*, 11171–11173.
- (94) Carter, M. S.; Zhang, X.; Huang, H.; Bouvier, J. T.; Francisco, B. S.; Vetting, M. W.; Al-Obaidi, N.; Bonanno, J. B.; Ghosh, A.; Zallot, R. G.; Andersen, H. M.; Almo, S. C.; Gerlt, J. A. Functional Assignment of Multiple Catabolic Pathways for D-Apiose. *Nat. Chem. Biol.* **2018**, *14*, 696–705.
- (95) Kim, S. M.; Lim, H. S.; Lee, S. B. Discovery of a Rubisco-Like Protein That Functions as an Oxygenase in the Novel D-Hamamelose Pathway. *Biotechnol. Bioeng.* **2018**, *23*, 490–499.
- (96) Andrews, T.; Lorimer, G.; Tolbert, N. Ribulose Diphosphate Oxygenase. I. Synthesis of Phosphoglycolate by Fraction-I Protein of Leaves. *Biochemistry* **1973**, *12*, 11–18.
- (97) Cegelski, L.; Schaefer, J. Nmr Determination of Photorespiration in Intact Leaves Using in Vivo ¹³CO₂ Labeling. *J. Magn. Reson.* **2006**, *178*, 1–10.
- (98) Eisenhut, M.; Roell, M. S.; Weber, A. P. Mechanistic Understanding of Photorespiration Paves the Way to a New Green Revolution. *New Phytologist* **2019**, *223*, 1762–1769.
- (99) Bathellier, C.; Tcherkez, G.; Lorimer, G. H.; Farquhar, G. D. Rubisco Is Not Really So Bad. *Plant Cell Environ* **2018**, *41*, 705–716.
- (100) Bathellier, C.; Yu, L. J.; Farquhar, G. D.; Coote, M. L.; Lorimer, G. H.; Tcherkez, G. Ribulose 1,5-Bisphosphate Carboxylase/Oxygenase Activates O₂ by Electron Transfer. *Proc. Natl. Acad. Sci. U. S. A.* **2020**, *117*, 24234–24242.
- (101) Turmo, A.; Gonzalez-Esquer, C. R.; Kerfeld, C. A. Carboxysomes: Metabolic Modules for CO₂ Fixation. *FEMS Microbiol. Lett.* **2017**, *364*, fnx176.
- (102) Barrett, J.; Girr, P.; Mackinder, L. C. Pyrenoids: CO₂-Fixing Phase Separated Liquid Organelles. *Biochim. Biophys. Acta, Mol. Cell Res.* **2021**, *1868*, 118949.
- (103) Bräutigam, A.; Schlüter, U.; Eisenhut, M.; Gowik, U. On the Evolutionary Origin of CAM Photosynthesis. *Plant Physiol.* **2017**, *174*, 473–477.
- (104) Edmondson, D. L.; Kane, H. J.; Andrews, T. J. Substrate Isomerization Inhibits Ribulosebisphosphate Carboxylase-Oxygenase During Catalysis. *FEBS Lett.* **1990**, *260*, 62–66.
- (105) Schloss, J. V.; Lorimer, G. H. The Stereochemical Course of Ribulosebisphosphate Carboxylase. Reductive Trapping of the 6-Carbon Reaction-Intermediate. *J. Biol. Chem.* **1982**, *257*, 4691–4694.
- (106) Parry, M. A.; Keys, A. J.; Madgwick, P. J.; Carmo-Silva, A. E.; Andralojc, P. J. Rubisco Regulation: A Role for Inhibitors. *J. Exp. Bot.* **2007**, *59*, 1569–1580.
- (107) Hayer-Hartl, M. From Chaperonins to Rubisco Assembly and Metabolic Repair. *Protein Sci.* **2017**, *26*, 2324–2333.
- (108) Matsumura, H.; Xie, Y.; Shirakata, S.; Inoue, T.; Yoshinaga, T.; Ueno, Y.; Izui, K.; Kai, Y. Crystal Structures of C4 Form Maize and Quaternary Complex of E. Coli Phosphoenolpyruvate Carboxylases. *Structure* **2002**, *10*, 1721–1730.
- (109) Gago, G.; Diacovich, L.; Arabolaza, A.; Tsai, S.-C.; Gramajo, H. Fatty Acid Biosynthesis in Actinomycetes. *FEMS Microbiol. Rev.* **2011**, *35*, 475–497.
- (110) Chuakrut, S.; Arai, H.; Ishii, M.; Igarashi, Y. Characterization of a Bifunctional Archaeal Acyl Coenzyme a Carboxylase. *J. Bacteriol.* **2003**, *185*, 938–947.
- (111) Chen, P. Y.-T.; Li, B.; Drennan, C. L.; Elliott, S. J. A Reverse TCA Cycle 2-Oxoacid: Ferredoxin Oxidoreductase That Makes CC Bonds from CO₂. *Joule* **2019**, *3*, 595–611.
- (112) Chen, P. Y.-T.; Aman, H.; Can, M.; Ragsdale, S. W.; Drennan, C. L. Binding Site for Coenzyme a Revealed in the Structure of Pyruvate: Ferredoxin Oxidoreductase from *Moorella Thermoacetica*. *Proc. Natl. Acad. Sci. U. S. A.* **2018**, *115*, 3846–3851.

- (113) Kim, S.; Lindner, S. N.; Aslan, S.; Yishai, O.; Wenk, S.; Schann, K.; Bar-Even, A. Growth of *E. Coli* on Formate and Methanol Via the Reductive Glycine Pathway. *Nat. Chem. Biol.* **2020**, *16*, 538–545.
- (114) Bang, J.; Hwang, C. H.; Ahn, J. H.; Lee, J. A.; Lee, S. Y. *Escherichia Coli* Is Engineered to Grow on CO₂ and Formic Acid. *Nat. Microbiol.* **2020**, *5*, 1459–1463.
- (115) Claassens, N. J.; Bordanaba-Florit, G.; Cotton, C. A. R.; De Maria, A.; Finger-Bou, M.; Friedeheim, L.; Giner-Laguarda, N.; Munar-Palmer, M.; Newell, W.; Scarinci, G.; et al. Replacing the Calvin Cycle with the Reductive Glycine Pathway in *Cupriavidus Necator*. *Metab. Eng.* **2020**, *62*, 30–41.
- (116) Dronsella, B.; Orsi, E.; Benito-Vaquero, S.; Glatter, T.; Bar-Even, A.; Erb, T. J.; Claassens, N. J. Engineered Synthetic One-Carbon Fixation Exceeds Yield of the Calvin Cycle. *bioRxiv* **2022**, 10.19.512895.
- (117) Bar-Even, A. Formate Assimilation: The Metabolic Architecture of Natural and Synthetic Pathways. *Biochemistry* **2016**, *55*, 3851–3863.
- (118) Bang, J.; Lee, S. Y. Assimilation of Formic Acid and CO₂ by Engineered *Escherichia Coli* Equipped with Reconstructed One-Carbon Assimilation Pathways. *Proc. Natl. Acad. Sci. U. S. A.* **2018**, *115*, E9271–E9279.
- (119) Bar-Even, A.; Noor, E.; Flamholz, A.; Milo, R. Design and Analysis of Metabolic Pathways Supporting Formatotrophic Growth for Electricity-Dependent Cultivation of Microbes. *Biochim. Biophys. Acta* **2013**, *1827*, 1039–1047.
- (120) Zhang, H.; Li, Y.; Nie, J.; Ren, J.; Zeng, A. P. Structure-Based Dynamic Analysis of the Glycine Cleavage System Suggests Key Residues for Control of a Key Reaction Step. *Commun. Biol.* **2020**, *3*, 756.
- (121) Moon, M.; Park, G. W.; Lee, J.-p.; Lee, J.-S.; Min, K. Recent Progress in Formate Dehydrogenase (FDH) as a Non-Photosynthetic CO₂ Utilizing Enzyme: A Short Review. *J. CO₂ Util.* **2020**, *42*, 101353.
- (122) Oliveira, A. R.; Mota, C.; Mourato, C. u.; Domingos, R. M.; Santos, M. F.; Gesto, D.; Guigliarelli, B.; Santos-Silva, T.; Romão, M. J. o.; Cardoso Pereira, I. s. A. Toward the Mechanistic Understanding of Enzymatic CO₂ Reduction. *ACS Catal.* **2020**, *10*, 3844–3856.
- (123) Wang, S.; Huang, H.; Kahnt, J.; Mueller, A. P.; Kopke, M.; Thauer, R. K. NADP-Specific Electron-Bifurcating [FeFe]-Hydrogenase in a Functional Complex with Formate Dehydrogenase in *Clostridium Autoethanogenum* Grown on CO. *J. Bacteriol.* **2013**, *195*, 4373–4386.
- (124) Wang, S.; Huang, H.; Kahnt, J.; Thauer, R. K. *Clostridium Acidurici* Electron-Bifurcating Formate Dehydrogenase. *Appl. Environ. Microbiol.* **2013**, *79*, 6176–6179.
- (125) Schuchmann, K.; Muller, V. Direct and Reversible Hydrogenation of CO₂ to Formate by a Bacterial Carbon Dioxide Reductase. *Science* **2013**, *342*, 1382–1385.
- (126) Schwarz, F. M.; Schuchmann, K.; Muller, V. Hydrogenation of CO₂ at Ambient Pressure Catalyzed by a Highly Active Thermostable Biocatalyst. *Biotechnol. Biofuels* **2018**, *11*, 237.
- (127) Reda, T.; Plugge, C. M.; Abram, N. J.; Hirst, J. Reversible Interconversion of Carbon Dioxide and Formate by an Electroactive Enzyme. *Proc. Natl. Acad. Sci. U. S. A.* **2008**, *105*, 10654–10658.
- (128) Meneghello, M.; Léger, C.; Fourmond, V. Electrochemical Studies of CO₂-Reducing Metalloenzymes. *Chem. Eur. J.* **2021**, *27*, 17542–17553.
- (129) Maia, L. B.; Fonseca, L.; Moura, I.; Moura, J. J. Reduction of Carbon Dioxide by a Molybdenum-Containing Formate Dehydrogenase: A Kinetic and Mechanistic Study. *J. Am. Chem. Soc.* **2016**, *138*, 8834–8846.
- (130) Niks, D.; Hille, R. Molybdenum- and Tungsten-Containing Formate Dehydrogenases and Formylmethanofuran Dehydrogenases: Structure, Mechanism, and Cofactor Insertion. *Protein Sci.* **2019**, *28*, 111–122.
- (131) Schrapers, P.; Hartmann, T.; Kositzki, R.; Dau, H.; Reschke, S.; Schulzke, C.; Leimkuhler, S.; Haumann, M. Sulfido and Cysteine Ligation Changes at the Molybdenum Cofactor During Substrate Conversion by Formate Dehydrogenase (FDH) from *Rhodobacter Capsulatus*. *Inorg. Chem.* **2015**, *54*, 3260–3271.
- (132) Drennan, C. L.; Heo, J.; Sintchak, M. D.; Schreiter, E.; Ludden, P. W. Life on Carbon Monoxide: X-Ray Structure of *Rhodospirillum Rubrum* Ni-Fe-S Carbon Monoxide Dehydrogenase. *Proc. Natl. Acad. Sci. U. S. A.* **2001**, *98*, 11973–11978.
- (133) Ragsdale, S. W. Life with Carbon Monoxide. *Crit. Rev. Biochem. Mol. Biol.* **2004**, *39*, 165–195.
- (134) Maynard, E. L.; Lindahl, P. A. Evidence of a Molecular Tunnel Connecting the Active Sites for CO₂ Reduction and Acetyl-CoA Synthesis in Acetyl-CoA Synthase from *Clostridium Thermoaceticum*. *J. Am. Chem. Soc.* **1999**, *121*, 9221–9222.
- (135) Wilson, M. C.; Moore, B. S. Beyond Ethylmalonyl-CoA: The Functional Role of Crotonyl-CoA Carboxylase/Reductase Homologs in Expanding Polyketide Diversity. *Nat. Prod. Rep.* **2012**, *29*, 72–86.
- (136) Vogeli, B.; Geyer, K.; Gerlinger, P. D.; Benkstein, S.; Cortina, N. S.; Erb, T. J. Combining Promiscuous Acyl-CoA Oxidase and Enoyl-CoA Carboxylase/Reductases for Atypical Polyketide Extender Unit Biosynthesis. *Cell Chem. Biol.* **2018**, *25*, 833–839.
- (137) Schwander, T.; Schada von Borzyskowski, L.; Burgener, S.; Cortina, N. S.; Erb, T. J. A Synthetic Pathway for the Fixation of Carbon Dioxide in Vitro. *Science* **2016**, *354*, 900–904.
- (138) Stoffel, G. M.; Saez, D. A.; DeMirci, H.; Vögeli, B.; Rao, Y.; Zarzycki, J.; Yoshikuni, Y.; Wakatsuki, S.; Vöhringer-Martinez, E.; Erb, T. J. Four Amino Acids Define the CO₂ Binding Pocket of Enoyl-CoA Carboxylases/Reductases. *Proc. Natl. Acad. Sci. U. S. A.* **2019**, *116*, 13964–13969.
- (139) Vögeli, B.; Erb, T. J. ‘Negative’ and ‘Positive Catalysis’: Complementary Principles That Shape the Catalytic Landscape of Enzymes. *Curr. Opin. Chem. Biol.* **2018**, *47*, 94–100.
- (140) Rosenthal, R. G.; Vogeli, B.; Wagner, T.; Shima, S.; Erb, T. J. A Conserved Threonine Prevents Self-Intoxication of Enoyl-Thioester Reductases. *Nat. Chem. Biol.* **2017**, *13*, 745–749.
- (141) Vogeli, B.; Rosenthal, R. G.; Stoffel, G. M. M.; Wagner, T.; Kiefer, P.; Cortina, N. S.; Shima, S.; Erb, T. J. Inha, the Enoyl-Thioester Reductase from *Mycobacterium Tuberculosis* Forms a Covalent Adduct During Catalysis. *J. Biol. Chem.* **2018**, *293*, 17200–17207.
- (142) Ishii, Y.; Narimatsu, Y.; Iwasaki, Y.; Arai, N.; Kino, K.; Kirimura, K. Reversible and Nonoxidative Gamma-Resorcylic Acid Decarboxylase: Characterization and Gene Cloning of a Novel Enzyme Catalyzing Carboxylation of Resorcinol, 1,3-Dihydroxybenzene, from *Rhizobium Radiobacter*. *Biochem. Biophys. Res. Co.* **2004**, *324*, 611–620.
- (143) Yoshida, T.; Hayakawa, Y.; Matsui, T.; Nagasawa, T. Purification and Characterization of 2,6-Dihydroxybenzoate Decarboxylase Reversibly Catalyzing Nonoxidative Decarboxylation. *Arch. Microbiol.* **2004**, *181*, 391–397.
- (144) Goto, M.; Hayashi, H.; Miyahara, I.; Hirotsu, K.; Yoshida, M.; Oikawa, T. Crystal Structures of Nonoxidative Zinc-Dependent 2,6-Dihydroxybenzoate (γ -Resorcyate) Decarboxylase from *Rhizobium Sp.* Strain MTP-10005. *J. Biol. Chem.* **2006**, *281*, 34365–34373.
- (145) Lindsey, A. S.; Jeskey, H. The Kolbe-Schmitt Reaction. *Chem. Rev.* **1957**, *57*, 583–620.
- (146) Saaret, A.; Balaikaite, A.; Leys, D. Biochemistry of Prenylated-FMN Enzymes. *Enzymes* **2020**, *47*, 517–549.
- (147) Zeug, M.; Markovic, N.; Iancu, C. V.; Tripp, J.; Oreb, M.; Choe, J. Y. Crystal Structures of Non-Oxidative Decarboxylases Reveal a New Mechanism of Action with a Catalytic Dyad and Structural Twists. *Sci. Rep.* **2021**, *11*, 3056.
- (148) Miyazaki, M.; Shibue, M.; Ogino, K.; Nakamura, H.; Maeda, H. Enzymatic Synthesis of Pyruvic Acid from Acetaldehyde and Carbon Dioxide. *Chem. Commun.* **2001**, 1800–1801.
- (149) Tong, X.; El-Zahab, B.; Zhao, X.; Liu, Y.; Wang, P. Enzymatic Synthesis of L-Lactic Acid from Carbon Dioxide and Ethanol with an Inherent Cofactor Regeneration Cycle. *Biotechnol. Bioeng.* **2011**, *108*, 465–469.
- (150) Peng, X.; Masai, E.; Kasai, D.; Miyauchi, K.; Katayama, Y.; Fukuda, M. A Second 5-Carboxyvanillate Decarboxylase Gene, LigW2, Is Important for Lignin-Related Biphenyl Catabolism in *Sphingomonas Paucimobilis* SYK-6. *Appl. Environ. Microbiol.* **2005**, *71*, 5014–5021.

- (151) Yoshida, M.; Fukuhara, N.; Oikawa, T. Thermophilic, Reversible γ -Resorcyate Decarboxylase from *Rhizobium* Sp. Strain MTP-10005: Purification, Molecular Characterization, and Expression. *J. Bacteriol.* **2004**, *186*, 6855–6863.
- (152) Wuensch, C.; Glueck, S. M.; Gross, J.; Koszelewski, D.; Schober, M.; Faber, K. Regioselective Enzymatic Carboxylation of Phenols and Hydroxystyrene Derivatives. *Org. Lett.* **2012**, *14*, 1974–1977.
- (153) Xu, S.; Li, W.; Zhu, J.; Wang, R.; Li, Z.; Xu, G.-L.; Ding, J. Crystal Structures of Isoorotate Decarboxylases Reveal a Novel Catalytic Mechanism of 5-Carboxyl-Uracil Decarboxylation and Shed Light on the Search for DNA Decarboxylase. *Cell Res.* **2013**, *23*, 1296.
- (154) Kino, K.; Hirokawa, Y.; Gawasawa, R.; Murase, R.; Tsuchihashi, R.; Hara, R. Screening, Gene Cloning, and Characterization of Orsellinic Acid Decarboxylase from *Arthrobacter* Sp. K8 for Regio-Selective Carboxylation of Resorcinol Derivatives. *J. Biotechnol.* **2020**, *323*, 128–135.
- (155) Hofer, G.; Sheng, X.; Braeuer, S.; Payer, S. E.; Plasch, K.; Goessler, W.; Faber, K.; Keller, W.; Himo, F.; Glueck, S. M. Metal Ion Promiscuity and Structure of 2,3-Dihydroxybenzoic Acid Decarboxylase of *Aspergillus Oryzae*. *ChemBioChem* **2021**, *22*, 652–656.
- (156) Sheng, X.; Patskovsky, Y.; Vladimirova, A.; Bonanno, J. B.; Almo, S. C.; Himo, F.; Raushel, F. M. Mechanism and Structure of γ -Resorcyate Decarboxylase. *Biochemistry* **2018**, *57*, 3167–3175.
- (157) Pesci, L.; Kara, S.; Liese, A. Evaluation of the Substrate Scope of Benzoic Acid (De)Carboxylases According to Chemical and Biochemical Parameters. *ChemBioChem* **2016**, *17*, 1845–1850.
- (158) Wuensch, C.; Gross, J.; Steinkellner, G.; Lyskowski, A.; Gruber, K.; Glueck, S. M.; Faber, K. Regioselective *Ortho*-Carboxylation of Phenols Catalyzed by Benzoic Acid Decarboxylases: A Biocatalytic Equivalent to the Kolbe-Schmitt Reaction. *RSC Adv.* **2014**, *4*, 9673–9679.
- (159) Pesci, L.; Gurikov, P.; Liese, A.; Kara, S. Amine-Mediated Enzymatic Carboxylation of Phenols Using CO₂ as Substrate Increases Equilibrium Conversions and Reaction Rates. *Biotechnol. J.* **2017**, *12*, 1700332.
- (160) Plasch, K.; Resch, V.; Hitce, J.; Popłoński, J.; Faber, K.; Glueck, S. M. Regioselective Enzymatic Carboxylation of Bioactive (Poly)-Phenols. *Adv. Synth. Catal.* **2017**, *359*, 959–965.
- (161) Meyer, L.-E.; Plasch, K.; Kragl, U.; von Langermann, J. Adsorbent-Based Downstream-Processing of the Decarboxylase-Based Synthesis of 2,6-Dihydroxy-4-Methylbenzoic Acid. *Org. Process Res. Dev.* **2018**, *22*, 963–970.
- (162) Peng, C.; Liu, Y.; Guo, X.; Liu, W.; Li, Q.; Zhao, Z. K. Selective Carboxylation of Substituted Phenols with Engineered *Escherichia Coli* Whole-Cells. *Tetrahedron Lett.* **2018**, *59*, 3810–3815.
- (163) Plasch, K.; Hofer, G.; Keller, W.; Hay, S.; Heyes, D. J.; Dennig, A.; Glueck, S. M.; Faber, K. Pressurized CO₂ as a Carboxylating Agent for the Biocatalytic *Ortho*-Carboxylation of Resorcinol. *Green Chem.* **2018**, *20*, 1754–1759.
- (164) Zhang, X.; Ren, J.; Yao, P.; Gong, R.; Wang, M.; Wu, Q.; Zhu, D. Biochemical Characterization and Substrate Profiling of a Reversible 2,3-Dihydroxybenzoic Acid Decarboxylase for Biocatalytic Kolbe-Schmitt Reaction. *Enzyme Microb. Technol.* **2018**, *113*, 37–43.
- (165) Song, M.; Zhang, X.; Liu, W.; Feng, J.; Cui, Y.; Yao, P.; Wang, M.; Guo, R. T.; Wu, Q.; Zhu, D. 2,3-Dihydroxybenzoic Acid Decarboxylase from *Fusarium Oxysporum*: Crystal Structures and Substrate Recognition Mechanism. *ChemBioChem* **2020**, *21*, 2950–2956.
- (166) Wuensch, C.; Schmidt, N.; Gross, J.; Grischek, B.; Glueck, S. M.; Faber, K. Pushing the Equilibrium of Regio-Complementary Carboxylation of Phenols and Hydroxystyrene Derivatives. *J. Biotechnol.* **2013**, *168*, 264–270.
- (167) Sato, M.; Sakurai, N.; Suzuki, H.; Shibata, D.; Kino, K. Enzymatic Carboxylation of Hydroxystilbenes by the γ -Resorcylic Acid Decarboxylase from *Rhizobium Radiobacter* WU-0108 under Reverse Reaction Conditions. *J. Mol. Catal. B: Enzym.* **2015**, *122*, 348–352.
- (168) Kirimura, K.; Gunji, H.; Wakayama, R.; Hattori, T.; Ishii, Y. Enzymatic Kolbe-Schmitt Reaction to Form Salicylic Acid from Phenol: Enzymatic Characterization and Gene Identification of a Novel Enzyme, *Trichosporon Moniliiforme* Salicylic Acid Decarboxylase. *Biochem. Biophys. Res. Co.* **2010**, *394*, 279–284.
- (169) Kirimura, K.; Yanaso, S.; Kosaka, S.; Koyama, K.; Hattori, T.; Ishii, Y. Production of *p*-Aminosalicylic Acid through Enzymatic Kolbe-Schmitt Reaction Catalyzed by Reversible Salicylic Acid Decarboxylase. *Chem. Lett.* **2011**, *40*, 206–208.
- (170) Ienaga, S.; Kosaka, S.; Honda, Y.; Ishii, Y.; Kirimura, K. *p*-Aminosalicylic Acid Production by Enzymatic Kolbe-Schmitt Reaction Using Salicylic Acid Decarboxylases Improved through Site-Directed Mutagenesis. *Bull. Chem. Soc. Jpn.* **2013**, *86*, 628–634.
- (171) Peng, X.; Masai, E.; Kitayama, H.; Harada, K.; Katayama, Y.; Fukuda, M. Characterization of the 5-Carboxyvanillate Decarboxylase Gene and Its Role in Lignin-Related Biphenyl Catabolism in *Sphingomonas Paucimobilis* SYK-6. *Appl. Environ. Microbiol.* **2002**, *68*, 4407–4415.
- (172) Vladimirova, A.; Patskovsky, Y.; Fedorov, A. A.; Bonanno, J. B.; Fedorov, E. V.; Toro, R.; Hillerich, B.; Seidel, R. D.; Richards, N. G. J.; Almo, S. C.; et al. Substrate Distortion and the Catalytic Reaction Mechanism of 5-Carboxyvanillate Decarboxylase. *J. Am. Chem. Soc.* **2016**, *138*, 826–836.
- (173) Sheng, X.; Plasch, K.; Payer, S. E.; Ertl, C.; Hofer, G.; Keller, W.; Braeuer, S.; Goessler, W.; Glueck, S. M.; Himo, F.; Faber, K. Reaction Mechanism and Substrate Specificity of Iso-Orotate Decarboxylase: A Combined Theoretical and Experimental Study. *Front. Chem.* **2018**, *6*, 608.
- (174) Sheng, X.; Zhu, W.; Huddleston, J.; Xiang, D. F.; Raushel, F. M.; Richards, N. G. J.; Himo, F. A Combined Experimental-Theoretical Study of the LigW-Catalyzed Decarboxylation of 5-Carboxyvanillate in the Metabolic Pathway for Lignin Degradation. *ACS Catal.* **2017**, *7*, 4968–4974.
- (175) Ohde, D.; Thomas, B.; Matthes, S.; Percin, Z.; Engelmann, C.; Bubenheim, P.; Terasaka, K.; Schluter, M.; Liese, A. Fine Bubble-Based CO₂ Capture Mediated by Triethanolamine Coupled to Whole Cell Biotransformation. *Chem. Ing. Tech.* **2019**, *91*, 1822–1826.
- (176) Wuensch, C.; Pavkov-Keller, T.; Steinkellner, G.; Gross, J.; Fuchs, M.; Hromic, A.; Lyskowski, A.; Fauland, K.; Gruber, K.; Glueck, S. M.; et al. Regioselective Enzymatic *Beta*-Carboxylation of *Para*-Hydroxy-Styrene Derivatives Catalyzed by Phenolic Acid Decarboxylases. *Adv. Synth. Catal.* **2015**, *357*, 1909–1918.
- (177) Tinikul, R.; Chenprakhon, P.; Maenpuen, S.; Chaiyen, P. Biotransformation of Plant-Derived Phenolic Acids. *Biotechnol. J.* **2018**, *13*, No. 1700632.
- (178) Kourist, R.; Guterl, J. K.; Miyamoto, K.; Sieber, V. Enzymatic Decarboxylation—an Emerging Reaction for Chemicals Production from Renewable Resources. *ChemCatChem* **2014**, *6*, 689–701.
- (179) Rodriguez, H.; Landete, J. M.; Curiel, J. A.; de Las Rivas, B.; Mancheno, J. M.; Munoz, R. Characterization of the *p*-Coumaric Acid Decarboxylase from *Lactobacillus Plantarum* CECT 748(T). *J. Agric. Food. Chem.* **2008**, *56*, 3068–3072.
- (180) Rodriguez, H.; Angulo, I.; de Las Rivas, B.; Campillo, N.; Paez, J. A.; Munoz, R.; Mancheno, J. M. *p*-Coumaric Acid Decarboxylase from *Lactobacillus Plantarum*: Structural Insights into the Active Site and Decarboxylation Catalytic Mechanism. *Proteins* **2010**, *78*, 1662–1676.
- (181) Jung, D. H.; Choi, W.; Choi, K. Y.; Jung, E.; Yun, H.; Kazlauskas, R. J.; Kim, B. G. Bioconversion of *p*-Coumaric Acid to *p*-Hydroxystyrene Using Phenolic Acid Decarboxylase from *B. Amyloliquefaciens* in Biphasic Reaction System. *Appl. Microbiol. Biotechnol.* **2013**, *97*, 1501–1511.
- (182) Frank, A.; Eborall, W.; Hyde, R.; Hart, S.; Turkenburg, J. P.; Grogan, G. Mutational Analysis of Phenolic Acid Decarboxylase from *Bacillus Subtilis* (BsPAD), Which Converts Bio-Derived Phenolic Acids to Styrene Derivatives. *Catal. Sci. Technol.* **2012**, *2*, 1568–1574.
- (183) Cavin, J. F.; Dartois, V.; Divies, C. Gene Cloning, Transcriptional Analysis, Purification, and Characterization of Phenolic Acid Decarboxylase from *Bacillus Subtilis*. *Appl. Environ. Microbiol.* **1998**, *64*, 1466–1471.
- (184) Gu, W.; Yang, J.; Lou, Z.; Liang, L.; Sun, Y.; Huang, J.; Li, X.; Cao, Y.; Meng, Z.; Zhang, K. Q. Structural Basis of Enzymatic Activity

for the Ferulic Acid Decarboxylase (FADase) from *Enterobacter* Sp. P_x6–4. *PLoS One* **2011**, 6, No. e16262.

(185) Sheng, X.; Lind, M. E.; Himo, F. Theoretical Study of the Reaction Mechanism of Phenolic Acid Decarboxylase. *FEBS J.* **2015**, 282, 4703–4713.

(186) Sasano, K.; Takaya, J.; Iwasawa, N. Palladium(II)-Catalyzed Direct Carboxylation of Alkenyl C–H Bonds with CO₂. *J. Am. Chem. Soc.* **2013**, 135, 10954–10957.

(187) Payer, S. E.; Marshall, S. A.; Barland, N.; Sheng, X.; Reiter, T.; Dordic, A.; Steinkellner, G.; Wuensch, C.; Kaltwasser, S.; Fisher, K.; et al. Regioselective *Para*-Carboxylation of Catechols with a Prenylated Flavin Dependent Decarboxylase. *Angew. Chem., Int. Ed.* **2017**, 56, 13893–13897.

(188) Meckenstock, R. U.; Boll, M.; Mouttaki, H.; Koelschbach, J. S.; Cunha Tarouco, P.; Weyrauch, P.; Dong, X.; Himmelberg, A. M. Anaerobic Degradation of Benzene and Polycyclic Aromatic Hydrocarbons. *J. Mol. Microbiol. Biotechnol.* **2016**, 26, 92–118.

(189) Gahloth, D.; Fisher, K.; Payne, K. A. P.; Cliff, M.; Levy, C.; Leys, D. Structural and Biochemical Characterisation of the Prenylated Flavin Mononucleotide-Dependent Indole-3-Carboxylic Acid Decarboxylase. *J. Biol. Chem.* **2022**, 298, 101771.

(190) Omura, H.; Wieser, M.; Nagasawa, T. Pyrrole-2-Carboxylate Decarboxylase from *Bacillus Megaterium* PYR2910, an Organic-Acid-Requiring Enzyme. *Eur. J. Biochem.* **1998**, 253, 480–484.

(191) Payne, K. A.; White, M. D.; Fisher, K.; Khara, B.; Bailey, S. S.; Parker, D.; Rattray, N. J.; Trivedi, D. K.; Goodacre, R.; Beveridge, R.; et al. New Cofactor Supports Alpha,Beta-Unsaturated Acid Decarboxylation Via 1,3-Dipolar Cycloaddition. *Nature* **2015**, 522, 497–501.

(192) Leys, D. Flavin Metamorphosis: Cofactor Transformation through Prenylation. *Curr. Opin. Chem. Biol.* **2018**, 47, 117–125.

(193) Leys, D.; Scrutton, N. S. Sweating the Assets of Flavin Cofactors: New Insight of Chemical Versatility from Knowledge of Structure and Mechanism. *Curr. Opin. Struct. Biol.* **2016**, 41, 19–26.

(194) Marshall, S. A.; Fisher, K.; Ni Cheallaigh, A.; White, M. D.; Payne, K. A.; Parker, D. A.; Rigby, S. E.; Leys, D. Oxidative Maturation and Structural Characterization of Prenylated FMN Binding by UbiD, a Decarboxylase Involved in Bacterial Ubiquinone Biosynthesis. *J. Biol. Chem.* **2017**, 292, 4623–4637.

(195) Abby, S. S.; Kazemzadeh, K.; Vragneau, C.; Pelosi, L.; Pierrel, F. Advances in Bacterial Pathways for the Biosynthesis of Ubiquinone. *Biochim. Biophys. Acta, Bioenerg.* **2020**, 1861, 148259.

(196) Aussel, L.; Pierrel, F.; Loiseau, L.; Lombard, M.; Fontecave, M.; Barras, F. Biosynthesis and Physiology of Coenzyme Q in Bacteria. *Biochim. Biophys. Acta* **2014**, 1837, 1004–1011.

(197) Kopeck, J.; Schnell, R.; Schneider, G. Structure of PA4019, a Putative Aromatic Acid Decarboxylase from *Pseudomonas Aeruginosa*. *Acta Crystallogr., Sect. F* **2011**, 67, 1184–1188.

(198) Marshall, S. A.; Payne, K. A. P.; Fisher, K.; White, M. D.; NiCheallaigh, A.; Balaikaite, A.; Rigby, S. E. J.; Leys, D. The UbiX Flavin Prenyltransferase Reaction Mechanism Resembles Class I Terpene Cyclase Chemistry. *Nat. Commun.* **2019**, 10, 2357.

(199) White, M. D.; Payne, K. A.; Fisher, K.; Marshall, S. A.; Parker, D.; Rattray, N. J.; Trivedi, D. K.; Goodacre, R.; Rigby, S. E.; Scrutton, N. S.; et al. UbiX Is a Flavin Prenyltransferase Required for Bacterial Ubiquinone Biosynthesis. *Nature* **2015**, 522, 502–506.

(200) Lin, F.; Ferguson, K. L.; Boyer, D. R.; Lin, X. N.; Marsh, E. N. G. Isofunctional Enzymes PAD1 and UbiX Catalyze Formation of a Novel Cofactor Required by Ferulic Acid Decarboxylase and 4-Hydroxy-3-Polyprenylbenzoic Acid Decarboxylase. *ACS Chem. Biol.* **2015**, 10, 1137–1144.

(201) Marshall, S. A.; Payne, K. A. P.; Leys, D. The UbiX-UbiD System: The Biosynthesis and Use of Prenylated Flavin (prFMN). *Arch. Biochem. Biophys.* **2017**, 632, 209–221.

(202) Balaikaite, A.; Chisanga, M.; Fisher, K.; Heyes, D. J.; Spiess, R.; Leys, D. Ferulic Acid Decarboxylase Controls Oxidative Maturation of the Prenylated Flavin Mononucleotide Cofactor. *ACS Chem. Biol.* **2020**, 15, 2466–2475.

(203) Bailey, S. S.; Payne, K. A. P.; Fisher, K.; Marshall, S. A.; Cliff, M. J.; Spiess, R.; Parker, D. A.; Rigby, S. E. J.; Leys, D. The Role of

Conserved Residues in Fdc Decarboxylase in Prenylated Flavin Mononucleotide Oxidative Maturation, Cofactor Isomerization, and Catalysis. *J. Biol. Chem.* **2018**, 293, 2272–2287.

(204) Mergelsberg, M.; Willstein, M.; Meyer, H.; Stark, H. J.; Bechtel, D. F.; Pierik, A. J.; Boll, M. Phthaloyl-Coenzyme a Decarboxylase from *Thauera Chlorobenzoica*: The Prenylated Flavin-, K(+) - and Fe(2+) -Dependent Key Enzyme of Anaerobic Phthalate Degradation. *Environ. Microbiol.* **2017**, 19, 3734–3744.

(205) Bergmann, F. D.; Selesi, D.; Meckenstock, R. U. Identification of New Enzymes Potentially Involved in Anaerobic Naphthalene Degradation by the Sulfate-Reducing Enrichment Culture N47. *Arch. Microbiol.* **2011**, 193, 241–250.

(206) Abu Laban, N.; Selesi, D.; Rattei, T.; Tischler, P.; Meckenstock, R. U. Identification of Enzymes Involved in Anaerobic Benzene Degradation by a Strictly Anaerobic Iron-Reducing Enrichment Culture. *Environ. Microbiol.* **2010**, 12, 2783–2796.

(207) Marshall, S. A.; Fisher, K.; Leys, D. The in Vitro Production of prFMN for Reconstitution of UbiD Enzymes. *Methods Mol. Biol.* **2021**, 2280, 219–227.

(208) Marshall, S. A.; Payne, K. A. P.; Fisher, K.; Gahloth, D.; Bailey, S. S.; Balaikaite, A.; Saaret, A.; Gostimskaya, I.; Aleku, G.; Huang, H. et al. Heterologous Production, Reconstitution and EPR Spectroscopic Analysis of prFMN Dependent Enzymes In *Methods in Enzymology*; Palfe, B. A., Ed.; Academic Press, 2019; Vol. 620, section 19, pp 489–508.

(209) Batyrova, K. A.; Khusnutdinova, A. N.; Wang, P. H.; Di Leo, R.; Flick, R.; Edwards, E. A.; Savchenko, A.; Yakunin, A. F. Biocatalytic in Vitro and in Vivo FMN Prenylation and (De)Carboxylase Activation. *ACS Chem. Biol.* **2020**, 15, 1874–1882.

(210) Annal, T.; Han, L.; Rudolf, J. D.; Xie, G.; Yang, D.; Chang, C.-Y.; Ma, M.; Crnovcic, I.; Miller, M. D.; Soman, J.; et al. Biochemical and Structural Characterization of TtnD, a Prenylated FMN-Dependent Decarboxylase from the Tautomycin Biosynthetic Pathway. *ACS Chem. Biol.* **2018**, 13, 2728–2738.

(211) Aleku, G. A.; Saaret, A.; Bradshaw-Allen, R. T.; Derrington, S. R.; Titchiner, G. R.; Gostimskaya, I.; Gahloth, D.; Parker, D. A.; Hay, S.; Leys, D. Enzymatic C–H Activation of Aromatic Compounds through CO₂ Fixation. *Nat. Chem. Biol.* **2020**, 16, 1255–1260.

(212) Aleku, G. A.; Prause, C.; Bradshaw-Allen, R. T.; Plasch, K.; Glueck, S. M.; Bailey, S. S.; Payne, K. A. P.; Parker, D. A.; Faber, K.; Leys, D. Terminal Alkenes from Acrylic Acid Derivatives Via Non-Oxidative Enzymatic Decarboxylation by Ferulic Acid Decarboxylases. *ChemCatChem* **2018**, 10, 3736–3745.

(213) Lan, C. L.; Chen, S. L. The Decarboxylation of Alpha,Beta-Unsaturated Acid Catalyzed by Prenylated FMN-Dependent Ferulic Acid Decarboxylase and the Enzyme Inhibition. *J. Org. Chem.* **2016**, 81, 9289–9295.

(214) Nagy, E. Z. A.; Nagy, C. L.; Filip, A.; Nagy, K.; Gál, E.; Tóth, R.; Poppe, L.; Paizs, C.; Bencze, L. C. Exploring the Substrate Scope of Ferulic Acid Decarboxylase (FDC1) from *Saccharomyces Cerevisiae*. *Sci. Rep.* **2019**, 9, 647.

(215) Ferguson, K. L.; Arunrattanamook, N.; Marsh, E. N. Mechanism of the Novel Prenylated Flavin-Containing Enzyme Ferulic Acid Decarboxylase Probed by Isotope Effects and Linear Free-Energy Relationships. *Biochemistry* **2016**, 55, 2857–2863.

(216) Bhuiya, M. W.; Lee, S. G.; Jez, J. M.; Yu, O. Structure and Mechanism of Ferulic Acid Decarboxylase (FDC1) from *Saccharomyces Cerevisiae*. *Appl. Environ. Microbiol.* **2015**, 81, 4216–4223.

(217) Duta, H.; Filip, A.; Nagy, L. C.; Nagy, E. Z. A.; Tóth, R.; Bencze, L. C. Toolbox for the Structure-Guided Evolution of Ferulic Acid Decarboxylase (FDC). *Sci. Rep.* **2022**, 12, 3347.

(218) Payne, K. A. P.; Marshall, S. A.; Fisher, K.; Cliff, M. J.; Cannas, D. M.; Yan, C.; Heyes, D. J.; Parker, D. A.; Larrosa, I.; Leys, D. Enzymatic Carboxylation of 2-Furoic Acid Yields 2,5-Furandicarboxylic Acid (FDCA). *ACS Catal.* **2019**, 9, 2854–2865.

(219) Lupa, B.; Lyon, D.; Gibbs, M. D.; Reeves, R. A.; Wiegel, J. Distribution of Genes Encoding the Microbial Non-Oxidative Reversible Hydroxyarylic Acid Decarboxylases/Phenol Carboxylases. *Genomics* **2005**, 86, 342–351.

- (220) Yoshida, T.; Inami, Y.; Matsui, T.; Nagasawa, T. Regioselective Carboxylation of Catechol by 3,4-Dihydroxybenzoate Decarboxylase of *Enterobacter Cloacae* P. *Biotechnol. Lett.* **2010**, *32*, 701–705.
- (221) Wieser, M.; Fujii, N.; Yoshida, T.; Nagasawa, T. Carbon Dioxide Fixation by Reversible Pyrrole-2-Carboxylate Decarboxylase from *Bacillus Megaterium* PYR2910. *Eur. J. Biochem.* **1998**, *257*, 495–499.
- (222) Wieser, M.; Yoshida, T.; Nagasawa, T. Microbial Synthesis of Pyrrole-2-Carboxylate by *Bacillus Megaterium* PYR2910. *Tetrahedron Lett.* **1998**, *39*, 4309–4310.
- (223) Matsuda, T.; Marukado, R.; Koguchi, S.; Nagasawa, T.; Mukouyama, M.; Harada, T.; Nakamura, K. Novel Continuous Carboxylation Using Pressurized Carbon Dioxide by Immobilized Decarboxylase. *Tetrahedron Lett.* **2008**, *49*, 6019–6020.
- (224) Payne, K. A. P.; Marshall, S. A.; Fisher, K.; Rigby, S. E. J.; Cliff, M. J.; Spiess, R.; Cannas, D. M.; Larrosa, I.; Hay, S.; Leys, D. Structure and Mechanism of *Pseudomonas Aeruginosa* PA0254/Huda, a prFMN-Dependent Pyrrole-2-Carboxylic Acid Decarboxylase Linked to Virulence. *ACS Catal.* **2021**, *11*, 2865–2878.
- (225) Jacewicz, A.; Izumi, A.; Brunner, K.; Schnell, R.; Schneider, G. Structural Insights into the UbiD Protein Family from the Crystal Structure of PA0254 from *Pseudomonas Aeruginosa*. *PLOS ONE* **2013**, *8*, No. e63161.
- (226) Yoshida, T.; Fujita, K.; Nagasawa, T. Novel Reversible Indole-3-Carboxylate Decarboxylase Catalyzing Nonoxidative Decarboxylation. *Biosci. Biotechnol. Biochem.* **2002**, *66*, 2388–2394.
- (227) Datar, P. M.; Marsh, E. N. G. Decarboxylation of Aromatic Carboxylic Acids by the Prenylated-FMN-Dependent Enzyme Phenazine-1-Carboxylic Acid Decarboxylase. *ACS Catal.* **2021**, *11*, 11723–11732.
- (228) Kawanabe, K.; Aono, R.; Kino, K. 2,5-Furandicarboxylic Acid Production from Furfural by Sequential Biocatalytic Reactions. *J. Biosci. Bioeng.* **2021**, *132*, 18–24.
- (229) Kaneshiro, A. K.; Koebke, K. J.; Zhao, C.; Ferguson, K. L.; Ballou, D. P.; Palfey, B. A.; Ruotolo, B. T.; Marsh, E. N. G. Kinetic Analysis of Transient Intermediates in the Mechanism of Prenyl-Flavin-Dependent Ferulic Acid Decarboxylase. *Biochemistry* **2021**, *60*, 125–134.
- (230) Beveridge, R.; Migas, L. G.; Payne, K. A.; Scrutton, N. S.; Leys, D.; Barran, P. E. Mass Spectrometry Locates Local and Allosteric Conformational Changes That Occur on Cofactor Binding. *Nat. Commun.* **2016**, *7*, 12163.
- (231) Marshall, S. A.; Payne, K. A. P.; Fisher, K.; Titchiner, G. R.; Levy, C.; Hay, S.; Leys, D. UbiD Domain Dynamics Underpins Aromatic Decarboxylation. *Nat. Commun.* **2021**, *12*, 5065.
- (232) Messiha, H. L.; Payne, K. A. P.; Scrutton, N. S.; Leys, D. A Biological Route to Conjugated Alkenes: Microbial Production of Hepta-1,3,5-Triene. *ACS Synth. Biol.* **2021**, *10*, 228–235.
- (233) Koelschbach, J. S.; Mouttaki, H.; Merl-Pham, J.; Arnold, M. E.; Meckenstock, R. U. Identification of Naphthalene Carboxylase Subunits of the Sulfate-Reducing Culture N47. *Biodegradation* **2019**, *30*, 147–160.
- (234) Junghare, M.; Spiteller, D.; Schink, B. Anaerobic Degradation of Xenobiotic Isophthalate by the Fermenting Bacterium *Syntrophorhabdus Aromaticivorans*. *ISME J.* **2019**, *13*, 1252–1268.
- (235) Matsui, T.; Yoshida, T.; Hayashi, T.; Nagasawa, T. Purification, Characterization, and Gene Cloning of 4-Hydroxybenzoate Decarboxylase of *Enterobacter Cloacae* P240. *Arch. Microbiol.* **2006**, *186*, 21–29.
- (236) Killenberg-Jabs, M.; König, S.; Eberhardt, I.; Hohmann, S.; Hubner, G. Role of Glu51 for Cofactor Binding and Catalytic Activity in Pyruvate Decarboxylase from Yeast Studied by Site-Directed Mutagenesis. *Biochemistry* **1997**, *36*, 1900–1905.
- (237) Kneen, M. M.; Stan, R.; Yep, A.; Tyler, R. P.; Saehuan, C.; McLeish, M. J. Characterization of a Thiamin Diphosphate-Dependent Phenylpyruvate Decarboxylase from *Saccharomyces Cerevisiae*. *FEBS J.* **2011**, *278*, 1842–1853.
- (238) Smit, B. A.; van Hylckama Vlieg, J. E.; Engels, W. J.; Meijer, L.; Wouters, J. T.; Smit, G. Identification, Cloning, and Characterization of a *Lactococcus Lactis* Branched-Chain Alpha-Keto Acid Decarboxylase Involved in Flavor Formation. *Appl. Environ. Microbiol.* **2005**, *71*, 303–311.
- (239) Hazelwood, L. A.; Daran, J. M.; van Maris, A. J.; Pronk, J. T.; Dickinson, J. R. The Ehrlich Pathway for Fusel Alcohol Production: A Century of Research on *Saccharomyces Cerevisiae* Metabolism. *Appl. Environ. Microbiol.* **2008**, *74*, 2259–2266.
- (240) Dodds, W. S.; Stutzman, L. F.; Sollami, B. J. Carbon Dioxide Solubility in Water. *Ind. Eng. Chem. Chem. Eng. Data Series* **1956**, *1*, 92–95.
- (241) Matsui, T.; Yoshida, T.; Yoshimura, T.; Nagasawa, T. Regioselective Carboxylation of 1,3-Dihydroxybenzene by 2,6-Dihydroxybenzoate Decarboxylase of *Pandora Sp.* 12B-2. *Appl. Microbiol. Biotechnol.* **2006**, *73*, 95–102.
- (242) Matsuda, T.; Ohashi, Y.; Harada, T.; Yanagihara, R.; Nagasawa, T.; Nakamura, K. Conversion of Pyrrole to Pyrrole-2-Carboxylate by Cells of in Supercritical CO₂. *Chem. Commun.* **2001**, 2194–2195.
- (243) Matsuda, T.; Harada, T.; Nakamura, K. Organic Synthesis Using Enzymes in Supercritical Carbon Dioxide. *Green Chem.* **2004**, *6*, 440–444.
- (244) Zhu, Y.; Huang, Z.; Chen, Q.; Wu, Q.; Huang, X.; So, P.-K.; Shao, L.; Yao, Z.; Jia, Y.; Li, Z.; et al. Continuous Artificial Synthesis of Glucose Precursor Using Enzyme-Immobilized Microfluidic Reactors. *Nat. Commun.* **2019**, *10*, 4049.
- (245) Badger, M. R.; Price, G. D. CO₂ Concentrating Mechanisms in Cyanobacteria: Molecular Components, Their Diversity and Evolution. *J. Exp. Bot.* **2003**, *54*, 609–622.
- (246) Li, Y.; Wen, L.; Tan, T.; Lv, Y. Sequential Co-Immobilization of Enzymes in Metal-Organic Frameworks for Efficient Biocatalytic Conversion of Adsorbed CO₂ to Formate. *Front. Bioeng. Biotechnol.* **2019**, *7*, 394.
- (247) Srikanth, S.; Alvarez-Gallego, Y.; Vanbroekhoven, K.; Pant, D. Enzymatic Electrosynthesis of Formic Acid through Carbon Dioxide Reduction in a Bioelectrochemical System: Effect of Immobilization and Carbonic Anhydrase Addition. *ChemPhysChem* **2017**, *18*, 3174–3181.
- (248) Chang, K. S.; Jeon, H.; Gu, M. B.; Pack, S. P.; Jin, E. Conversion of Carbon Dioxide to Oxaloacetate Using Integrated Carbonic Anhydrase and Phosphoenolpyruvate Carboxylase. *Bioprocess Biosyst. Eng.* **2013**, *36*, 1923–1928.
- (249) Ji, X.; Su, Z.; Wang, P.; Ma, G.; Zhang, S. Tethering of Nicotinamide Adenine Dinucleotide inside Hollow Nanofibers for High-Yield Synthesis of Methanol from Carbon Dioxide Catalyzed by Coencapsulated Multienzymes. *ACS Nano* **2015**, *9*, 4600–4610.
- (250) Gandomkar, S.; Zadlo-Dobrowolska, A.; Kroutil, W. Extending Designed Linear Biocatalytic Cascades for Organic Synthesis. *ChemCatChem* **2019**, *11*, 225–243.
- (251) Schrittwieser, J. H.; Velikogne, S.; Hall, M.; Kroutil, W. Artificial Biocatalytic Linear Cascades for Preparation of Organic Molecules. *Chem. Rev.* **2018**, *118*, 270–348.
- (252) Claessens, N. J.; Burgener, S.; Vogeli, B.; Erb, T. J.; Bar-Even, A. A Critical Comparison of Cellular and Cell-Free Bioproduction Systems. *Curr. Opin. Biotechnol.* **2019**, *60*, 221–229.
- (253) Xiao, L.; Liu, G.; Gong, F.; Zhu, H.; Zhang, Y.; Cai, Z.; Li, Y. A Minimized Synthetic Carbon Fixation Cycle. *ACS Catal.* **2022**, *12*, 799–808.
- (254) Pandi, A.; Diehl, C.; Yazdizadeh Kharrazi, A.; Scholz, S. A.; Bobkova, E.; Faure, L.; Nattermann, M.; Adam, D.; Chapin, N.; Foroughijabbari, Y.; et al. A Versatile Active Learning Workflow for Optimization of Genetic and Metabolic Networks. *Nat. Commun.* **2022**, *13*, 3876.
- (255) Cai, T.; Sun, H.; Qiao, J.; Zhu, L.; Zhang, F.; Zhang, J.; Tang, Z.; Wei, X.; Yang, J.; Yuan, Q.; et al. Cell-Free Chemoenzymatic Starch Synthesis from Carbon Dioxide. *Science* **2021**, *373*, 1523–1527.
- (256) Fuchs, G. Alternative Pathways of Carbon Dioxide Fixation: Insights into the Early Evolution of Life? *Annu. Rev. Microbiol.* **2011**, *65*, 631–658.
- (257) Ren, J.; Yao, P.; Yu, S.; Dong, W.; Chen, Q.; Feng, J.; Wu, Q.; Zhu, D. An Unprecedented Effective Enzymatic Carboxylation of Phenols. *ACS Catal.* **2016**, *6*, 564–567.

- (258) Ohde, D.; Thomas, B.; Bubenheim, P.; Liese, A. Enhanced CO₂ Fixation in the Biocatalytic Carboxylation of Resorcinol: Utilization of Amines for Amine Scrubbing and in Situ Product Precipitation. *Biochem. Eng. J.* **2021**, *166*, 107825.
- (259) Mueller-Cajar, O.; Whitney, S. M. Directing the Evolution of Rubisco and Rubisco Activase: First Impressions of a New Tool for Photosynthesis Research. *Photosynth. Res.* **2008**, *98*, 667–675.
- (260) Prywes, N.; Phillips, N. R.; Tuck, O. T.; Valentin-Alvarado, L. E.; Savage, D. F. Rubisco Function, Evolution, and Engineering. *arXiv* **2022**, 2207.10773.
- (261) Arnold, F. H. Directed Evolution: Bringing New Chemistry to Life. *Angew. Chem., Int. Ed.* **2018**, *57*, 4143–4148.
- (262) Li, G.; Dong, Y.; Reetz, M. T. Can Machine Learning Revolutionize Directed Evolution of Selective Enzymes? *Adv. Synth. Catal.* **2019**, *361*, 2377–2386.
- (263) McLure, R. J.; Radford, S. E.; Brockwell, D. J. High-Throughput Directed Evolution: A Golden Era for Protein Science. *Trends Chem.* **2022**, *4*, 378–391.
- (264) Markel, U.; Essani, K. D.; Besirlioglu, V.; Schiffels, J.; Streit, W. R.; Schwaneberg, U. Advances in Ultrahigh-Throughput Screening for Directed Enzyme Evolution. *Chem. Soc. Rev.* **2020**, *49*, 233–262.
- (265) Romero-Fernandez, M.; Paradisi, F. Protein Immobilization Technology for Flow Biocatalysis. *Curr. Opin. Chem. Biol.* **2020**, *55*, 1–8.
- (266) Basso, A.; Serban, S. Industrial Applications of Immobilized Enzymes—a Review. *Mol. Catal.* **2019**, *479*, 110607.
- (267) Sheldon, R. A. Enzyme Immobilization: The Quest for Optimum Performance. *Adv. Synth. Catal.* **2007**, *349*, 1289–1307.
- (268) Landman, A. D.; Lampert, J. Activation of Immobilized Acetyl-Coenzyme A Carboxylase. *Biochem. J.* **1978**, *169*, 255–256.
- (269) Chakrabarti, S.; Bhattacharya, S.; Bhattacharya, S. K. Immobilization of D-Ribulose-1,5-Bisphosphate Carboxylase/Oxygenase: A Step toward Carbon Dioxide Fixation Bioprocess. *Biotechnol. Bioeng.* **2003**, *81*, 705–711.
- (270) Satagopan, S.; Sun, Y.; Parquette, J. R.; Tabita, F. R. Synthetic CO₂-Fixation Enzyme Cascades Immobilized on Self-Assembled Nanostructures That Enhance CO₂/O₂ Selectivity of Rubisco. *Biotechnol. Biofuels* **2017**, *10*, 175.
- (271) Hwang, E. T.; Seo, B.-K.; Gu, M. B.; Zeng, A.-P. Successful Bi-Enzyme Stabilization for the Biomimetic Cascade Transformation of Carbon Dioxide. *Catal. Sci. Technol.* **2016**, *6*, 7267–7272.
- (272) Cazelles, R.; Drone, J.; Fajula, F.; Ersen, O.; Moldovan, S.; Galarneau, A. Reduction of CO₂ to Methanol by a Polyzymatic System Encapsulated in Phospholipids-Silica Nanocapsules. *New J. Chem.* **2013**, *37*, 3721.
- (273) Wang, X. L.; Li, Z.; Shi, J. F.; Wu, H.; Jiang, Z. Y.; Zhang, W. Y.; Song, X. K.; Ai, Q. H. Bioinspired Approach to Multienzyme Cascade System Construction for Efficient Carbon Dioxide Reduction. *ACS Catal.* **2014**, *4*, 962–972.
- (274) Castaneda-Losada, L.; Adam, D.; Paczia, N.; Buesen, D.; Steffler, F.; Sieber, V.; Erb, T. J.; Richter, M.; Plumere, N. Bioelectrocatalytic Cofactor Regeneration Coupled to CO₂ Fixation in a Redox-Active Hydrogel for Stereoselective C-C Bond Formation. *Angew. Chem., Int. Ed.* **2021**, *60*, 21056–21061.
- (275) Schweiger, A. K.; Rios-Lombardia, N.; Winkler, C. K.; Schmidt, S.; Moris, F.; Kroutil, W.; Gonzalez-Sabin, J.; Kourist, R. Using Deep Eutectic Solvents to Overcome Limited Substrate Solubility in the Enzymatic Decarboxylation of Bio-Based Phenolic Acids. *ACS Sustainable Chemistry & Engineering* **2019**, *7*, 16364–16370.
- (276) Mordhorst, S.; Andexer, J. N. Round, Round We Go - Strategies for Enzymatic Cofactor Regeneration. *Nat. Prod. Rep.* **2020**, *37*, 1316–1333.
- (277) Zhang, W.; Hollmann, F. Nonconventional Regeneration of Redox Enzymes - a Practical Approach for Organic Synthesis? *Chem. Commun.* **2018**, *54*, 7281–7289.
- (278) Miller, T. E.; Beneyton, T.; Schwander, T.; Diehl, C.; Girault, M.; McLean, R.; Chotel, T.; Claus, P.; Cortina, N. S.; Baret, J. C.; et al. Light-Powered CO₂ Fixation in a Chloroplast Mimic with Natural and Synthetic Parts. *Science* **2020**, *368*, 649–654.
- (279) Calvin, M.; Benson, A. A. The Path of Carbon in Photosynthesis. *Science* **1948**, *107*, 476–480.
- (280) Evans, M.; Buchanan, B. B.; Arnon, D. I. A New Ferredoxin-Dependent Carbon Reduction Cycle in a Photosynthetic Bacterium. *Proc. Natl. Acad. Sci. U. S. A.* **1966**, *55*, 928.
- (281) Mall, A.; Sobotta, J.; Huber, C.; Tschirner, C.; Kowarschik, S.; Bacnik, K.; Mergelsberg, M.; Boll, M.; Hugler, M.; Eisenreich, W.; et al. Reversibility of Citrate Synthase Allows Autotrophic Growth of a Thermophilic Bacterium. *Science* **2018**, *359*, 563–567.
- (282) Steffens, L.; Pettinato, E.; Steiner, T. M.; Mall, A.; König, S.; Eisenreich, W.; Berg, I. A. High CO₂ Levels Drive the TCA Cycle Backwards Towards Autotrophy. *Nature* **2021**, *592*, 784–788.
- (283) Schulman, M.; Parker, D.; Ljungdahl, L. G.; Wood, H. G. Total Synthesis of Acetate from CO₂. V. Determination by Mass Analysis of the Different Types of Acetate Formed from ¹³CO₂ by Heterotrophic Bacteria. *J. Bacteriol.* **1972**, *109*, 633–644.
- (284) Figueroa, I. A.; Barnum, T. P.; Somasekhar, P. Y.; Carlström, C. I.; Engelbrektson, A. L.; Coates, J. D. Metagenomics-Guided Analysis of Microbial Chemolithoautotrophic Phosphite Oxidation Yields Evidence of a Seventh Natural CO₂ Fixation Pathway. *Proc. Natl. Acad. Sci. U. S. A.* **2018**, *115*, E92–E101.
- (285) Huber, H.; Gallenberger, M.; Jahn, U.; Eylert, E.; Berg, I. A.; Kockelkorn, D.; Eisenreich, W.; Fuchs, G. A Dicarboxylate/4-Hydroxybutyrate Autotrophic Carbon Assimilation Cycle in the Hyperthermophilic *Archaeum Ignicoccus Hospitalis*. *Proc. Natl. Acad. Sci. U. S. A.* **2008**, *105*, 7851–7856.
- (286) Berg, I. A.; Kockelkorn, D.; Buckel, W.; Fuchs, G. A 3-Hydroxypropionate/4-Hydroxybutyrate Autotrophic Carbon Dioxide Assimilation Pathway in Archaea. *Science* **2007**, *318*, 1782–1786.
- (287) Strauss, G.; Fuchs, G. Enzymes of a Novel Autotrophic CO₂ Fixation Pathway in the Phototrophic Bacterium *Chloroflexus Aurantiacus*, the 3-Hydroxypropionate Cycle. *Eur. J. Biochem.* **1993**, *215*, 633–643.
- (288) Liu, Z.; Wang, K.; Chen, Y.; Tan, T.; Nielsen, J. Third-Generation Biorefineries as the Means to Produce Fuels and Chemicals from CO₂. *Nat. Catal.* **2020**, *3*, 274–288.
- (289) Gong, F.; Cai, Z.; Li, Y. Synthetic Biology for CO₂ Fixation. *Sci. China: Life Sci.* **2016**, *59*, 1106–1114.
- (290) Nunoura, T.; Chikaraishi, Y.; Izaki, R.; Suwa, T.; Sato, T.; Harada, T.; Mori, K.; Kato, Y.; Miyazaki, M.; Shimamura, S.; et al. A Primordial and Reversible TCA Cycle in a Facultatively Chemolithoautotrophic Thermophile. *Science* **2018**, *359*, 559–563.
- (291) Ragsdale, S. W.; Pierce, E. Acetogenesis and the Wood-Ljungdahl Pathway of CO₂ Fixation. *Biochim. Biophys. Acta, Proteins Proteomics* **2008**, *1784*, 1873–1898.
- (292) Claassens, N. J.; Satanowski, A.; Bysani, V. R.; Dronsella, B.; Orsi, E.; Rainaldi, V.; Yilmaz, S.; Wenk, S.; Lindner, S. N. Engineering the Reductive Glycine Pathway: A Promising Synthetic Metabolism Approach for C1-Assimilation. In *One-Carbon Feedstocks for Sustainable Bioproduction*; Advances in Biochemical Engineering/Biotechnology; Springer International: Cham, 2022; Vol. 180, p 299.
- (293) Zarzycki, J.; Brecht, V.; Müller, M.; Fuchs, G. Identifying the Missing Steps of the Autotrophic 3-Hydroxypropionate CO₂ Fixation Cycle in *Chloroflexus Aurantiacus*. *Proc. Natl. Acad. Sci. U. S. A.* **2009**, *106*, 21317–21322.
- (294) Luo, S. S.; Lin, P. P.; Nieh, L. Y.; Liao, G. B.; Tang, P. W.; Chen, C.; Liao, J. C. A Cell-Free Self-Replenishing CO₂-Fixing System. *Nat. Catal.* **2022**, *5*, 154–162.
- (295) Ivanovsky, R. N.; Sintsov, N. V.; Kondratieva, E. N. ATP-Linked Citrate Lyase Activity in the Green Sulfur Bacterium *Chlorobium-Limicola Forma Thiosulfatophilum*. *Arch. Microbiol.* **1980**, *128*, 239–241.
- (296) Aoshima, M.; Ishii, M.; Igarashi, Y. A Novel Enzyme, Citryl-CoA Synthetase, Catalysing the First Step of the Citrate Cleavage Reaction in *Hydrogenobacter Thermophilus* TK-6. *Mol. Microbiol.* **2004**, *52*, 751–761.
- (297) Aoshima, M.; Ishii, M.; Igarashi, Y. A Novel Enzyme, Citryl-CoA Lyase, Catalysing the Second Step of the Citrate Cleavage

- Reaction in *Hydrogenobacter Thermophilus* TK-6. *Mol. Microbiol.* **2004**, *52*, 763–770.
- (298) Shiba, H.; Kawasumi, T.; Igarashi, Y.; Kodama, T.; Minoda, Y. The CO₂ Assimilation Via the Reductive Tricarboxylic Acid Cycle in an Obligately Autotrophic, Aerobic Hydrogen-Oxidizing Bacterium, *Hydrogenobacter Thermophilus*. *Arch. Microbiol.* **1985**, *141*, 198–203.
- (299) Bar-Even, A.; Noor, E.; Lewis, N. E.; Milo, R. Design and Analysis of Synthetic Carbon Fixation Pathways. *Proc. Natl. Acad. Sci. U. S. A.* **2010**, *107*, 8889–8894.
- (300) Berg, I. A.; Ramos-Vera, W. H.; Petri, A.; Huber, H.; Fuchs, G. Study of the Distribution of Autotrophic CO₂ Fixation Cycles in *Crenarchaeota*. *Microbiology* **2010**, *156*, 256–269.
- (301) Wurtzel, E. T.; Vickers, C. E.; Hanson, A. D.; Millar, A. H.; Cooper, M.; Voss-Fels, K. P.; Nikel, P. I.; Erb, T. J. Revolutionizing Agriculture with Synthetic Biology. *Nat. Plants* **2019**, *5*, 1207–1210.
- (302) Cotton, C. A.; Edlich-Muth, C.; Bar-Even, A. Reinforcing Carbon Fixation: CO₂/Reduction Replacing and Supporting Carboxylation. *Curr. Opin. Biotechnol.* **2018**, *49*, 49–56.
- (303) Bar-Even, A.; Noor, E.; Savir, Y.; Liebermeister, W.; Davidi, D.; Tawfik, D. S.; Milo, R. The Moderately Efficient Enzyme: Evolutionary and Physicochemical Trends Shaping Enzyme Parameters. *Biochemistry* **2011**, *50*, 4402–4410.
- (304) Moreno-Sanchez, R.; Saavedra, E.; Rodriguez-Enriquez, S.; Olin-Sandoval, V. Metabolic Control Analysis: A Tool for Designing Strategies to Manipulate Metabolic Pathways. *J. Biomed. Biotechnol.* **2008**, *2008*, 597913.
- (305) Noor, E.; Bar-Even, A.; Flamholz, A.; Reznik, E.; Liebermeister, W.; Milo, R. Pathway Thermodynamics Highlights Kinetic Obstacles in Central Metabolism. *PLoS Comput. Biol.* **2014**, *10*, No. e1003483.
- (306) Hadicke, O.; von Kamp, A.; Aydogan, T.; Klamt, S. Optmdfpathway: Identification of Metabolic Pathways with Maximal Thermodynamic Driving Force and Its Application for Analyzing the Endogenous CO₂ Fixation Potential of *Escherichia Coli*. *PLoS Comput. Biol.* **2018**, *14*, No. e1006492.
- (307) Kamp, A. V.; Klamt, S. MEMO: A Method for Computing Metabolic Modules for Cell-Free Production Systems. *ACS Synth. Biol.* **2020**, *9*, 556–566.
- (308) Erb, T. J.; Jones, P. R.; Bar-Even, A. Synthetic Metabolism: Metabolic Engineering Meets Enzyme Design. *Curr. Opin. Chem. Biol.* **2017**, *37*, 56–62.
- (309) Walker, B. J.; VanLoocke, A.; Bernacchi, C. J.; Ort, D. R. The Costs of Photorespiration to Food Production Now and in the Future. *Annu. Rev. Plant Biol.* **2016**, *67*, 107–129.
- (310) Desmons, S.; Grayson-Steel, K.; Nunez-Dallos, N.; Vendier, L.; Hurtado, J.; Clapes, P.; Faure, R.; Dumon, C.; Bontemps, S. Enantioselective Reductive Oligomerization of Carbon Dioxide into L-Erythrulose Via a Chemoenzymatic Catalysis. *J. Am. Chem. Soc.* **2021**, *143*, 16274–16283.
- (311) Yishai, O.; Lindner, S. N.; Gonzalez de la Cruz, J.; Tenenboim, H.; Bar-Even, A. The Formate Bio-Economy. *Curr. Opin. Chem. Biol.* **2016**, *35*, 1–9.
- (312) Satanowski, A.; Bar-Even, A. A One-Carbon Path for Fixing CO₂: C1 Compounds, Produced by Chemical Catalysis and Upgraded Via Microbial Fermentation, Could Become Key Intermediates in the Valorization of CO₂ into Commodity Chemicals. *EMBO Rep.* **2020**, *21*, No. e50273.
- (313) Burgener, S.; Schwander, T.; Romero, E.; Fraaije, M. W.; Erb, T. J. Molecular Basis for Converting (2S)-Methylsuccinyl-CoA Dehydrogenase into an Oxidase. *Molecules* **2018**, *23*, 68.
- (314) Sundaram, S.; Diehl, C.; Cortina, N. S.; Bamberger, J.; Paczia, N.; Erb, T. J. A Modular in Vitro Platform for the Production of Terpenes and Polyketides from CO₂. *Angew. Chem., Int. Ed.* **2021**, *60*, 16420–16425.
- (315) Güner, S.; Wegat, V.; Pick, A.; Sieber, V. Design of a Synthetic Enzyme Cascade for the in Vitro Fixation of a C1 Carbon Source to a Functional C4 Sugar. *Green Chem.* **2021**, *23*, 6583–6590.
- (316) Löwe, H.; Kremling, A. In-Depth Computational Analysis of Natural and Artificial Carbon Fixation Pathways. *BioDesign Res.* **2021**, *2021*, 9898316.
- (317) Trudeau, D. L.; Edlich-Muth, C.; Zarzycki, J.; Scheffen, M.; Goldsmith, M.; Khersonsky, O.; Avizemer, Z.; Fleishman, S. J.; Cotton, C. A. R.; Erb, T. J.; Tawfik, D. S.; Bar-Even, A. Design and in Vitro Realization of Carbon-Conserving Photorespiration. *Proc. Natl. Acad. Sci. U. S. A.* **2018**, *115*, E11455–E11464.
- (318) Antonovsky, N.; Gleizer, S.; Noor, E.; Zohar, Y.; Herz, E.; Barenholz, U.; Zelcbuch, L.; Amram, S.; Wides, A.; Tepper, N.; et al. Sugar Synthesis from CO₂ in *Escherichia Coli*. *Cell* **2016**, *166*, 115–125.
- (319) Gleizer, S.; Ben-Nissan, R.; Bar-On, Y. M.; Antonovsky, N.; Noor, E.; Zohar, Y.; Jona, G.; Krieger, E.; Shamshoum, M.; Bar-Even, A.; et al. Conversion of *Escherichia Coli* to Generate All Biomass Carbon from CO₂. *Cell* **2019**, *179*, 1255–1263.
- (320) Flamholz, A. I.; Dugan, E.; Blikstad, C.; Gleizer, S.; Ben-Nissan, R.; Amram, S.; Antonovsky, N.; Ravishankar, S.; Noor, E.; Bar-Even, A.; Milo, R.; Savage, D. F. Functional Reconstitution of a Bacterial CO₂ Concentrating Mechanism in *Escherichia Coli*. *eLife* **2020**, *9*, No. e59882.
- (321) Wu, C.; Lo, J.; Urban, C.; Gao, X.; Yang, B.; Humphreys, J.; Shinde, S.; Wang, X.; Chou, K. J.; Maness, P.; Tsesmetzis, N.; Parker, D.; Xiong, W. Acetyl-CoA Synthesis through a Bicyclic Carbon-Fixing Pathway in Gas-Fermenting Bacteria. *Nat. Synth.* **2022**, *1*, 615–625.
- (322) Chen, F. Y. H.; Jung, H. W.; Tsuei, C. Y.; Liao, J. C. Converting *Escherichia Coli* to a Synthetic Methylophilic Growing Solely on Methanol. *Cell* **2020**, *182*, 933–946.
- (323) He, H.; Edlich-Muth, C.; Lindner, S. N.; Bar-Even, A. Ribulose Monophosphate Shunt Provides Nearly All Biomass and Energy Required for Growth of *E. Coli*. *ACS Synth. Biol.* **2018**, *7*, 1601–1611.
- (324) Keller, P.; Noor, E.; Meyer, F.; Reiter, M. A.; Anastassov, S.; Kiefer, P.; Vorholt, J. A. Methanol-Dependent *Escherichia Coli* Strains with a Complete Ribulose Monophosphate Cycle. *Nat. Commun.* **2020**, *11*, 5403.
- (325) Claassens, N. J.; Cotton, C. A. R.; Kopljar, D.; Bar-Even, A. Making Quantitative Sense of Electromicrobial Production. *Nat. Catal.* **2019**, *2*, 437–447.
- (326) Nielsen, C. F.; Lange, L.; Meyer, A. S. Classification and Enzyme Kinetics of Formate Dehydrogenases for Biomanufacturing Via CO₂ Utilization. *Biotechnol. Adv.* **2019**, *37*, 107408.
- (327) Calzadiaz-Ramirez, L.; Calvo-Tusell, C.; Stoffel, G. M. M.; Lindner, S. N.; Osuna, S.; Erb, T. J.; Garcia-Borras, M.; Bar-Even, A.; Acevedo-Rocha, C. G. In Vivo Selection for Formate Dehydrogenases with High Efficiency and Specificity toward NADP⁺. *ACS Catal.* **2020**, *10*, 7512–7525.
- (328) Calzadiaz-Ramirez, L.; Meyer, A. S. Formate Dehydrogenases for CO₂ Utilization. *Curr. Opin. Biotechnol.* **2022**, *73*, 95–100.
- (329) Hu, B.; Harris, D. F.; Dean, D. R.; Liu, T. L.; Yang, Z. Y.; Seefeldt, L. C. Electrocatalytic CO₂ Reduction Catalyzed by Nitrogenase MoFe and FeFe Proteins. *Bioelectrochemistry* **2018**, *120*, 104–109.
- (330) Schaub, T. CO₂-Based Hydrogen Storage: CO₂ Hydrogenation to Formic Acid, Formaldehyde and Methanol. *Phys. Sci. Rev.* **2018**, *3*, 20170015.
- (331) Zell, T.; Langer, R. CO₂-Based Hydrogen Storage - Formic Acid Dehydrogenation. *Phys. Sci. Rev.* **2018**, *3*, 20170012.
- (332) Kemp, M. B.; Quayle, J. R. Microbial Growth on C1 Compounds. Incorporation of C1 Units into Allulose Phosphate by Extracts of *Pseudomonas Methanica*. *Biochem. J.* **1966**, *99*, 41–48.
- (333) Van Dijken, J. P.; Harder, W.; Beardsmore, A. J.; Quayle, J. R. Dihydroxyacetone: An Intermediate in the Assimilation of Methanol by Yeasts? *FEMS Microbiol. Lett.* **1978**, *4*, 97–102.
- (334) Large, P. J.; Peel, D.; Quayle, J. R. Microbial Growth on C(1) Compounds. 3. Distribution of Radioactivity in Metabolites of Methanol-Grown *Pseudomonas AM1* after Incubation with [¹⁴C]-Methanol and [¹⁴C]Bicarbonate. *Biochem. J.* **1962**, *82*, 483–488.
- (335) Ljungdahl, L. G.; Wood, H. G. Total Synthesis of Acetate from CO₂ by Heterotrophic Bacteria. *Annu. Rev. Microbiol.* **1969**, *23*, 515–538.

- (336) Cox, R. B.; Quayle, J. R. The Autotrophic Growth of *Micrococcus Denitrificans* on Methanol. *Biochem. J.* **1975**, *150*, 569–571.
- (337) Yu, H.; Liao, J. C. A Modified Serine Cycle in *Escherichia Coli* Coverts Methanol and CO₂ to Two-Carbon Compounds. *Nat. Commun.* **2018**, *9*, 3992.
- (338) He, H.; Hoper, R.; Dodenhoft, M.; Marliere, P.; Bar-Even, A. An Optimized Methanol Assimilation Pathway Relying on Promiscuous Formaldehyde-Condensing Aldolases in *E. Coli*. *Metab. Eng.* **2020**, *60*, 1–13.
- (339) Chou, A.; Lee, S. H.; Zhu, F.; Clomburg, J. M.; Gonzalez, R. An Orthogonal Metabolic Framework for One-Carbon Utilization. *Nat. Metab.* **2021**, *3*, 1385–1399.
- (340) Hu, G.; Li, Z.; Ma, D.; Ye, C.; Zhang, L.; Gao, C.; Liu, L.; Chen, X. Light-Driven CO₂ Sequestration in *Escherichia Coli* to Achieve Theoretical Yield of Chemicals. *Nat. Catal.* **2021**, *4*, 395–406.
- (341) Lu, X.; Liu, Y.; Yang, Y.; Wang, S.; Wang, Q.; Wang, X.; Yan, Z.; Cheng, J.; Liu, C.; Yang, X.; et al. Constructing a Synthetic Pathway for Acetyl-Coenzyme a from One-Carbon through Enzyme Design. *Nat. Commun.* **2019**, *10*, 1378.
- (342) Hu, G.; Guo, L.; Gao, C.; Song, W.; Liu, L.; Chen, X. Synergistic Metabolism of Glucose and Formate Increases the Yield of Short-Chain Organic Acids in *Escherichia Coli*. *ACS Synth. Biol.* **2022**, *11*, 135–143.
- (343) Wang, X.; Wang, Y.; Liu, J.; Li, Q.; Zhang, Z.; Zheng, P.; Lu, F.; Sun, J. Biological Conversion of Methanol by Evolved *Escherichia Coli* Carrying a Linear Methanol Assimilation Pathway. *Bioresour. Bioprocess.* **2017**, *4*, 41.
- (344) Maden, B. E. Tetrahydrofolate and Tetrahydromethanopterin Compared: Functionally Distinct Carriers in C1 Metabolism. *Biochem. J.* **2000**, *350*, 609–629.
- (345) He, H.; Noor, E.; Ramos-Parra, P. A.; Garcia-Valencia, L. E.; Patterson, J. A.; Diaz de la Garza, R. I.; Hanson, A. D.; Bar-Even, A. In Vivo Rate of Formaldehyde Condensation with Tetrahydrofolate. *Metabolites* **2020**, *10*, 65.
- (346) Yishai, O.; Goldbach, L.; Tenenboim, H.; Lindner, S. N.; Bar-Even, A. Engineered Assimilation of Exogenous and Endogenous Formate in *Escherichia Coli*. *ACS Synth. Biol.* **2017**, *6*, 1722–1731.
- (347) Ragsdale, S. W. Enzymology of the Wood-Ljungdahl Pathway of Acetogenesis. *Ann. N.Y. Acad. Sci.* **2008**, *1125*, 129–136.
- (348) Santatiwongchai, J.; Gleeson, D.; Gleeson, M. P. Theoretical Evaluation of the Reaction Mechanism of Serine Hydroxymethyltransferase. *J. Phys. Chem. B* **2019**, *123*, 407–418.
- (349) Trivedi, V.; Gupta, A.; Jala, V. R.; Saravanan, P.; Rao, G. S.; Rao, N. A.; Savithri, H. S.; Subramanya, H. S. Crystal Structure of Binary and Ternary Complexes of Serine Hydroxymethyltransferase from *Bacillus Stearothermophilus*: Insights into the Catalytic Mechanism. *J. Biol. Chem.* **2002**, *277*, 17161–17169.
- (350) Schirch, V.; Szebenyi, D. M. Serine Hydroxymethyltransferase Revisited. *Curr. Opin. Chem. Biol.* **2005**, *9*, 482–487.
- (351) Fernandes, H. S.; Ramos, M. J.; Cerqueira, N. M. F. S. A. Catalytic Mechanism of the Serine Hydroxymethyltransferase: A Computational ONIOM QM/MM Study. *ACS Catal.* **2018**, *8*, 10096–10110.
- (352) Chiba, Y.; Terada, T.; Kameya, M.; Shimizu, K.; Arai, H.; Ishii, M.; Igarashi, Y. Mechanism for Folate-Independent Aldolase Reaction Catalyzed by Serine Hydroxymethyltransferase. *FEBS J.* **2012**, *279*, 504–514.
- (353) Kim, S. J.; Yoon, J.; Im, D. K.; Kim, Y. H.; Oh, M. K. Adaptively Evolved *Escherichia Coli* for Improved Ability of Formate Utilization as a Carbon Source in Sugar-Free Conditions. *Biotechnol. Biofuels* **2019**, *12*, 207.
- (354) Wise, E. L.; Yew, W. S.; Akana, J.; Gerlt, J. A.; Rayment, I. Evolution of Enzymatic Activities in the Orotidine 5'-Monophosphate Decarboxylase Suprafamily: Structural Basis for Catalytic Promiscuity in Wild-Type and Designed Mutants of 3-Keto-L-Gulonate 6-Phosphate Decarboxylase. *Biochemistry* **2005**, *44*, 1816–1823.
- (355) Orita, I.; Kita, A.; Yurimoto, H.; Kato, N.; Sakai, Y.; Miki, K. Crystal Structure of 3-Hexulose-6-Phosphate Synthase, a Member of the Orotidine 5'-Monophosphate Decarboxylase Suprafamily. *Proteins* **2010**, *78*, 3488–3492.
- (356) Claessens, N. J.; He, H.; Bar-Even, A. Synthetic Methanol and Formate Assimilation Via Modular Engineering and Selection Strategies. *Curr. Issues Mol. Biol.* **2019**, *33*, 237–248.
- (357) Bogorad, I. W.; Chen, C.-T.; Theisen, M. K.; Wu, T.-Y.; Schlenz, A. R.; Lam, A. T.; Liao, J. C. Building Carbon-Carbon Bonds Using a Biocatalytic Methanol Condensation Cycle. *Proc. Natl. Acad. Sci. U.S.A.* **2014**, *111*, 15928–15933.
- (358) Poust, S.; Piety, J.; Bar-Even, A.; Louw, C.; Baker, D.; Keasling, J. D.; Siegel, J. B. Mechanistic Analysis of an Engineered Enzyme That Catalyzes the Formose Reaction. *ChemBioChem* **2015**, *16*, 1950–1954.
- (359) Burgener, S.; Cortina, N. S.; Erb, T. J. Oxalyl-CoA Decarboxylase Enables Nucleophilic One-Carbon Extension of Aldehydes to Chiral Alpha-Hydroxy Acids. *Angew. Chem., Int. Ed.* **2020**, *59*, 5526–5530.
- (360) Nattermann, M.; Burgener, S.; Pfister, P.; Chou, A.; Schulz, L.; Lee, S. H.; Paczia, N.; Zarzycki, J.; Gonzalez, R.; Erb, T. J. Engineering a Highly Efficient Carboligase for Synthetic One-Carbon Metabolism. *ACS Catal.* **2021**, *11*, 5396–5404.
- (361) Dai, Z.; Gu, H.; Zhang, S.; Xin, F.; Zhang, W.; Dong, W.; Ma, J.; Jia, H.; Jiang, M. Metabolic Construction Strategies for Direct Methanol Utilization in *Saccharomyces Cerevisiae*. *Bioresour. Technol.* **2017**, *245*, 1407–1412.
- (362) Siegel, J. B.; Smith, A. L.; Poust, S.; Wargacki, A. J.; Bar-Even, A.; Louw, C.; Shen, B. W.; Eiben, C. B.; Tran, H. M.; Noor, E.; et al. Computational Protein Design Enables a Novel One-Carbon Assimilation Pathway. *Proc. Natl. Acad. Sci. U.S.A.* **2015**, *112*, 3704–3709.
- (363) Jo, H.-J.; Kim, J.-H.; Kim, Y.-N.; Seo, P.-W.; Kim, C.-Y.; Kim, J.-W.; Yu, H.-n.; Cheon, H.; Lee, E. Y.; Kim, J.-S.; et al. Glyoxylate Carboligase-Based Whole-Cell Biotransformation of Formaldehyde into Ethylene Glycol Via Glycolaldehyde. *Green Chem.* **2022**, *24*, 218–226.
- (364) Chou, A.; Clomburg, J. M.; Qian, S.; Gonzalez, R. 2-Hydroxyacyl-CoA Lyase Catalyzes Acyloln Condensation for One-Carbon Bioconversion. *Nat. Chem. Biol.* **2019**, *15*, 900–906.
- (365) Zelcbuch, L.; Lindner, S. N.; Zegman, Y.; Vainberg Slutskin, I.; Antonovsky, N.; Gleizer, S.; Milo, R.; Bar-Even, A. Pyruvate Formate-Lyase Enables Efficient Growth of *Escherichia Coli* on Acetate and Formate. *Biochemistry* **2016**, *55*, 2423–2426.
- (366) Kirst, H.; Ferlez, B. H.; Lindner, S. N.; Cotton, C. A. R.; Bar-Even, A.; Kerfeld, C. A. Toward a Glycyl Radical Enzyme Containing Synthetic Bacterial Microcompartment to Produce Pyruvate from Formate and Acetate. *Proc. Natl. Acad. Sci. U.S.A.* **2022**, *119*, e2116871119.
- (367) Becker, A.; Fritz-Wolf, K.; Kabsch, W.; Knappe, J.; Schultz, S.; Volker Wagner, A. F. Structure and Mechanism of the Glycyl Radical Enzyme Pyruvate Formate-Lyase. *Nat. Struct. Biol.* **1999**, *6*, 969–975.
- (368) Topham, S.; Bazzanella, A.; Schiebahn, S.; Luhr, S.; Zhao, L.; Otto, A.; Stoltén, D. Carbon Dioxide. In *Ullmann's Encyclopedia of Industrial Chemistry*; Wiley-VCH: Weinheim, 2014; pp 1–43.
- (369) Wang, X.; Song, C. Carbon Capture from Flue Gas and the Atmosphere: A Perspective. *Front. Eng. Res.* **2020**, *8*, 560849.
- (370) Rochelle, G. T. Amine Scrubbing for CO₂ Capture. *Science* **2009**, *325*, 1652–1654.
- (371) Erans, M.; Sanz-Perez, E. S.; Hanak, D. P.; Clulow, Z.; Reiner, D. M.; Mutch, G. A. Direct Air Capture: Process Technology, Techno-Economic and Socio-Political Challenges. *Energy Environ. Sci.* **2022**, *15*, 1360–1405.
- (372) Williamson, P. Emissions Reduction: Scrutinize CO₂ Removal Methods. *Nature* **2016**, *530*, 153–155.
- (373) Laing, W. A.; Ogren, W. L.; Hageman, R. H. Regulation of Soybean Net Photosynthetic CO(2) Fixation by the Interaction of CO(2), O(2), and Ribulose 1,5-Diphosphate Carboxylase. *Plant. Physiol.* **1974**, *54*, 678–685.
- (374) Yeoh, H. H.; Badger, M. R.; Watson, L. Variations in K(m)(CO(2)) of Ribulose-1,5-Bisphosphate Carboxylase among Grasses. *Plant. Physiol.* **1980**, *66*, 1110–1112.

- (375) Sander, R. Compilation of Henry's Law Constants (Version 4.0) for Water as Solvent. *Atmos. Chem. Phys.* **2015**, *15*, 4399–4981.
- (376) Simic, S.; Zukic, E.; Schmermund, L.; Faber, K.; Winkler, C. K.; Kroutil, W. Shortening Synthetic Routes to Small Molecule Active Pharmaceutical Ingredients Employing Biocatalytic Methods. *Chem. Rev.* **2022**, *122*, 1052–1126.
- (377) Beer, C.; Reichstein, M.; Tomelleri, E.; Ciaia, P.; Jung, M.; Carvalhais, N.; Rodenbeck, C.; Arain, M. A.; Baldocchi, D.; Bonan, G. B.; et al. Terrestrial Gross Carbon Dioxide Uptake: Global Distribution and Covariation with Climate. *Science* **2010**, *329*, 834–838.
- (378) Potapov, P.; Turubanova, S.; Hansen, M. C.; Tyukavina, A.; Zalles, V.; Khan, A.; Song, X.-P.; Pickens, A.; Shen, Q.; Cortez, J. Global Maps of Cropland Extent and Change Show Accelerated Cropland Expansion in the Twenty-First Century. *Nat. Food* **2022**, *3*, 19–28.
- (379) Alston, J. M.; Beddow, J. M.; Pardey, P. G. Agriculture. Agricultural Research, Productivity, and Food Prices in the Long Run. *Science* **2009**, *325*, 1209–1210.
- (380) Kircher, M. Sustainability of Biofuels and Renewable Chemicals Production from Biomass. *Curr. Opin. Chem. Biol.* **2015**, *29*, 26–31.
- (381) Rogelj, J.; Luderer, G.; Pietzcker, R. C.; Kriegler, E.; Schaeffer, M.; Krey, V.; Riahi, K. Energy System Transformations for Limiting End-of-Century Warming to Below 1.5 Degrees C. *Nat. Clim. Change* **2015**, *5*, 519.
- (382) Napier, J. A.; Olsen, R.-E.; Tocher, D. R. Update on Gm Canola Crops as Novel Sources of Omega-3 Fish Oils. *Plant Biotechnol. J.* **2019**, *17*, 703–705.
- (383) Fayyaz, M.; Chew, K. W.; Show, P. L.; Ling, T. C.; Ng, I. S.; Chang, J.-S. Genetic Engineering of Microalgae for Enhanced Biorefinery Capabilities. *Biotechnol. Adv.* **2020**, *43*, 107554.
- (384) Sebesta, J.; Xiong, W.; Guarnieri, M. T.; Yu, J. Biocontainment of Genetically Engineered Algae. *Front. Plant Sci.* **2022**, *13*, 839446.
- (385) Salimijazi, F.; Parra, E.; Barstow, B. Electrical Energy Storage with Engineered Biological Systems. *J. Biol. Eng.* **2019**, *13*, 38.
- (386) Hoff, B.; Plassmeier, J.; Blankschien, M.; Letzel, A.-C.; Kourtz, L.; Schröder, H.; Koch, W.; Zelder, O. Unlocking Nature's Biosynthetic Power—Metabolic Engineering for the Fermentative Production of Chemicals. *Angew. Chem., Int. Ed.* **2021**, *60*, 2258–2278.
- (387) Cok, B.; Tsiropoulos, I.; Roes, A. L.; Patel, M. K. Succinic Acid Production Derived from Carbohydrates: An Energy and Greenhouse Gas Assessment of a Platform Chemical toward a Bio-Based Economy. *Biofuels, Bioprod. Biorefin.* **2014**, *8*, 16–29.
- (388) Ahn, J. H.; Jang, Y.-S.; Lee, S. Y. Production of Succinic Acid by Metabolically Engineered Microorganisms. *Curr. Opin. Biotechnol.* **2016**, *42*, 54–66.
- (389) Xiberras, J.; Klein, M.; de Hulster, E.; Mans, R.; Nevoigt, E. Engineering *Saccharomyces Cerevisiae* for Succinic Acid Production from Glycerol and Carbon Dioxide. *Front. Bioeng. Biotechnol.* **2020**, *8*, 3389.
- (390) Heijstra, B. D.; Leang, C.; Juminaga, A. Gas Fermentation: Cellular Engineering Possibilities and Scale Up. *Microb. Cell Fact.* **2017**, *16*, 60.
- (391) Oehlmann, N. N.; Rebelein, J. G. The Conversion of Carbon Monoxide and Carbon Dioxide by Nitrogenases. *ChemBioChem* **2022**, *23*, No. e202100453.
- (392) Yang, Z. Y.; Dean, D. R.; Seefeldt, L. C. Molybdenum Nitrogenase Catalyzes the Reduction and Coupling of CO to Form Hydrocarbons. *J. Biol. Chem.* **2011**, *286*, 19417–19421.
- (393) Lee, C. C.; Hu, Y.; Ribbe, M. W. Vanadium Nitrogenase Reduces CO. *Science* **2010**, *329*, 642.
- (394) Hu, Y.; Lee, C. C.; Ribbe, M. W. Extending the Carbon Chain: Hydrocarbon Formation Catalyzed by Vanadium/Molybdenum Nitrogenases. *Science* **2011**, *333*, 753–755.
- (395) Seefeldt, L. C.; Rasche, M. E.; Ensign, S. A. Carbonyl Sulfide and Carbon Dioxide as New Substrates, and Carbon Disulfide as a New Inhibitor, of Nitrogenase. *Biochemistry* **1995**, *34*, 5382–5389.
- (396) Rebelein, J. G.; Hu, Y.; Ribbe, M. W. Differential Reduction of CO(2) by Molybdenum and Vanadium Nitrogenases. *Angew. Chem., Int. Ed.* **2014**, *53*, 11543–11546.
- (397) Kang, F.; Yu, L.; Xia, Y.; Yu, M.; Xia, L.; Wang, Y.; Yang, L.; Wang, T.; Gong, W.; Tian, C.; et al. Rational Design of a Miniature Photocatalytic CO₂-Reducing Enzyme. *ACS Catal.* **2021**, *11*, 5628–5635.
- (398) South, P. F.; Cavanagh, A. P.; Liu, H. W.; Ort, D. R. Synthetic Glycolate Metabolism Pathways Stimulate Crop Growth and Productivity in the Field. *Science* **2019**, *363*, 609–616.